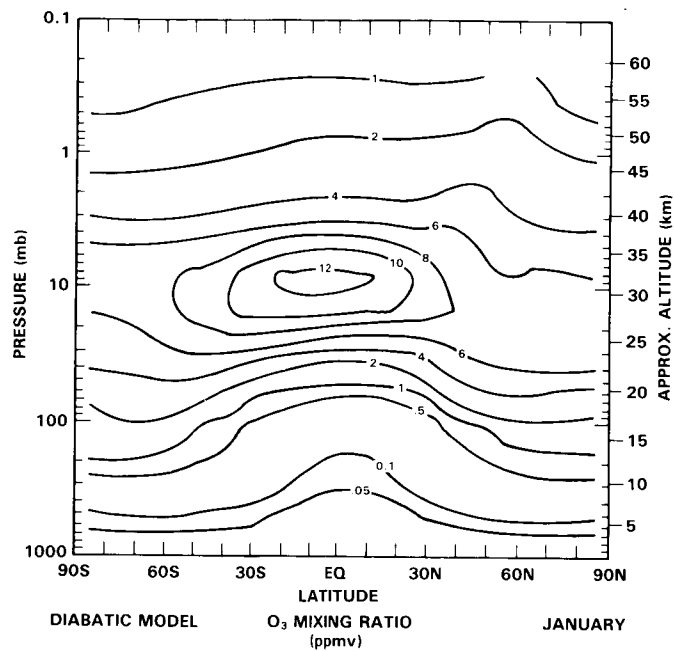


# ASSESSMENT MODELS



## Panel Members

J.A. Pyle, Chairman

D.M. Butler

D. Cariolle

R.R. Garcia

W.L. Grose

P.D. Guthrie

M. Ko

A.J. Owens

R.A. Plumb

M.J. Prather

U. Schmailzl

M.R. Schoeberl

S. Solomon

F. Stordal

N.D. Sze

K.K. Tung

G. Visconti

D.J. Wuebbles

## CHAPTER 12

### ASSESSMENT MODELS

#### TABLE OF CONTENTS

12.0	INTRODUCTION .....	649
12.1	ON THE COMPARISON OF MODELS AND DATA .....	649
12.2	1-D MODELS: FORMULATION AND INTERPRETATION - RECENT DEVELOPMENTS .....	654
12.3	1-D MODELS: INTERCOMPARISON OF NO <sub>y</sub> DIFFERENCES .....	658
12.4	TWO-DIMENSIONAL MODELS - SOME THEORETICAL IDEAS .....	662
12.5	CURRENT MODELS .....	670
12.6	A COMPARISON OF TWO-DIMENSIONAL MODELS .....	681
12.7	CHEMISTRY IN THREE-DIMENSIONAL MODELS .....	711
12.8	ON THE USE OF MODELS FOR ASSESSMENT STUDIES .....	714
12.9	CONCLUSIONS .....	719

## 12.0 INTRODUCTION

In this chapter the types of models used in assessment of possible chemical perturbations to the stratosphere will be reviewed. One-dimensional models have traditionally been used for this task. Their limitations are well known: the parameterisation of transport in one-dimensional models has a poor physical basis (but see Mahlman (1984), Holton (1985)); the hybrid nature of the models - part local, part global (or hemispheric) average - makes interpretation and validation non-trivial (although this problem is generally ignored). The models' great strength lies in their use as a test bed for photochemical theories; a variety of pollution studies, including multiple perturbations, can be carried out inexpensively. An additional important role in the future may lie in developing complete and efficient photochemical schemes for multi-dimensional models. One-dimensional models are discussed in Sections 12.2 and 12.3.

Two-dimensional models have been used for assessment studies in the past by relatively few groups (e.g. Vupputuri, 1978/79, Pyle, 1980, Brasseur and Bertin, 1978/79, Whitten *et al.*, 1981, Gidel *et al.*, 1983). In recent years there have been considerable advances in the theoretical basis for these models and the advantages of the better dynamical treatment have led many groups to embark on a two-dimensional modelling effort. In Sections 12.4 and 12.5 are discussed the present status of two-dimensional modelling, with a comparison of model results in Section 12.6.

Three-dimensional models have so far been little used for photochemical studies. There are beginning to be some efforts to incorporate simple chemical schemes and these are reviewed in Section 12.7.

Before a discussion of the status of photochemical modelling efforts, the problem of model validation will be mentioned. It is clear that simply to compare a model calculated profile of a particular gas with a measured profile, while being a necessary step, is unsatisfactory as a critical test for the theory behind the model. In the next Section a hierarchy of tests for photochemical models is presented.

### 12.1 ON THE COMPARISON OF MODELS AND DATA

To have some confidence in the models which are used to study both the current atmosphere and to make predictions about its future development, comparisons between model and data are required. In this Section, types of comparison are discussed. These vary considerably in their usefulness for testing various aspects of model behaviour. In order to reduce the subjectivity of the comparisons, strategies for field observations are suggested.

While the simplest test of the photochemical components of a model is the identification in the atmosphere of the species described in that model (a test not currently satisfied for at least HOCl and HNO<sub>4</sub>), the next category of test is usually the comparison of modelled and observed profiles. While this is a necessary step it is certainly insufficient as a critical test. Firstly, the decision as to the goodness of fit is subjective. Differences, for example, in ozone in the upper stratosphere of about 20% are generally thought to constitute 'poor' agreement, while factors of two in comparison between modelled and measured OH are labelled as 'satisfactory'. Secondly, one and two-dimensional models are incapable of modelling the specific dynamical conditions appropriate to a given observation. Thus any discrepancy could be due to inadequately modelled transport or photochemistry. The comparison does not constitute a test because it cannot isolate the physical process being tested. The comparison is at best suggestive (consider, for example, the case of the ClO profile where systematic differences in the slope at around 30 km suggested possible inadequacies in HO<sub>x</sub> chemistry (Whitten *et al.*, 1981)). Given these problems, single measurements of

## ASSESSMENT MODELS

stratospheric species for which a reasonable data base already exists do not appear to add much to the testing of models.

In order to isolate the photochemical from the dynamical contributions, a better test is to compare modelled and measured ratios of species which should be in photochemical steady state. A critical test requires the measurement of all the terms contributing to the ratio expression, which for some ratios would constitute a major logistical problem. Harries (1982) has shown that to test the ratio of NO to NO<sub>2</sub> measurements of O, O<sub>3</sub>, ClO, HO<sub>2</sub>, temperature and upward and downward solar flux are required. For the test to be critical, the measurements need to be made at exactly the same time and location. Furthermore, the requirement is for high absolute accuracies on the measurements if a useful test is to be made. Harries points to the need for measurements with absolute accuracies of  $\sim \pm 2\%$  to test the NO/NO<sub>2</sub> ratio to  $\sim \pm 10\%$ .

Anderson (NASA meeting, Feldafing, 1984) has discussed the possibility of simultaneously measuring a number of important stratospheric radicals. In his resonance fluorescence technique stratospheric air flows through a chamber where the measurements are made. A rapid response will allow nearly simultaneous, highly accurate measurements of O(<sup>3</sup>P), NO, NO<sub>2</sub>, OH, HO<sub>2</sub> and ClO. If O<sub>3</sub>, CH<sub>4</sub>, H<sub>2</sub>O and temperature are also measured, many of the important ratios can be determined.

The rapid response is also an advantage for investigations of correlations between species within the laminar layers encountered in the stratosphere. These structures, well known for O<sub>3</sub> (e.g. Dobson, 1973) and recently seen in H<sub>2</sub>O (Kley *et al.*, 1980), may be typically a few hundred metres in vertical extent. Kley *et al.* note an anticorrelation between O<sub>3</sub> and H<sub>2</sub>O. Observation of similar relationships between, for example, O<sub>3</sub> and OH would be a powerful test of photochemical theory.

An extremely informative test, with less stringent measurement requirements, is the comparison of diurnal variations which in most situations should be independent of atmospheric dynamics. Here, the comparison of the gross behaviour of model and data is useful; failure to reproduce the observed structure points to model inadequacies. Furthermore, since it is the relative diurnal changes which are important, the observations need only have high precision with the absolute accuracy being relatively unimportant.

Two examples showing the usefulness of this approach are chosen. Figure 12-1 shows modelled and observed NO<sub>2</sub> in the upper stratosphere (Roscoe *et al.*, 1985b). Although the absolute magnitudes are different, the gross behaviour is modelled well, including the smaller night-time variation seen at the higher altitude, caused in the model by a less important role for N<sub>2</sub>O<sub>5</sub> with increasing height in the upper stratosphere.

Figure 12-2 shows modelled and observed measurements of the vertical column of ClO (Ko and Sze 1984). The difference in the daytime time increase has led to important suggestions regarding the role of ClONO<sub>2</sub> (see Chapter 11).

Pallister and Tuck (1983) have suggested a particularly important role for high precision measurements of diurnal variations. Figure 12-3 shows the relative variation in ozone at altitudes between 40 and 50 km. The diurnal changes vary significantly with height as the relative roles of O<sub>x</sub>, HO<sub>x</sub>, NO<sub>x</sub> and ClO<sub>x</sub> change. For atmospheres with different levels of odd chlorine, they calculate different variations. Measurement of these variations (which would place extremely stringent requirements on the experimental technique) would be particularly useful for assessing our understanding of upper stratospheric photochemistry.

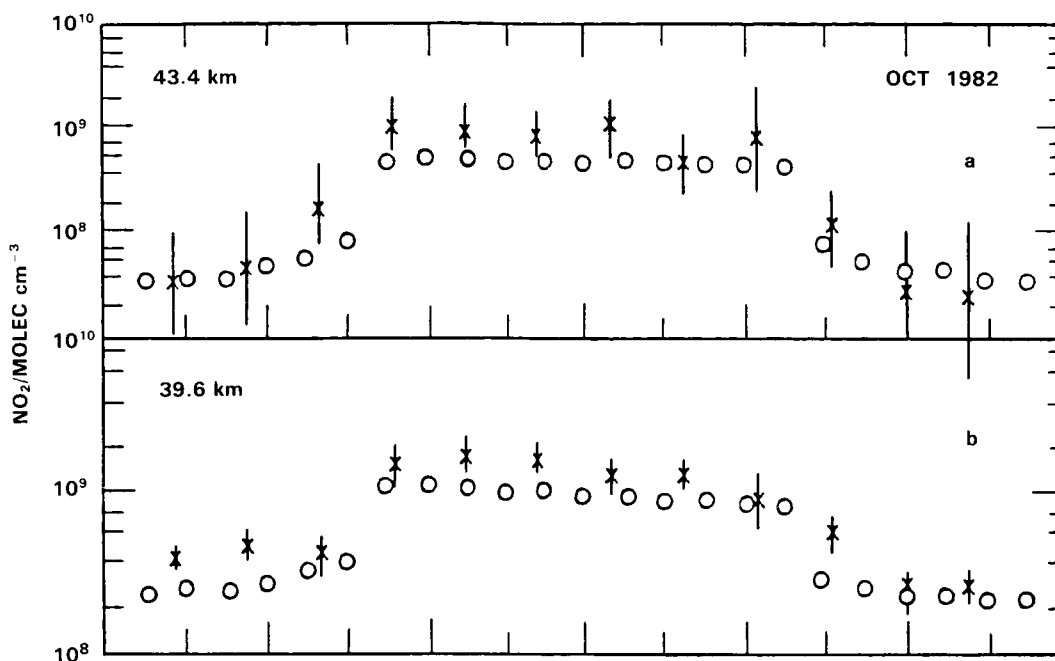


**Figure 12-1.** Diurnal variation of  $\text{NO}_2$  concentration at  $32^\circ\text{N}$ , October at (a)  $\sim 43$  Km and (b)  $\sim 40$  Km. \* are observations by a pressure modulator radiometer; o represents model calculations. See Roscoe *et al.* (1985b).

A further category of model-data comparisons is provided by major natural perturbations to the stratosphere. These would include solar proton events, eclipses, sudden stratospheric warmings, injection of volcanic material, etc. As an example, Figure 12-4 shows the calculated decrease in ozone following the major solar proton event of August 1972. The expected decrease in ozone following the predicted increases in nitrogen oxides is modelled well.

The comparisons outlined above depend for their usefulness on the photochemical time scale being considerably less than the dynamical time scale. For many stratospheric species this is not the case and additional tests are required. To avoid the particular problems with these species and the dependence of their distributions on the synoptic situation (such that comparison of a single measured profile with a modelled profile is quite unsatisfactory) calls for more extensive data requirements. Two particular approaches can be identified. A trajectory approach can be followed in which the problem of dynamics is separated from the photochemistry by considering an isolated air parcel. Secondly, use can be made of large satellite data sets from which meaningful mean quantities can be extracted, thus avoiding the problem of day to day variability.

Austin *et al.* (1985b) have described trajectory analyses using LIMS and SAMS satellite data. Starting from a LIMS observation they calculate air parcel trajectories for periods of up to ten days (beyond which time the parcel can be expected to lose its integrity). A photochemical box model is initialised with LIMS and SAMS data and one-dimensional model results and then the photochemical calculation is carried out along the parcel trajectory, with appropriate temperatures and solar zenith angles. The parcel typically intersects one LIMS observation per day so that the model and data can be compared. Figure 12-5 shows the calculated  $\text{O}_3$  and  $\text{NO}_2$  at  $\sim 35$  km compared with observations. It can be seen that the model reproduces the observed fluctuations quite well. Figure 12-6 shows scatter diagram for  $\text{O}_3$ ,  $\text{HNO}_3$  and  $\text{NO}_2$  and the

## ASSESSMENT MODELS

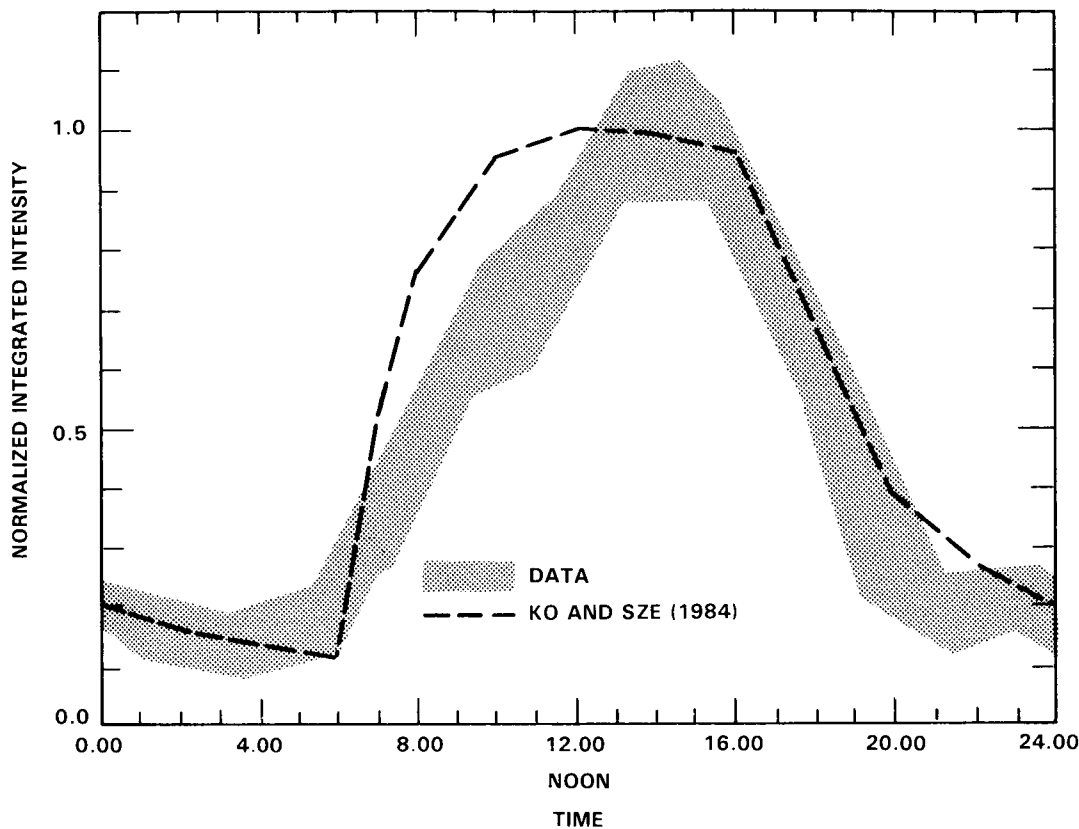


**Figure 12-2.** Comparison between the normalized observed integrated intensity of the ClO emission (Solomon *et al.*, 1984) and the synthetic intensity derived from calculated concentration of ClO by Ko and Sze (1984) for December, 19°N.

corresponding correlation coefficients. The good fits suggest an important future role for this kind of study, especially if more data to initialize the model becomes available. In this context, ATMOS and then the experiments on UARS provide excellent opportunities for further study.

The LIMS and SAMS experiments allow studies to be performed which rely on the extremely large amounts of data providing a good statistical base. Crutzen and Schmailzl (1983) have studied the  $O_x$ ,  $NO_y$  and the  $HO_x$  budgets by using combinations of balloon and satellite data, while Jones *et al.* (1985) have investigated the role of  $CH_4$  oxidation in the  $H_2O$  budget, using SAMS and LIMS (see Chapter 9).

Pyle and Zavody (1985a) and Jackman *et al.* (1985a) have tested some aspects of  $HO_x$  photochemistry by deriving OH fields using LIMS and SAMS data by two independent methods. One method assumes equilibrium between  $HNO_3$  and  $NO_2$  while the other calculates OH from its sources and sinks. The two methods agree within the errors expected of the derivations (see Chapters 9, 10.)

Finally, correlation studies using satellite data can also be used to study photochemistry. For example, the correlation between  $O_3$  and temperature throws some light on the relative strength of the catalytic cycles affecting ozone (Barnett *et al.*, 1975a).

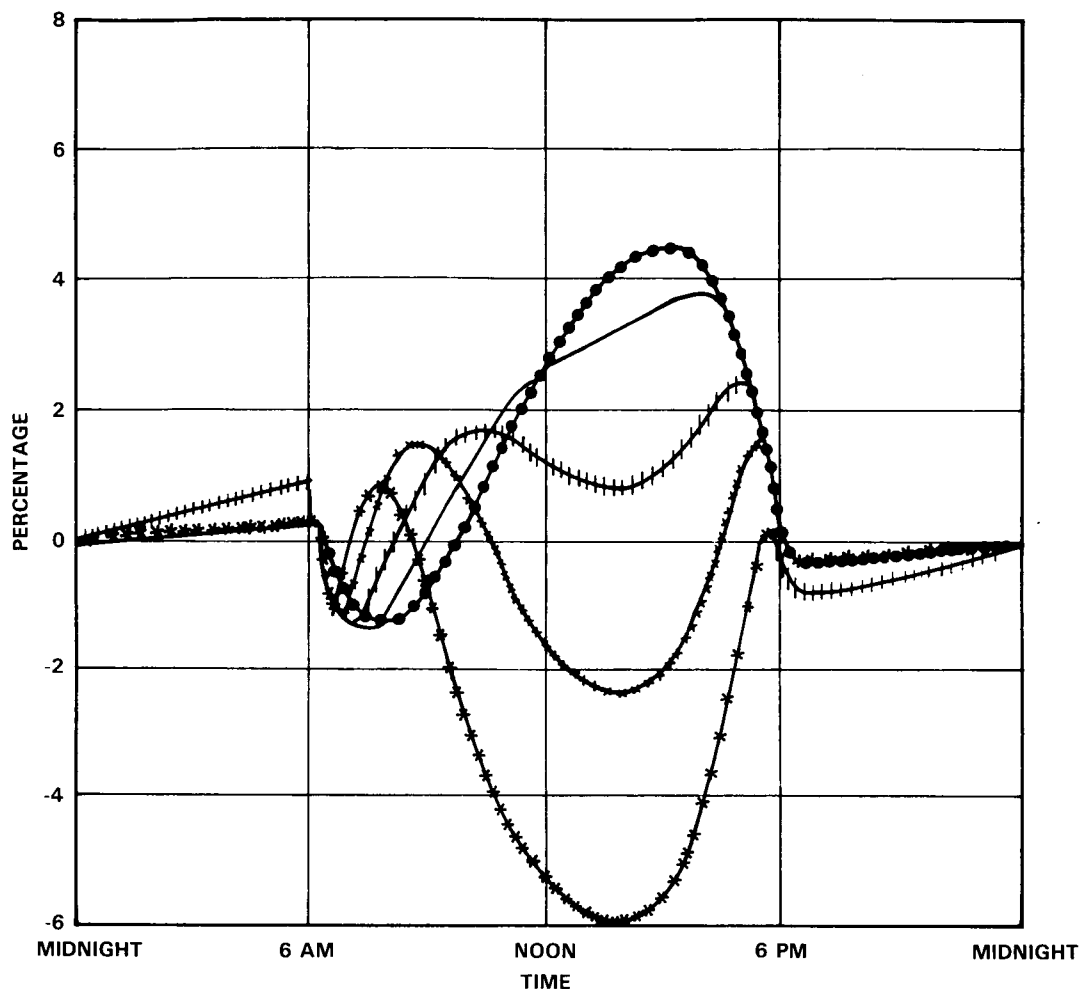


**Figure 12-3.** Percentage deviation from midnight values of ozone concentrations for a diurnal cycle. Key: ● ≡ 40 km; — ≡ 42 km; | ≡ 44 km; X ≡ 46 km; \* ≡ 48 km. From Pallister and Tuck (1983).

In conclusion, fast photochemistry can in principle be tested using good measurements at a fixed pressure. The photochemical model then reduces to a box model and a treatment of dynamics is unnecessary. Two types of measurements appear particularly useful: measurements to test both photochemical ratios and correlations, and diurnal measurements. The former may place severe requirements on measurement accuracy while the latter requires measurements with high precision but not necessarily high absolute accuracy.

The testing of model behaviour for longer lived species is most difficult. Various methods are available. The approach needs to allow for transport so that multi-dimensional models have a particular role to play. Combinations of models and large satellite data sets are particularly useful. Trajectory analyses in which the problems of dynamics can be separated from photochemistry should be especially useful when large data sets become available.

Whichever method is used to compare model and measurements, there is a need for a careful estimate of errors in both the models and data, as pointed out by Harries (1982). While a detailed model error

## ASSESSMENT MODELS

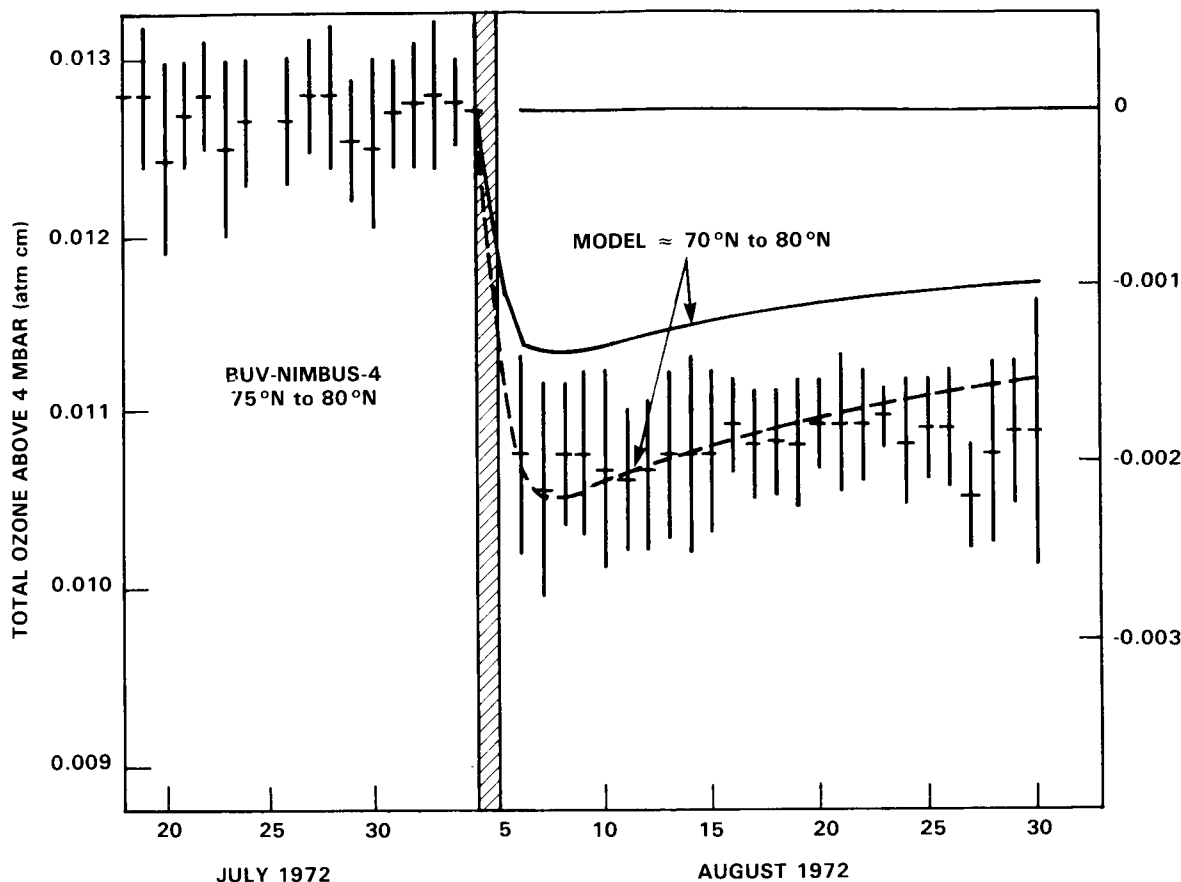


**Figure 12-4.** Comparison of BUUV-NIMBUS-4 ozone data with model prediction for high latitudes. The model results are plotted as relative depletions with respect to the 'undisturbed' level on 4 August, before a major SPE occurred. The solid line and dashed line represent different assumed NO production rates. See Fabian *et al.* (1979).

analysis is difficult and can be an unwieldy problem, by isolating specific aspects of the model (e.g., the ratio of  $\text{HNO}_3$  to  $\text{NO}_2$ ) the comparison does become amenable to a critical examination of errors. Modellers should be encouraged to carry out such studies.

The limitations which are apparent in the present testing of models must be borne in mind when considering the discussion of the detailed comparison of models and data (Chapters 8 to 11) and, of course, in considering the assessment studies.

### 12.2 1-D MODELS: FORMULATION AND INTERPRETATION — RECENT DEVELOPMENTS

One-dimensional coupled transport and chemical kinetics models have been one of the basic research tools in theoretical studies of the stratosphere. In fact, much of the current theoretical understanding of the chemical structure of the stratosphere and the photochemical processes governing it has been derived with the help of one-dimensional models. Most past analyses of man's potential influence on stratospheric ozone have been done with the aid of one-dimensional models. Despite the detailed representations of

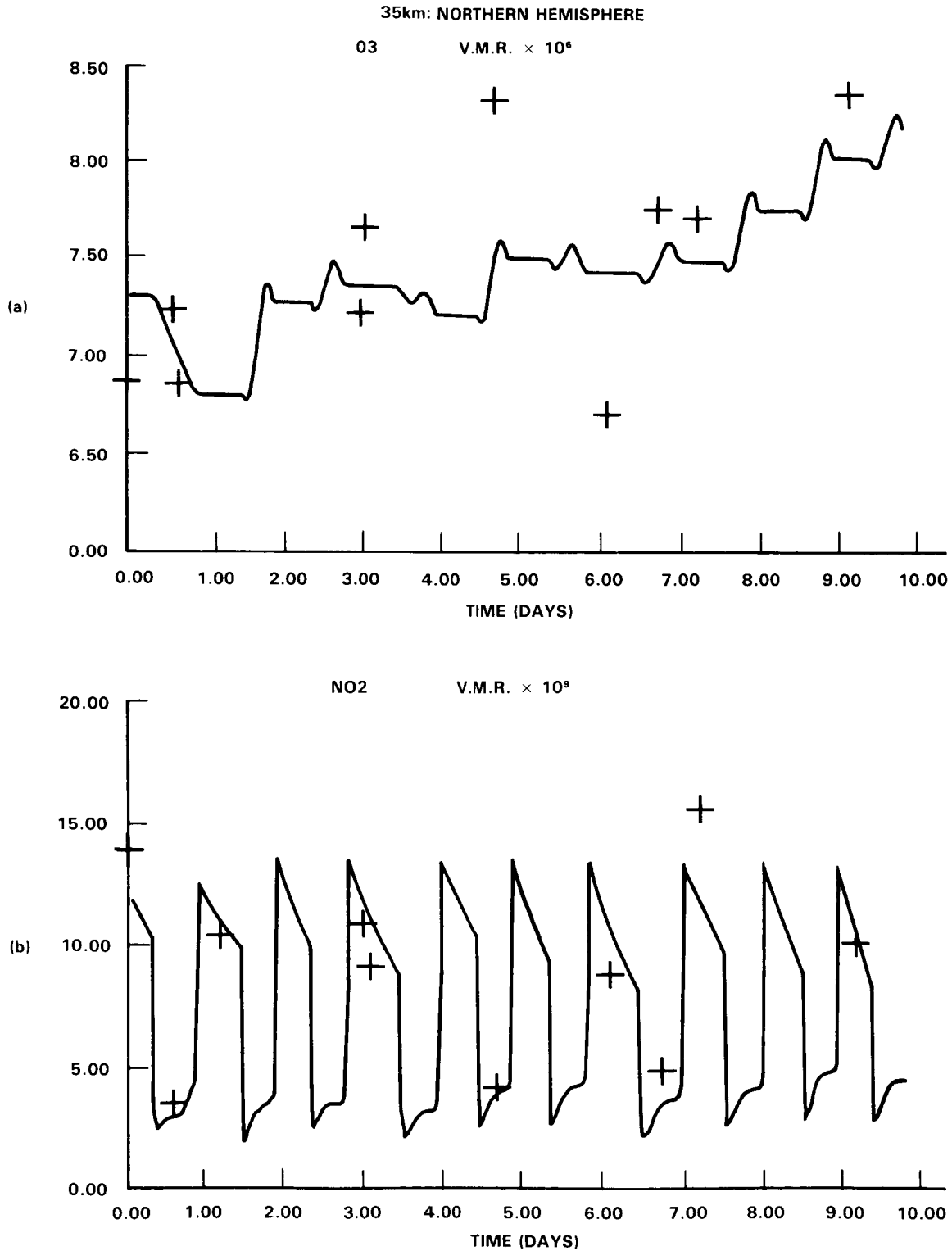


**Figure 12-5.** Ten-day time histories of species observed by LIMS along a trajectory at  $\sim 35$  km ( $\theta = 1100\text{K}$ ) during February 1979. Curve is model calculation, crosses are LIMS observations within the coincidence criterion of 5 great circle degrees radius (a)  $\text{O}_3$  (b)  $\text{NO}_2$ . After Austin *et al.* (1985b).

ASSESSMENT MODELS

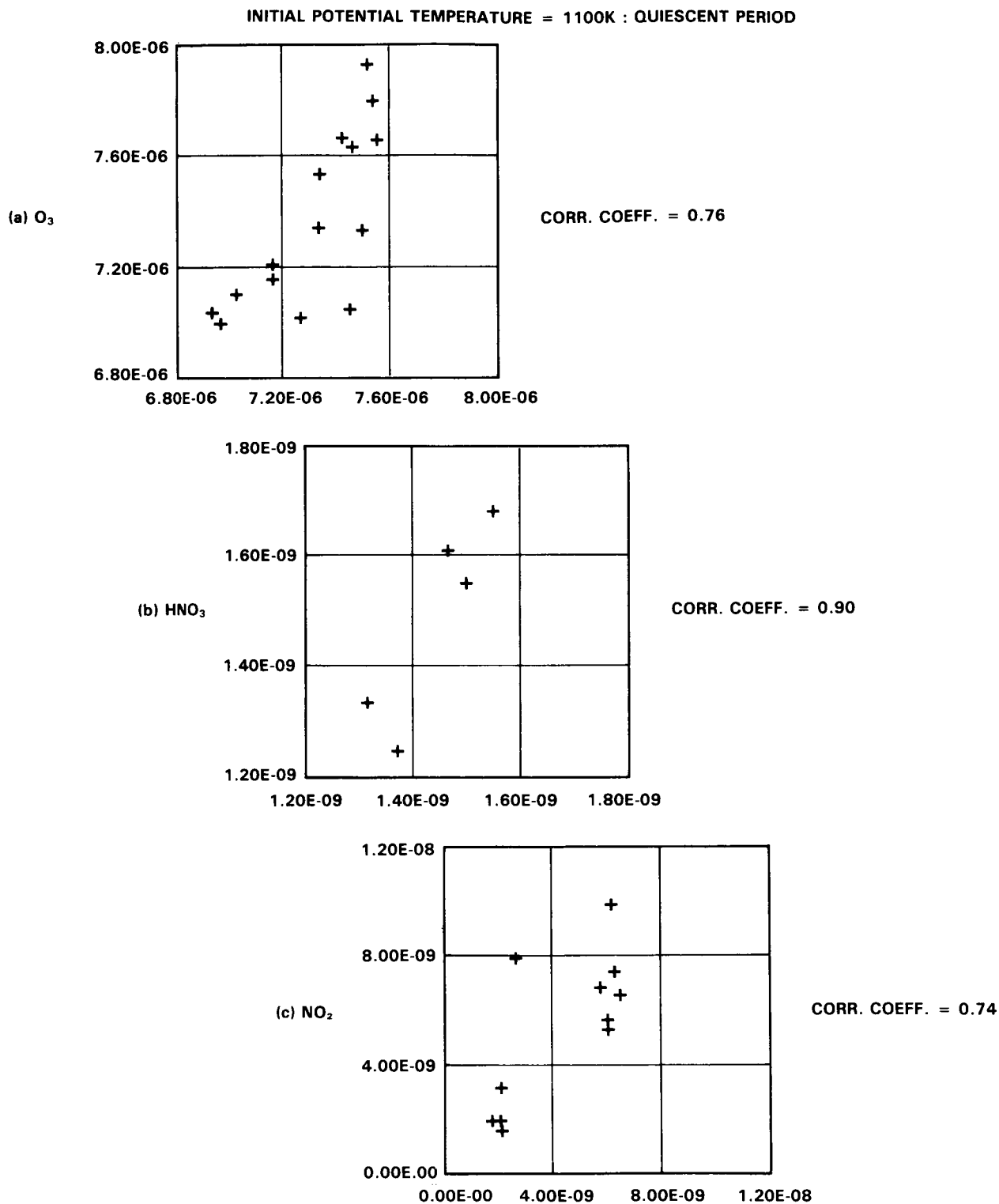


Figure 12-6. Scattergram of calculated volume mixing ratios and coincident LIMS observations. (a) O<sub>3</sub>, (b) HNO<sub>3</sub>, (c) NO<sub>2</sub>. The correlation coefficient is given on each plot. ~ 35 km trajectory, March, from Austin *et al.* (1985b).

atmospheric chemical and radiative processes in these models, there remain recognized limitations in their formulation and interpretation.

In the 1-D model, the chemical and physical processes determining the temporal variation in the concentration of the atmospheric constituent,  $c$ , can be represented in mathematical form by the continuity equation,

$$\frac{\partial c}{\partial t} = \frac{\partial}{\partial z} \left\{ K_z \rho \frac{\partial}{\partial z} (c/\rho) \right\} + P - Lc + S$$

where  $t$  is time,  $z$  is altitude,  $K_z$  is the one-dimensional vertical diffusion coefficient,  $\rho$  is air density,  $P$  and  $Lc$  are, respectively, the photochemical production and loss rates, and  $S$  represents any other possible sources and sinks for  $c$ . In deriving this equation, a longitudinal and latitudinal global average of the transport flux is taken, and it is assumed that the resulting net vertical transport flux can be represented as a diffusive process.

The diffusive treatment of transport in the 1-D model is a purely empirical representation. It does not utilize observed atmospheric motions directly but rather is based on the observations of the temporal and spatial distributions of selected tracers. The  $K_z$  profiles used in different models have typically been based on chemical tracers such as  $\text{CH}_4$  and  $\text{N}_2\text{O}$  and radionuclides from past nuclear tests. For such tracers, it is assumed that the value of  $K_z$  determined is a function of only the transporting motions, and within the scope of 1-D models is independent of both the details of the tracer field and the specific structure of the tracer source and sink distributions. While adopted profiles differ by as much as an order of magnitude at some altitudes, these  $K_z$  profiles tend to have similar characteristics: large values in the troposphere, much reduced values in the region near the tropopause, increasing with altitude in the stratosphere (see WMO 1981).

Generally, a single  $K_z$  profile is chosen to represent the transport of all species in the atmosphere. In practice, the representation of transport in the 1-D model has been limited by the lack of well-determined globally averaged data for the tracers and by uncertainties in understanding of the balances among sources, sinks and transport processes affecting the trace species distributions. Recent analyses suggest that it may not be possible to find a  $K_z$  at least with current chemistry that adequately fits atmospheric data for all long-lived tracers, such as  $\text{N}_2\text{O}$  and  $\text{CH}_4$ , at the same time (e.g. Wuebbles 1983b). Using a separate  $K_z$  for each species would provide additional variables in the model that would enable any observational data to be fit, but without necessarily representing any physical aspect of the atmosphere. Unless there is established a physically well-defined basis for each species to have its own  $K_z$  it would not be reasonable to consider this.

Dynamically based transport parameterizations have been proposed in which  $K_z$  depends on species and chemical gradients (Holton 1985, Mahlman *et al.*, 1985). Although not fully developed and exploited, these techniques may provide a better physical basis for representation of globally averaged transport in 1-D models.

A further limitation of 1-D models is that it is difficult to average accurately the global rates for photochemical production and loss. Only local variables, such as solar flux intensity, ozone concentrations, and temperature, can be used. This complicates interpretation of 1-D results, and has led to much discussion on the meaning of calculated distributions of various species. Despite these difficulties, the

## ASSESSMENT MODELS

1-D model has nonetheless been found to capture many of the important features of trace gas behaviour in the stratosphere, and remains a useful theoretical tool.

For multi-year time-dependent calculations, such as those for assessment analyses, it is extremely expensive to calculate the full diurnal variations throughout the calculation. To get around this, several different techniques for simplified diurnal treatments or diurnal averaging have been developed. Some models treat diurnal averaging by occasionally updating multiplicative factors on each photodissociation rate and chemical rate constant based on detailed diurnal models. Others simplify this approach in various ways. Still others simplify diurnal changes by calculating day-time and night-time averages separately throughout their calculations. For those models that do not continually update the effects of diurnal variations, several studies (e.g. Herman and McQuillan 1985; Wuebbles and Connell 1985) indicate that the influence of diurnal averaging must be carefully considered for the perturbed atmosphere. Herman (1985) indicates that significant errors in the calculated ozone change can result unless diurnal averaging factors calculated for the ambient atmosphere are updated for the perturbed atmosphere. Wuebbles and Connell (1985) show that much of this error appears to result from "false" increases in  $\text{NO}_3$  and  $\text{N}_2\text{O}_5$ , that can be corrected for simply by recognizing that almost all  $\text{NO}_3$  produced during the day would be photolyzed. The remaining error appears to be related to significant difference in  $\text{NO}_2/\text{NO}$ ,  $\text{HO}_2/\text{OH}$  and  $\text{ClO}/\text{Cl}$  ratios between the current atmosphere and a highly perturbed atmosphere.

### 12.3 1-D MODELS: INTERCOMPARISON OF $\text{NO}_y$ DIFFERENCES

The current interest in assessment studies, particularly cases with very high chlorine amounts, has led to a recent intercomparison of 1-D models. The initial intercomparison revealed major differences in the calculated stratospheric total odd nitrogen. Possible reasons for these differences, which have an important impact on the calculated ozone perturbation, are discussed in this section.

Organizations participating in the initial stages of the 1-D model intercomparison are shown in Table 12-1. For the present atmosphere, each using the "best case" versions of the models, with 1985 NASA recommended chemical rate constants, as given in Appendix A, resulted in maximum total odd-nitrogen in the upper stratosphere ranging from 13 ppbv (in the Harvard model) to 23 ppbv (in the NASA GSFC model of Stolarski).

A special series of calculations was done with each model to analyze the causes of the large differences in calculated  $\text{NO}_y$ . In these calculations, along with using the same chemical rate constants, each

**Table 12-1.** Initial participants in 1-D model intercomparison. Numbers are used to identify models corresponding to plotted results in Figures 12-7–12-11.

Model	Organization
1	Du Pont (A Owens)
2	NASA GSFC (J Herman)
3	AER, Inc. (N D Sze)
4	Harvard Univ. (M Prather)
5	NASA GSFC (R Stolarski)
6	NASA Langley (L Callis)
7	LLNL (D Wuebbles)

model assumed the same  $K_z$  profile (based on the DuPont model), the same atmosphere (U.S. Standard Atmosphere, 1976), the same boundary conditions, the same tropospheric water vapor, same albedo (25%), and generally the same solar zenith angle (30° equinox). For these calculations, model calculated  $\text{NO}_y$  ranged from 12 to 22 ppbv. A detailed comparison of results indicated strong differences between models in the photodissociation rates of  $\text{O}_2$ ,  $\text{N}_2\text{O}$ , and  $\text{NO}$ . Since photolysis is the major sink for  $\text{N}_2\text{O}$ , the production of odd-nitrogen, through  $\text{O}(^1\text{D}) + \text{N}_2\text{O} \rightarrow 2\text{NO}$ , is dependent on differences in calculated  $\text{N}_2\text{O}$  amounts and, therefore, in photolysis rates of  $\text{N}_2\text{O}$  in the upper stratosphere. In turn,  $\text{N}_2\text{O}$  photolysis is dependent on  $\text{O}_2$  absorption in the Schumann-Runge bands. Likewise, the major sink for odd-nitrogen in the upper stratosphere is through the reaction  $\text{N} + \text{NO} \rightarrow \text{N}_2 + \text{O}$ , where the atomic nitrogen,  $\text{N}$ , is produced through the photolysis of  $\text{NO}$ .

In order to narrow further the differences between models, another special calculation was suggested (the NASA test case shown in Figures 12-7–12-11) in which the prior conditions were combined with a fixed ozone distribution based on the U.S. Standard Atmosphere (1976). The results to be discussed include an updated photodissociation treatment of  $\text{O}_2$  in model 5 (a change from the approach of Hudson and Mahle (1972) to Frederick and Hudson (1979a)), and changes in the treatment of both  $\text{O}_2$  and  $\text{NO}$  photolysis for model 4 (for  $\text{O}_2$ , Logan *et al.* (1978) with reduced continuum is used and, for  $\text{NO}$ , 67% predissociation with  $\text{N}_2$  quenching as in Nicolet and Cieslik (1980) is employed). The results for this test case gave a range in  $\text{NO}_y$ , shown in Figure 12-7, of 13 to 19 ppbv, with most of the decrease in the spread of  $\text{NO}_y$  coming primarily from the changes in photodissociation treatments described above.

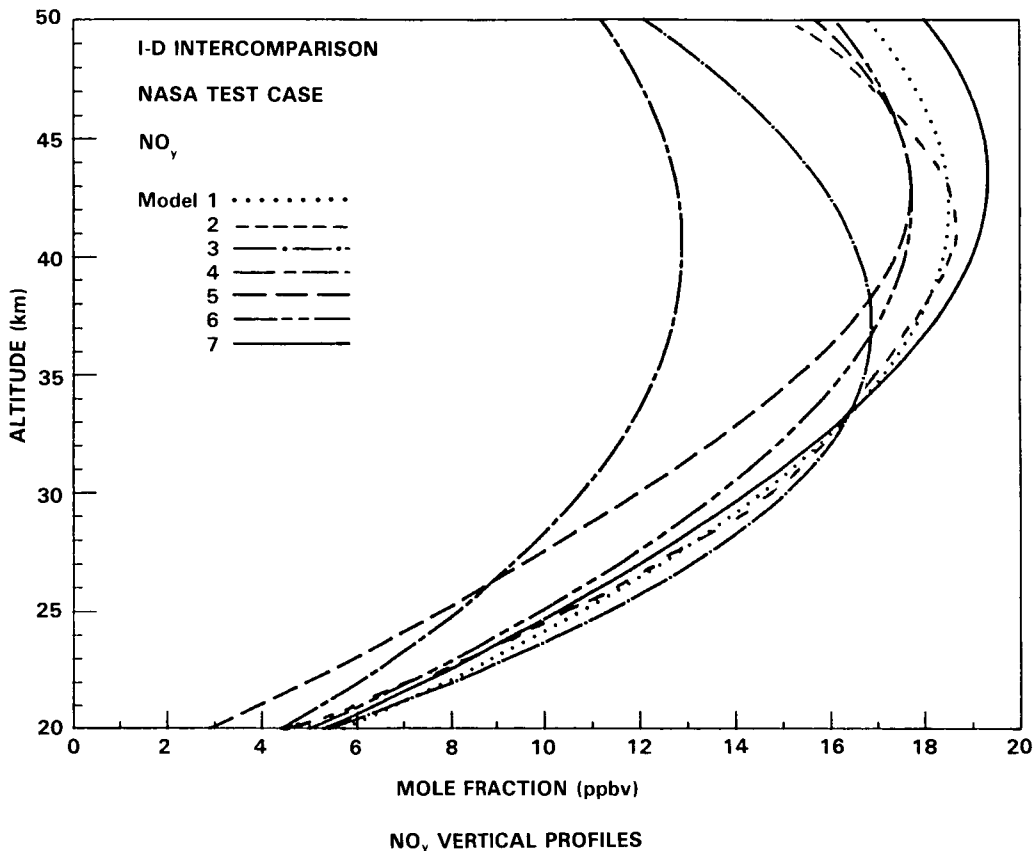


Figure 12-7.  $\text{NO}_y$  as calculated by the 1-D models of Table 12-1.

## ASSESSMENT MODELS

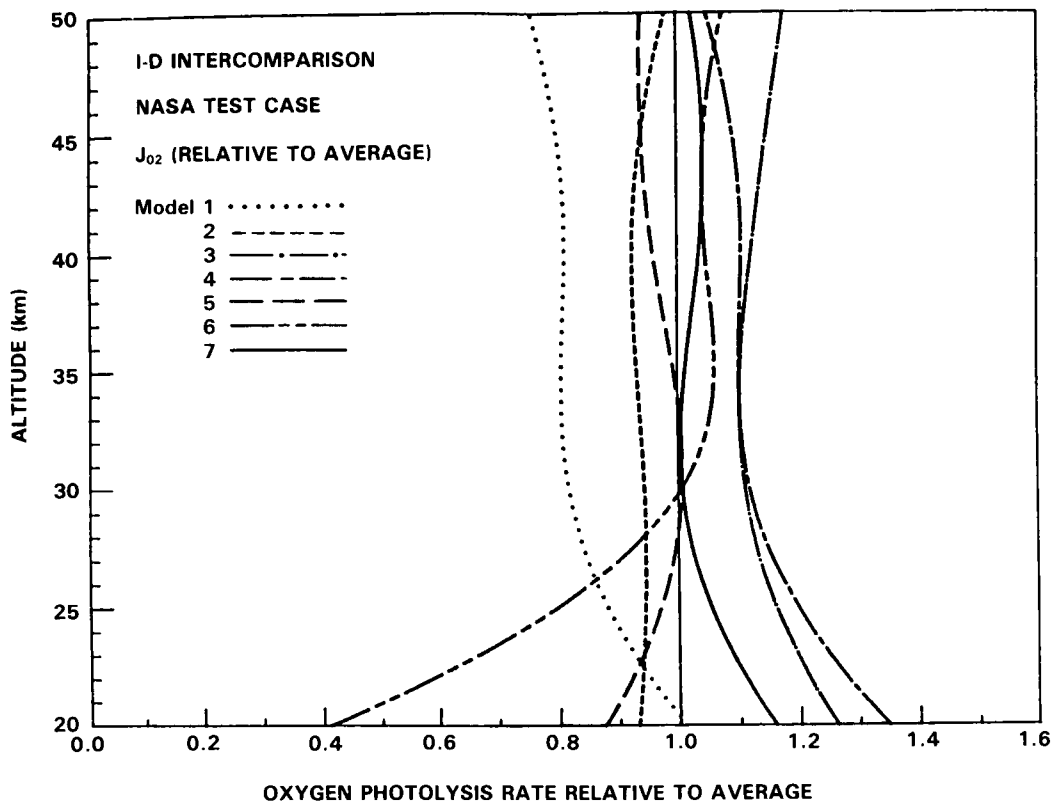


Figure 12-8.  $J_{O_2}$  for the 1-D models of Table 12-1 relative to the average of all model results.

Calculated photodissociation rates for  $O_2$ ,  $N_2O$ ,  $NO$  and  $O_3$  are shown in Figure 12-8 through 12-11 respectively, relative to the average of all model results. Note that the relative scale for each figure is different. The photodissociation rate of  $O_2$  differs by about twenty percent in the upper stratosphere, if the DuPont results are not included (the DuPont model calculates photodissociation rates based on a global integration of zenith angle rather than the  $30^\circ$  equinox used in all other models for the NASA test case). The much larger apparent differences in the photodissociation rates for  $N_2O$ , shown in Figure 12-9, suggest that discrepancies in  $O_2$  Schumann-Runge band absorption is primarily responsible for the model differences. The calculated photodissociation rates for  $N_2O$  differ by about 20% in the upper stratosphere increasing with decreasing altitude to 60% by 30 km. As shown in Figure 12-10, much larger differences are found for nitric oxide photodissociation rates, with a factor of about 2 difference at 50 km, increasing to almost a factor of 3 at 40 km. Much smaller differences of approximately 10-15% were found in the photodissociation rates for ozone in Figure 12-11.

The underlying causes of the variations in the  $NO_y$  are possibly indicated by examining the differences in photodissociation rates. For example, the low  $NO_y$  levels calculated in the Harvard model correspond to larger  $N_2O$  and  $NO$  photodissociation rates in the upper stratosphere than found in other models, and therefore less production and more destruction of total odd-nitrogen than calculated in other models.

The results described above suggest that the major differences between models for calculated  $NO_y$  are possibly related to the formulations used for the Schumann-Runge bands. All models basically use the formulation recommended in chapter 7, with the exception of the Harvard model, which employs opacity

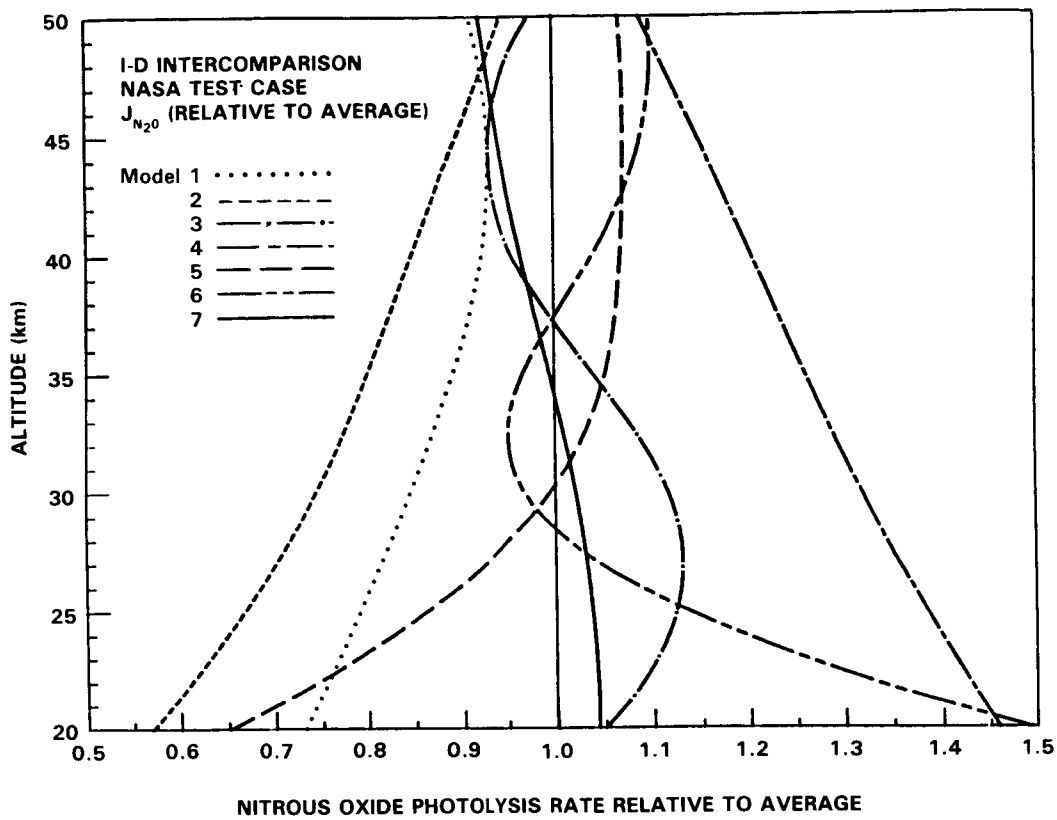


Figure 12-9. As Figure 12-8 for  $J_{N_2O}$ .

distributions as described in Logan *et al.* (1978), and the DuPont model, which used the formulation of Nicolet and Peetermans (1980).

Production of stratospheric ozone is dominated by photolysis of  $O_2$  in the Herzberg continuum (205-240nm). All models used similar cross-sections for the Herzberg continuum, resulting in similar photolysis rates for  $O_2$  in the stratosphere. Penetration of sunlight in the region of the S-R bands (180-205nm) is responsible for the primary losses of  $N_2O$  and  $NO$ . The  $N_2O$  cross-section increases more than a factor of 10 from 205nm to 185nm, emphasizing differences in the treatment of radiative transfer for S-R bands (1,0) through (10,0). Similarly, photolysis of  $NO$  occurs in the  $\delta(0,0)$  and  $\delta(1,0)$  bands which overlie the S-R(5,0) and (10,0) bands of  $O_2$ , respectively. Stratospheric photolysis is dominated by the  $\delta(0,0)$  band, which when excited may either predissociate, radiate or be kinetically quenched (see Nicolet and Cieslik 1980). The Harvard formulation (Logan *et al.*, 1978, updated with new continuum values from 192nm to 240nm from Cheung *et al.*, 1984b) allows for deeper penetration of ultraviolet in the S-R bands than that of Frederick *et al.* (1981).

These results point to two fundamental uncertainties in the treatment of ultraviolet radiation in stratospheric models. First, there is considerable diversity in calculated photolysis rates even among models which are purportedly using the same treatment of radiative transfer. Second, there are different formulations currently in the literature for ultraviolet transmission in the Schumann-Runge bands. Both of these differences have significant effects on model calculations for odd-nitrogen. The first discrepancy may be resolved simply by comparing results for a few restricted cases with more accurate solutions of radiative

## ASSESSMENT MODELS

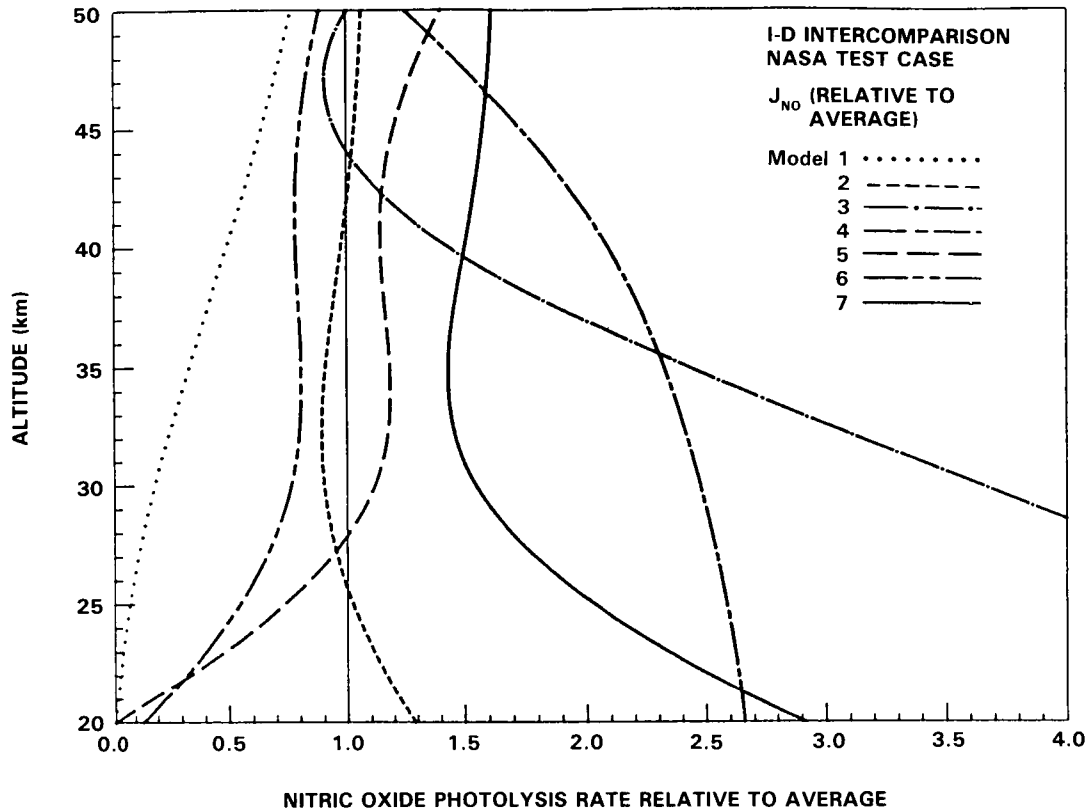


Figure 12-10. As Figure 12-8 for JNO.

transfer. The second problem requires validation of the S-R band models with both laboratory (Yoshino *et al.* 1983) and *in situ* stratospheric data (Herman and Mentall, 1982a, Frederick and Mentall, 1982, Anderson and Hall 1983). Improved models will need both further laboratory data for  $O_2$  at lower temperatures and observations of stratospheric transmission of sunlight with a resolution of approximately 0.1nm in the S-R bands.

Assessing perturbations to the stratosphere requires an ability to simulate the response of ozone to changes in odd-nitrogen or nitrous oxide. Discrepancies among theoretical treatments of the Schumann-Runge bands of  $O_2$  have lead to differing amounts of  $NO_y$  and thence to varying changes in total ozone for a given increase in chlorine. Validation of radiative schemes - in the ultraviolet where the greatest differences occur - is essential for both 1-D and 2-D photochemical models.

### 12.4 TWO-DIMENSIONAL MODELS — SOME THEORETICAL IDEAS

While 1-D models have been the principal tool for assessment studies of the effects of stratospheric pollutants, in recent years a number of two-dimensional models with detailed descriptions of radiation, dynamics and photochemistry has been developed. Some of these models have been used for assessment purposes (e.g. Vupputuri 1978/79; Pyle 1980; Haigh and Pyle 1982; Steed *et al.*, 1982, Brasseur and Bertin 1978/79) and they are expected to play an increasingly important role in the next few years.

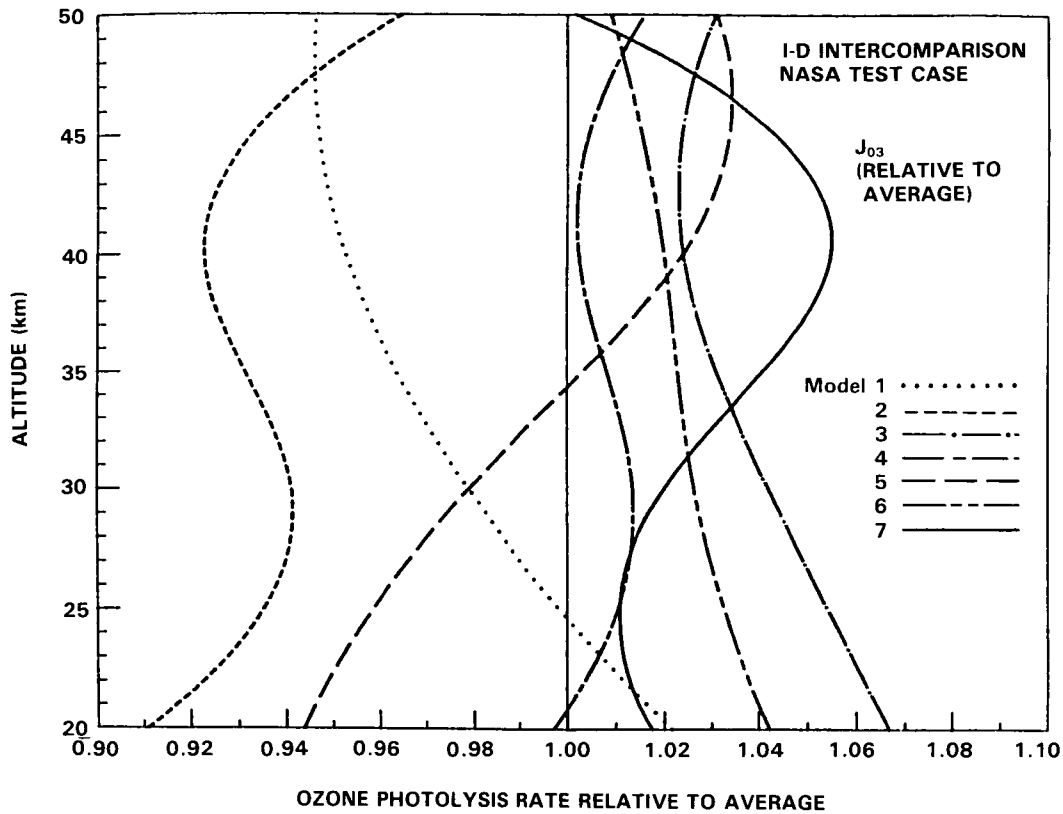


Figure 12-11. As Figure 12-8. for  $J_{O_3}$ .

The two-dimensional approach has a number of advantages compared with that using one-dimensional models. The total ozone record is a convincing demonstration of the vital role of meridional motions in the stratosphere. Two-dimensional models can include this transport; one-dimensional models cannot. Recent developments using satellites, balloons, aircraft and ground based measurements have significantly increased the geographical coverage of data; a two-dimensional approach (at least) is an advantage in interpreting this data. Two-dimensional models also have the considerable benefit for assessment purposes that they can include a number of the important feedbacks between dynamics, radiation and photochemistry.

While the advantages of the two-dimensional approach are clear, how best to construct a two-dimensional model of the three dimensional atmosphere has been a vexed question for some time. Taking  $y$  and  $z$  as meridional and vertical coordinates, the zonal mean continuity equation for tracer of mixing ratio  $\chi$  can be written

$$\frac{\partial}{\partial t} \bar{\chi} + \bar{v} \frac{\partial}{\partial y} \bar{\chi} + \bar{w} \frac{\partial}{\partial z} \bar{\chi} = -\frac{1}{\cos\phi} \frac{\partial}{\partial y} (\overline{v'\chi'} \cos\phi) - \frac{1}{\rho} \frac{\partial}{\partial z} (\rho \overline{w'\chi'}) + \bar{S} \quad (12.1)$$

where  $v$ ,  $w$  are meridional and vertical velocity components,  $\partial y = a d\phi$ ,  $a$  is the Earth's radius,  $\phi$  is latitude,  $\rho$  is density and  $S$  is the net source of  $\chi$ .  $(\bar{\quad})$  represents a zonal average,  $(\bar{\quad}) = 1/2\pi \int_0^{2\pi} (\quad) d\lambda$ , and  $(\quad)'$  a departure therefrom,  $(\quad) = (\bar{\quad}) + (\quad)'$ . The transport terms on the left hand side of 12.1 represent advection by a zonal mean circulation. The transport terms on the right hand side contain departures from

## ASSESSMENT MODELS

the zonal mean (eddy) for which in a two-dimensional framework there is no *a priori* description. A central problem in two-dimensional modelling is the treatment and the proper interpretation of the eddy terms.

Much debate has centred on the relative roles of mean meridional motions and eddy motions in transporting heat, momentum and tracer mixing ratios. In his classic paper, Brewer (1949) explained the dryness of the stratosphere in terms of a mean meridional circulation with rising motion at the equator, poleward flow in the stratosphere with sinking motion at higher latitudes. As discussed by Dobson (1956), such a circulation, hereafter referred to as the Brewer-Dobson circulation, also appeared to be required to explain the observations of ozone.

Murgatroyd and Singleton (1961) calculated the meridional circulation of the middle atmosphere driven by radiative sources and sinks. The circulation is similar to the Brewer-Dobson circulation in the lower stratosphere and has a single cell from summer pole to winter pole in the upper stratosphere and mesosphere. Murgatroyd and Singleton concluded that their circulation was supported by the observed zonal mean tracer distributions, although they stressed the limitations of their calculations which followed the neglect of eddy processes. Thus these authors concluded that tracer transport is controlled mainly by a mean meridional circulation.

The alternative view was taken by Godson (1960). He studied the distribution of ozone in polar latitudes, noting that ozone is carried polewards in episodes which he associated with baroclinic eddies. Newell (1963a) also argued that eddy motions produced dominant transport in the lower stratosphere. Similarly, the observations of the spread of Tungsten-185 from nuclear bomb tests could best be explained in terms of diffusive mixing rather than a mean meridional transport (Feely and Spar 1960).

Subsequent theoretical studies, both analytical and modelling, have shown that the debate about the principal transport process, whether it be a mean circulation or the eddies, was based on false premises. In the conventional Eulerian formalism, the mean meridional circulation and eddy transports are not in fact independent but are intimately related to one another. For example, the close cancellation of mean and eddy transport has been demonstrated in many three-dimensional modelling studies (see e.g. Hunt and Manabe 1968). Theoretically, this result is expected and is summarized in various "non-acceleration" or "non-transport" theorems (see e.g. Andrews and McIntyre 1976) which state that in the absence of transience or damping of a small amplitude wave, the wave exerts no effects on the zonal mean state. A circulation is driven by the wave which exactly cancels the effect of the wave on the zonal mean.

There have been a number of excellent reviews of these ideas (see e.g. Murgatroyd 1982, Mahlman *et al.*, 1984) which it is not necessary to repeat. Instead, we will sketch here the impact of theoretical and observational studies on attempts to build two-dimensional tracer transport models, starting with the early work of Prabhakara (1963) and tracing developments to the present day. It is clear from Equation (12.1) that the definition of advective and eddy transport is not unique. Given the same three-dimensional circulations, different sets of mean circulation and eddy fluxes can be obtained depending on the averaging processes and coordinates adopted. It will be seen that different approaches to describing both the mean motions and the eddies are possible and that the state of the art is dynamic and not static. The different approaches currently in use will be discussed in Section 12.6. No one approach will be pronounced correct (indeed the diversity of approaches is important). Some approaches have particular advantages and these will be stressed. The chosen approach needs a firm physical base and analysis of model results must be carried out with due consideration of the limitations of the model.

The first two-dimensional numerical model for tracer transport was developed by Prabhakara (1963), who attempted to combine mean meridional motions with the diffusion model suggested by the observa-

tions of radioactive fallout (Feely and Spar 1960). Prabhakara used the Murgatroyd and Singleton mean circulation, which was scaled to be only 20 per cent of the original value in a pragmatic attempt to model the ozone distribution. Eddy transport was modelled by Fickian diffusion with the zonal mean horizontal and vertical fluxes of the mixing ratio of  $\chi$  given by

$$\overline{v'\chi'} = -K_y \frac{\partial \bar{\chi}}{\partial y} ; \quad \overline{w'\chi'} = -K_z \frac{\partial \bar{\chi}}{\partial z} \quad (12.2)$$

where  $K_y$ ,  $K_z$  are horizontal and vertical diffusion coefficients. With some adjustments to the estimated  $K_y$  and  $K_z$  (the estimates based on the distribution of radioactive tracers) Prabhakara was able to obtain realistic latitudinal and temporal variations in total ozone. As will become evident, Prabhakara's work is of particular interest in view of the recent developments in two-dimensional modelling.

Subsequent work lead to criticism of Prabhakara's model on two counts. Firstly, the circulation obtained by Murgatroyd and Singleton did not correspond to the circulation deduced from Eulerian eddy statistics, particularly in the winter lower stratosphere where such statistics imply an indirect cell with rising motion at the pole and sinking in middle latitudes (see, e.g. Vincent 1968). Of course, as we see below, there is no *a priori* reason to expect the transport circulation to be identical to the mean meridional circulation in pressure coordinates. Secondly, observed horizontal eddy fluxes in the lower stratosphere were found to be counter-gradient (Newell 1964). Simple Fickian diffusion will only model downgradient fluxes.

The next advance was a treatment of eddy transport by Reed and German (1965) in which counter-gradient fluxes were permitted. They described the fluxes of a quasi-conservation tracer  $\chi$  using a tensor of diffusion coefficients such that

$$\begin{pmatrix} \overline{v'\chi'} \\ \overline{w'\chi'} \end{pmatrix} = - \begin{pmatrix} K_{yy} & K_{yz} \\ K_{zy} & K_{zz} \end{pmatrix} \begin{pmatrix} \frac{d\bar{\chi}}{dy} \\ \frac{d\bar{\chi}}{dz} \end{pmatrix} \quad (12.3)$$

Expressions for the  $K$ s were based on a mixing length hypothesis, with parcel trajectories assumed to be straight lines at some known angle to the mean isentropes. These assumptions lead to the result  $K_{yz} = K_{zy}$ , which produces a symmetric tensor and a diffusive flux. If the slope of the mixing surface (the parcel trajectory) is greater than the slope of the isentropes (and  $K_{yz}$ ,  $K_{zy}$  depend on these mean quantities) then the horizontal component of the flux calculated from Equation 12.3 will be countergradient.

Reed and German's work paved the way for a number of numerical models which included both the mean circulation and eddy transports (Rao 1973, Harwood and Pyle 1975). The mean circulation can be calculated using the momentum and thermodynamic equations:

$$\frac{\partial \bar{u}}{\partial t} + \bar{v} \frac{\partial \bar{u}}{\partial y} + \bar{w} \frac{\partial \bar{u}}{\partial z} - f\bar{v} = -\frac{1}{\cos^2 \phi} \frac{\partial}{\partial y} (\overline{u'v'} \cos^2 \phi) - \frac{1}{\rho} \frac{\partial}{\partial z} (\rho \overline{u'w'}) \quad (12.4)$$

$$\frac{\partial \bar{\theta}}{\partial t} + \bar{v} \frac{\partial \bar{\theta}}{\partial y} + \bar{w} \frac{\partial \bar{\theta}}{\partial z} = -\frac{1}{\cos \phi} \frac{\partial}{\partial y} (\overline{v'\theta'} \cos \phi) - \frac{1}{\rho} \frac{\partial}{\partial z} (\rho \overline{w'\theta'}) + \bar{Q} \quad (12.5)$$

## ASSESSMENT MODELS

where  $\bar{u}$  is the mean zonal wind,  $\bar{\theta}$  is potential temperature,  $f$  is the Coriolis parameter, and  $\bar{Q}$  is the net diabatic heating rate.

Both equations contain eddy flux terms. The eddy heat fluxes can be written in terms of the K-tensor. If the eddy momentum flux is known, then solution for the mean circulation is straightforward. However, angular momentum is not a rationally conserved quantity and Reed and German's approach cannot be used. Rao (1973) described the momentum fluxes in terms of the vertical wind shear. Harwood and Pyle (1975) chose instead to specify the horizontal eddy momentum fluxes using values derived from satellite data. These models, which will here be called classical Eulerian models, succeeded in producing realistic fields of stratospheric winds, temperatures and constituent mixing ratios. They still play a role in assessment studies.

Although some features of these models are satisfactory, the treatment of the eddies is open to criticism. Mahlman (1975) used results from a GCM to study the flux gradient relationship and found that the flux was not always diffusive in character. Other studies criticised the approximations made by Reed and German (1965): their assumptions regarding the conservative nature of the tracer, the particle trajectory (a straight line) and the mean mixing surface slope and its variance were all considered dubious (e.g. Matsuno 1980, Danielsen 1981). It is these approximations which determine the nature of the K tensor and the ensuing transport.

More generally, specification of a fixed K-tensor, particularly for assessment purposes, is unsatisfactory for several reasons. If the mean meridional circulation and the K tensor are specified independently, there is no guarantee that the sum of mean advection and eddy fluxes will give the correct net transport. Further, the specification of fixed Ks inhibits dynamical feedback whereby the eddies depend on the background zonal wind field which is related, via solar heating, to the temperature and ozone fields. Finally, the treatment of the eddy momentum fluxes can also be criticised. The physical basis for a K-theory approach for momentum is especially poor. On the other hand, if the fluxes are specified from observations, these values may not be consistent with the eddy fluxes of heat and tracers which are determined using the K-tensors.

The interest during the 1970s in possible perturbations to the ozone layer prompted analytical studies of transport in the middle atmosphere and, in particular, a reappraisal of simple models of the atmosphere and their treatments of eddy processes. These studies produced two significant advances. Firstly, the relationship between the mean meridional circulation and the eddies was clarified. The two are mutually dependent. As we have seen, under certain restricted circumstances (steady waves with no damping — and see the remarks at the end of Section 6.3.3), the wave produces no net effect on the zonal mean atmosphere.

Secondly, explicit solutions of the eddy perturbation equations using linear wave theory led to a complete reassessment of Reed and German's work. To summarise, (and see Plumb 1979, Matsuno 1980, Holton 1980, Danielsen 1981, Pyle and Rogers 1980b, etc.) although a tensor approach is possible, it was found that because many of Reed and German's approximations were invalid, the form of the tensor became quite different from that originally proposed.

These results led to various new approaches in two-dimensional modelling. Ideally, Andrews and McIntyre's work pointed to the desirability of using a Lagrangian procedure for defining eddy and mean transport. In such a system, averages are taken following the trajectories of air parcels, rather than around some fixed latitude circle. Thus the mean circulation in this system is the mass transport circulation. However, experience tracing air parcels in a GCM indicates that in practice such an approach is impractical. Hsu (1980), for example, showed how material tubes can become hopelessly entangled, since on the time scale

of a few tens of days dispersion and diffusion cannot be ignored. Some of the practical problems of the Lagrangian system have been discussed by McIntyre (1980a) who suggested that the phenomena demonstrated by Hsu, which violate the premises of the non-acceleration, non-transport theorems, should be thought of as planetary wave 'braking.' (See Section 6.3.4)

Nevertheless, in the spirit of the work of Andrews and McIntyre, Dunkerton (1978) proposed a mass transport circulation based on a reformulated thermodynamic equation. Adopting the definition of Andrews and McIntyre (1976), a residual circulation is defined as

$$\bar{v}^R = \bar{v} - \frac{1}{\rho} \frac{\partial}{\partial z} \left( \rho \frac{\overline{v'\theta'}}{\bar{\theta}_z} \right) \quad (12.6)$$

$$\bar{w}^R = \bar{w} + \frac{1}{\cos\phi} \frac{\partial}{\partial y} \left( \frac{\overline{v'\theta'} \cos\phi}{\bar{\theta}_z} \right) \quad (12.7)$$

then the thermodynamic and continuity equations become, after some approximation,

$$\bar{w}^R \frac{\partial \bar{\theta}}{\partial z} = \bar{Q} \quad (12.8)$$

$$\frac{1}{\cos\phi} \frac{\partial}{\partial y} (\bar{v}^R \cos\phi) + \frac{1}{\rho} \frac{\partial}{\partial z} (\rho \bar{w}^R) = 0 \quad (12.9)$$

Equation 12.8 contains no eddy terms following the transformation in Equations 12.6-12.7. Thus the residual circulation depends just on the diabatic heating and the lapse rate and is similar to the diabatic circulation. Dunkerton then identified this circulation with a Lagrangian mean circulation of air parcels in the stratosphere provided that the waves are approximately steady and conservative. This would be the net circulation for tracer transport and is similar to the circulation proposed by Brewer (1949) and Dobson (1956). Although Dunkerton ignored diffusion, his work represented a significant conceptual improvement in the understanding of the net transport stream function.

Next, the tracer equation, in the absence of diffusion or transience and ignoring the effect of the photochemical lifetime on eddy transport, becomes

$$\frac{\partial \bar{\chi}}{\partial t} + \bar{v}^R \frac{\partial \bar{\chi}}{\partial y} + \bar{w}^R \frac{\partial \bar{\chi}}{\partial z} = \bar{S} \quad (12.10)$$

The approximations of no chemistry (except in the zonal mean source,  $\bar{S}$ ), transience, dissipation or dispersion lead to a particularly simple tracer continuity equation.

Following Dunkerton's work there have been a number of 2-D model studies which have used the diabatic circulation, or alternatively the residual circulation, as the transport circulation. (In this chapter the term 'transport circulation' is used somewhat loosely. For definitions of different circulations and their relationships see Table 6.1). The studies include Pyle and Rogers (1980a), Holton (1981), Garcia and Solomon

## ASSESSMENT MODELS

(1983), Guthrie *et al.*, (1984) Ko *et al.*, (1985). For example, Holton (1981), including some of the terms dropped by Dunkerton (1978), obtained the following thermodynamic equation.

$$\frac{\partial \bar{\theta}}{\partial t} + \bar{v}^R \frac{\partial \bar{\theta}}{\partial y} + \bar{w}^R \frac{\partial \bar{\theta}}{\partial z} = \bar{Q} - \frac{1}{\rho} \frac{\partial}{\partial z} \left\{ \rho \frac{\overline{v'\theta'} \cdot \nabla \bar{\theta}}{\bar{\theta}_z} \right\} \quad (12.11)$$

For steady and conservative waves the flux  $\overline{v'\theta'}$  is parallel to the  $\theta$  surface and the eddy forcing vanishes (Andrews and McIntyre 1976, Clark and Rogers 1978, Plumb 1979). Thus in this case, too, the transport circulation is driven by the diabatic heating. A more complete residual circulation (e.g. Garcia and Solomon 1983) would include the eddy term in both the thermodynamic and momentum equations.

Finally, the work of Tung (1982) should be mentioned, as it offers some conceptual advantages for tracer modelling. The isentropic coordinate system used by Tung adopts the potential temperature as the vertical coordinate. The vertical velocity is proportional to the diabatic heating. The zonal mean circulation in isentropic coordinates is a close approximation to the diabatic circulation and the definition of a residual circulation is not required. (Notice that the zonal mean circulations in isobaric and isentropic coordinates are not identical).

It is clear that to neglect of eddies from Equation 12.11 is an oversimplification. In the absence of any friction, the circulation would be strongly zonal with extremely weak meridional flows (see, e.g. Mahman *et al.*, 1984). It is precisely the irreversible effects of chemistry, transience, dissipation and dispersion which give rise to a transport circulation and thus these processes must somehow be included. It cannot be argued that these are small terms which can be ignored since those same arguments would imply that the transport circulation itself is negligible. After the cancellation of the large standing wave components and the induced mean circulation it is these very terms which become important in driving the mean circulation and possibly in leading to enhanced mixing. A fully self-consistent interactive two-dimensional model is not possible without an adequate description of these processes, at present not available. This relationship between the eddies and the induced circulation and the subsequent formulation of the eddy treatment has been discussed by a number of authors (Plumb 1979, Matsuno 1980, Pyle and Rogers 1980b, Danielson 1981, Tung 1982). An important result, where relevance to Equation 12.11 was pointed out by Andrews and McIntyre (1976), is that

$$\overline{v'\chi'} \cdot \nabla \bar{\chi} = \overline{\chi'S'} - \frac{1}{2} \frac{\partial}{\partial t} \overline{\chi'^2} \quad (12.12)$$

Thus the eddy flux of  $\chi$  is directed along the surfaces of constant mixing ratios (and not across them) if  $\chi$  is exactly conserved or the waves are steady and frictionless. In this case it is clear that the fluxes are not diffusive in character. On the other hand, photochemistry or a growing or decaying wave can produce cross-gradient flux components.

Solving the eddy perturbation equation with the linear wave approximation and expressing the fluxes in K-tensor form it is found that the Ks can be separated into symmetric and antisymmetric components (Plumb 1979, Matsuno 1980).

$$\underline{\underline{K}} = \underline{\underline{K}}_s + \underline{\underline{K}}_a$$

(Notice that this shows the approximation  $K_{yz} = K_{zy}$ , used by Reed and German (1965), is not generally valid (i.e. when  $\underline{\underline{K}}_a$  is significant compared with  $\underline{\underline{K}}_s$ )).

These K tensors depend on Lagrangian eddy statistics and the dissipation or photochemical relaxation rates. The eddy flux arising from the antisymmetric component is advective in character and can thus be conveniently combined with the mean circulation to give an effective transport circulation. This eddy-induced advection opposes the mean circulation (Dunkerton 1978, Plumb 1979). Plumb and Mahlman (1985) point out that the transport circulation is related to the Lagrangian circulation, the diabatic circulation and the residual circulation but is not identical to any (see Table 6.1). The difference between the circulations is related to the breakdown of non-acceleration conditions. Nevertheless, GCM results (Plumb and Mahlman, 1985) show that in the stratosphere the transport, diabatic and residual circulations are very similar and, in practice, many modellers have implicitly assumed them to be equal.

The symmetric, diffusive components can be further separated. A part simply depends on the time dependence of Lagrangian eddy statistics (the parcel displacements) which are difficult to determine in practice. (Note, however, that Lagrangian eddy statistics can easily be determined within linear wave theory - see Chapter 6 for a more complete discussion). This part represents dispersion. Secondly, an additional part depends also on the photochemical relaxation rates. Matsuno (1980) argued that this part would be small but Pyle and Rogers (1980b, 1984) have shown that it can play a non-negligible role.

A number of methods of deriving the Ks arising from the transient eddies have been discussed. Luther (1973) used Reed and German's approach to derive Ks from heat flux data. His values have been much used in classical Eulerian models. Typical values for  $K_{yy}$  are found to be a few  $\times 10^6 \text{m}^2 \text{s}^{-1}$  and for  $K_{zz}$ ,  $0.1\text{-}1 \text{m}^2 \text{s}^{-1}$ .

Kida (1983a, b) has derived a global average  $K_{yy}$  from the tracer dispersion in a simple GCM and obtains a  $K_{yy} \sim 3 \times 10^5 \text{m}^2 \text{s}^{-1}$  and  $K_{zz} \sim 10^{-1} \text{m}^2 \text{s}^{-1}$ , considerably smaller than Luther's values. Tung (1982) argued that the eddy motions are predominantly directed along the isentropes in the atmosphere. This implies that the effects from  $K_{yz}$  and  $K_{zz}$  are considerably smaller than that from  $K_{yy}$  in isentropic coordinates. Tung (1984) has studied observed atmospheric Eulerian statistics and argues for a  $K_{yy}$  value  $\sim 4 \times 10^5 \text{m}^2 \text{s}^{-1}$  in the stratosphere, although this number could be an order of magnitude greater in disturbed conditions. In subsequent model studies, Ko *et al.*, (1985) found that the calculated distributions of  $\text{HNO}_3$  are quite sensitive to the  $K_{yy}$  and that the observed  $\text{HNO}_3$  distribution can best be simulated using  $K_{yy} \sim 3 \times 10^5 \text{m}^2 \text{s}^{-1}$ .

Newman, Schoeberl and Plumb (1985b) have investigated the possibility of deriving  $K_{yy}$  from the observed fluxes of potential vorticity. Since  $q$  is conserved on pressure surfaces they argue that  $K_{zz}$  is unimportant for potential vorticity and derive  $K_{yy}$  from  $\overline{v'q'} = -K_{yy} \partial \bar{q} / \partial y$ . Using stratospheric data they find a maximum  $K_{yy} \sim 4 \times 10^6 \text{m}^2 \text{s}^{-1}$  at  $\sim 1 \text{mb}$  with a value of  $\sim 5 \times 10^5 \text{m}^2 \text{s}^{-1}$  typical of the middle stratosphere. They also find some regions of negative  $K_{yy}$  in high latitudes when the vortex is displaced from the pole. Clearly, simple two-dimensional ideas of transport must be used with caution in high latitudes.

Yet another approach has been taken by Plumb and Mahlman (1985). They have used the flux of pairs of tracers from a GCM to derive latitudinally dependent Ks (and the transport circulation). They find  $K_{yy}$  in the stratosphere to be generally  $\sim$  a few  $\times 10^5 \text{m}^2 \text{s}^{-1}$  but with significant regions (the 'surf zones' of McIntyre and Palmer (1983)) where  $K_{yy} \sim 4 \times 10^6 \text{m}^2 \text{s}^{-1}$ .  $K_{zz}$  is important in the troposphere but much smaller in the stratosphere when it arises from small scale, but resolved motions. A pragmatic conclusion of their work is that although the wave amplitudes can become very large, theories based on small amplitude disturbances seem to work reasonably well, if used as above to motivate the formulatic of the K tensor.

The part of the K tensor that depends on photochemical relaxation (leading to the so-called chemical eddies) has been determined by Pyle and Rogers (1980b), among others. They showed how this component

## ASSESSMENT MODELS

of the tensor could be related to chemical lifetimes and eddy statistics. Expanding small amplitude waves into Fourier components and assuming linearity they calculated Eulerian statistics by solution of the quasi-geostrophic potential vorticity equation (not a particularly convenient method for purely chemically-orientated problems). Pyle and Rogers calculate photochemical Kyy values in excess of  $10^6 \text{m}^2 \text{s}^{-1}$  for ozone in the mid stratosphere.

The limitations of the various derivations of the Ks must be remembered. Calculations based on satellite data use Eulerian statistics and necessarily only allow for the planetary scale since the smaller scales are not resolved. Calculations based on GCM results will be limited by the accuracy of the GCM itself. Most GCMs appear to have relatively weak eddies compared with the atmosphere (see Chapter 6).

In summary, the results discussed above on the residual circulation and the treatment of eddy transport have an important bearing on approaches to two-dimensional modelling. Firstly, various of Reed and German's approximations lead to an incorrect treatment of eddy fluxes. The parcel trajectories are, in fact, ellipses and not straight lines (Matsuno 1980) and the fluxes due to steady and conservative planetary waves are advective and not diffusive in character. A K-tensor treatment should therefore include an anti-symmetric component. That the Reed and German approach has in practice worked reasonably satisfactorily perhaps suggests that the fluxes modelled by the symmetric component, due to dispersion, photochemistry, etc., play a major role. Nevertheless the Reed and German derivation of the Ks cannot be justified in principle.

Secondly, the residual and diabatic circulations are only approximations to the transport circulation, but good approximations in the stratosphere. They are not as good an approximation in the troposphere and during disturbed situations such as stratospheric sudden warmings. These are situations where, in any case, any two-dimensional model treatment should not be expected to be satisfactory.

Thirdly, if the residual circulation approach is used, there must nevertheless still be some eddy transport to be treated, otherwise an inconsistency arises: without eddy forcing in the zonal momentum equation, we expect only a weak circulation.

Fourthly, the relative importance of advective and eddy processes in the transport of tracers can only be determined on a species by species basis. It is clear that the role of chemical eddies depends on the chemical reactivity of the individual species. The contribution from transient motions depends on both the K and local gradient of species concentrations. (See Chapter 6 for a detailed discussion of transience). Eddy transport could be particularly important for species that exhibit large gradients created by advection and/or chemical interactions.

Finally, the eddy transport is related to global Lagrangian statistics which to date have not been derived from observations. Approximate relationships to Eulerian statistics derived from linear wave theory have been used, but nevertheless a totally satisfactory determination of the Ks is difficult. In lieu of theoretical methods for determining the Ks, one could derive or validate the values of Ks by comparing the calculated tracer distributions with observed distributions. This will be discussed in the next section.

## 12.5 CURRENT MODELS

In parallel with the development in the formulation of transport processes in 2-D models, the chemical contents of 2-D models have also matured over the past decade. Most 2-D models now contain realis-

tic chemistry packages, comparable or identical to those in current 1-D models both in the number of species, reactions and diurnal treatment.

Current two-dimensional models can usefully be categorised in at least two ways. Firstly, they can be separated, according to their dynamical treatment of the mean circulation and the eddies, into so-called classical Eulerian models or models which employ a residual (or similar) circulation. The traditional models thus have a mean circulation with, for example, an indirect circulation in middle and high latitudes of the winter hemisphere. They use a similar approach to Reed and German for the description of the eddy transport. On the other hand the diabatic/residual circulation models explicitly recognize the cancellation between eddies and the mean motions and generally use somewhat smaller K values.

Secondly, the models can be classified by the degree to which the model is interactive. The role played by non-conservative eddy processes in driving the atmosphere away from equilibrium must not be forgotten (see Sections 12.4, 12.8 and Chapter 6); until these processes can be modelled adequately two-dimensional models cannot be fully interactive and will be driven by the *specified* eddy forcing. Nevertheless, even a limited degree of feedback within the models can be extremely useful in assisting understanding. For example, the ultraviolet heating in the upper stratosphere is dependent on the ozone concentration, which is temperature dependent. A change in ozone will change the heating rate and probably the temperature, thus altering the ozone concentration. These are potentially important feedbacks for inclusion in any assessment of ozone perturbation. For example, experiments with and without this feedback using a 2-D model showed significantly different results for the calculated ozone depletion by fluorocarbons (STRAC, 1979, pp 167-175).

The importance of an interactive model is also seen in results discussed by Harwood and Pyle (1980). They showed that the ozone column amounts in their model were extremely sensitive to the radiative heating rate in the lower stratosphere, a difficult region in which to make accurate radiation calculations. Moving from a model which assumed radiative equilibrium in the lower stratosphere to one which employed fixed, calculated heating rates there (both reasonable approximations) changed the ozone column by up to 70 D.U. The reason for such large sensitivity lies in the heating rates in both experiments being fixed. In this region of the stratosphere the model meridional circulation, and hence the temperature and tracer distributions, will be largely dominated by the diabatic forcing (which should depend on the nonconservative eddy processes). Radiative feedback in which changed temperatures alter the heating rates could also be expected to change the ozone distributions and reduce the sensitivity. Ignoring the radiative feedback (albeit for the understandable reason that the radiative calculation is very difficult) probably leads to an erroneous conclusion (and this cautions against overinterpretation of a 2-D feedback). In this case it seems likely that a Newtonian cooling scheme, necessarily of low accuracy but including the feedback capability, would be advantageous.

Other dynamical feedbacks are also important. For example the propagation of waves depends on the background zonal wind field. Thus planetary wave transport in the stratosphere and gravity wave mixing in the mesosphere should depend on the background fields, which themselves will be related to the momentum transport by the waves.

While the feedback processes are not always necessarily important for assessment studies, inclusion in simple two-dimensional models is nevertheless an extremely useful method of examining the important processes which govern the fields of temperature and trace gases in the middle atmosphere. The problems of interactive modelling are discussed in detail in Chapter 6 (see also Section 12.8).

## ASSESSMENT MODELS

Table 12.2 summarizes some current two-dimensional models, categorising the approaches from the most simple, with specified circulations, to more complex models including many of the important feedback processes. In the remaining part of this section some of these models will be discussed in more detail with an emphasis on the more important results.

Table 12-2

### Classical Eulerian Models

Specified mean circulation, fixed Ks	Hidalgo & Crutzen	(1977)
	Brasseur	(1978/79)
	Ko <i>et al.</i>	(1984)
	Pyle	(1980)
	Whitten <i>et al.</i>	(1981)
Calculated mean circulation, fixed Ks	Rao Vupputuri	(1973)
	Harwood & Pyle	(1975)
	Haigh & Pyle	(1982)
	Haigh	(1984)

### Transformed and other alternative formulations

Diabatic Circulation	Examples	
Fixed heating rates, fixed Ks (often small)	Prabhakara	(1963)
	Pyle & Rogers	(1980)
	Guthrie <i>et al.</i>	(1984)
	Stordal <i>et al.</i>	(1985)
Fixed heating rates, Luther's Ks	Miller <i>et al.</i>	(1981)
	Cariolle & Brard	(1984)
Isentropic coordinate system, fixed heating rates	Ko <i>et al.</i>	(1985)
Computed heating rates + chemical eddies	Rogers & Pyle	(1984)
<b>Residual Circulation</b>		
Fields derived from a circulation model.	Holton	(1981)
Calculated fields.	Garcia & Solomon	(1983)
<b>Transport Circulation</b>		
Derived from GCMs	Plumb & Mahlman	(1985)
	Pitari and Visconti	(1985)

There have been a number of modelling studies employing the classical Eulerian approach with a specified mean circulation and a fixed K tensor. The circulation and temperature may be taken from various compilations (e.g. Newell *et al.* 1974, Louis 1974) or be precomputed. Luther's (1973) K tensor has been extensively used, although some workers have chosen to modify the Ks to produce a satisfactory fit to certain observations. This latter approach presupposes that any discrepancy between observation and theory is due to inadequately modelled eddy transport rather than, for example, a deficiency in the model photochemical scheme. While the Ks should by no means be regarded as fixed, unique quantities, treating them as adjustable parameters is equally unsatisfactory. This applies whether the approach is the classical Eulerian or uses a transformed mean circulation. These specified circulation models have been used to study stratospheric perturbations by high flying aircraft (Cunnold *et al.* 1977, Hidalgo and Crutzen 1977) and by fluorocarbons (Pyle 1980, Gidel *et al.* 1983).

Recently, using a specified circulation model with complete chemistry, Ko *et al.* (1984) have presented a very detailed analysis of the latitudinal and seasonal distribution of stratospheric trace gases and addressed the question of the role of transport and chemistry in determining trace gas distributions. Their model consistently underestimated the concentration of the upward diffusing species (e.g.  $N_2O$ ) in the tropical stratosphere while at the same time overestimating the abundance of the downward diffusing species in the lower stratosphere. This suggests that the transport parameterization in this classical Eulerian model may have underestimated the upwelling at the equatorial tropopause either because of too weak a circulation or too strong horizontal mixing. The authors identified  $N_2O_5$  as a major reservoir for NOy in the winter hemisphere at high latitudes and identified this sequestration by  $N_2O_5$  as responsible for the winter minimum in  $NO_2$  column produced in the model. However, the observed  $NO_2$  column abundances show much larger seasonal contrast.

The study described by Pyle (1980) produced the interesting result that the predicted depletion of ozone due to fluorocarbons showed significant latitudinal and seasonal variations with the largest depletions occurring in the winter polar latitudes. This argues for the need for multi-dimensional models in any assessment studies and, furthermore, suggests the importance of a monitoring programme with sufficient high latitude stations.

Two-dimensional classical Eulerian models in which the mean circulation is calculated have been described by Rao Vupputuri (1973) and Harwood and Pyle (1975). As discussed in the previous section, Harwood and Pyle circumvented the problem of modelling the horizontal eddy flux of momentum by using values derived from satellite data. This removes some degree of dynamic feedback with, in some regions, the mean circulation depending strongly on the prescribed momentum fluxes. The other terms which drive the circulation, the net diabatic heating and the eddy fluxes of heat, are however model dependent. This model does produce a hemispherically asymmetric total ozone distribution in good qualitative agreement with observations (see Figure 12-12, from Haigh (1984)), due to the circulation driven by the specified, asymmetric momentum fluxes.

In common with more sophisticated models, the temperature structure in the above model, while qualitatively satisfactory, has somewhat too cold a winter polar lower stratosphere and correspondingly too strong a polar night jet. For these calculations a detailed radiation code is used with the  $15\mu$   $CO_2$  band modelled using a Curtis matrix approach (Williams 1971). When the ozone, temperature and net heating rates are all calculated self consistently, the summer stratopause is found to be very close to radiative equilibrium, in agreement with the arguments of Dickinson (1975). Somewhat different results were obtained by Kuhn and London (1969) and Murgatroyd and Goody (1958) who presumably used ozone and temperature data which were not necessarily mutually compatible.

## ASSESSMENT MODELS

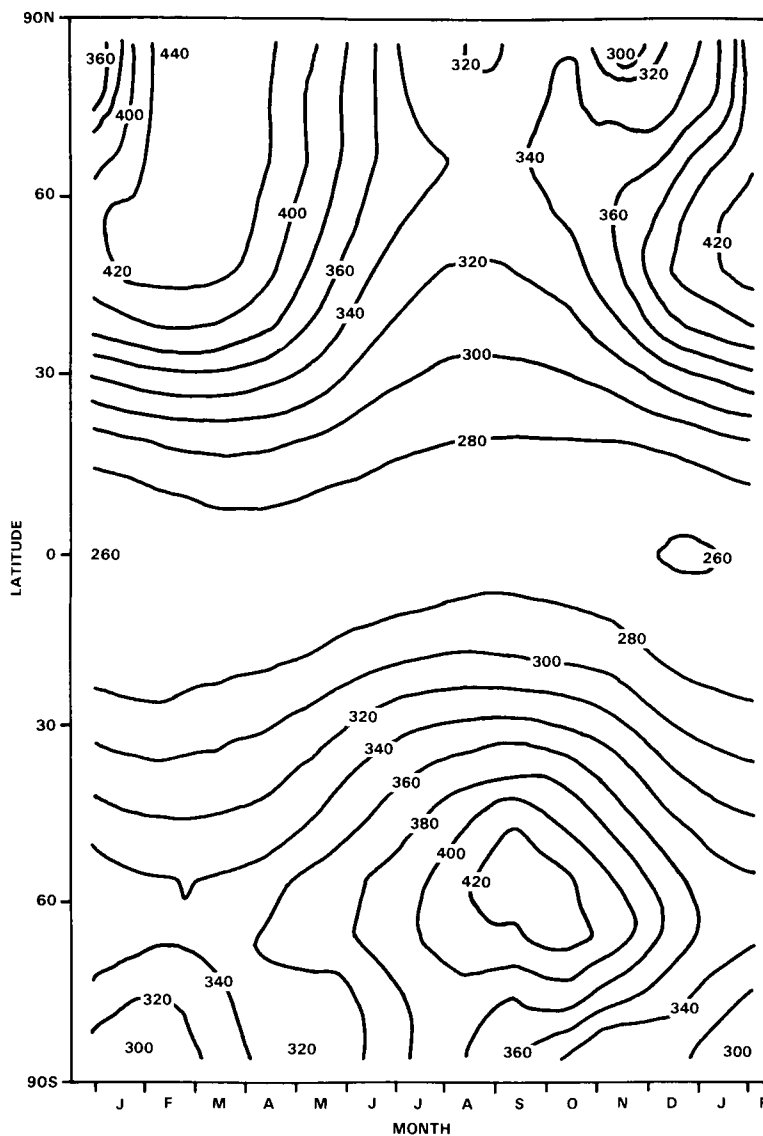


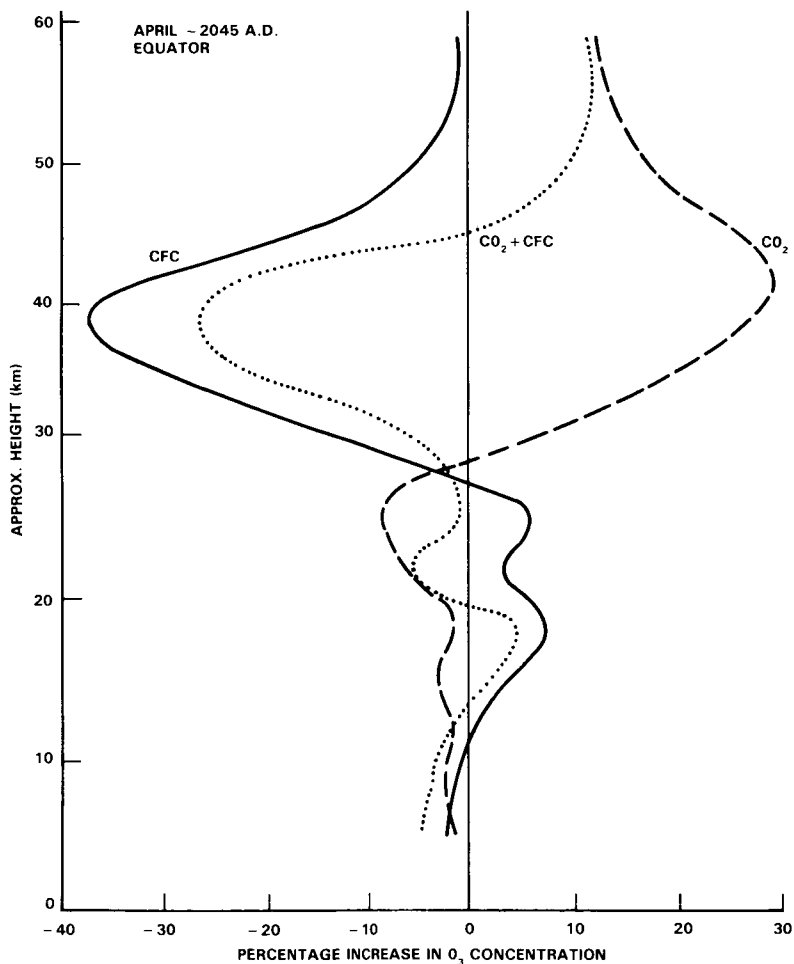
**Figure 12-12.** Latitude-time section of total ozone (matm-cm) from Haigh (1984).

These classical Eulerian circulation models also show a strong cancellation between eddy and mean motion transport. Some of this may be for the reasons discussed (nonacceleration, etc.), but given the diffusive nature of the model eddy transport, the cancellation perhaps is not unexpected. What is perhaps most surprising is that the modelling of satisfactory tracer distributions seems to suggest that the small residual between eddy and mean transport has also been modelled well (see, e.g. Harwood and Pyle 1977, Ko *et al.*, 1984). It could simply reflect a suitable choice of  $K_{yz}/K_{yy}$  to simulate successfully the observed slope of the mixing surfaces in the model.

Haigh and Pyle (1982) have used their model with calculated circulations to investigate stratospheric perturbations. Experiments were carried out to study the effect of emitted fluorocarbons and increasing levels of  $\text{CO}_2$ , singly and together, on stratospheric ozone. Without radiation feedback the  $\text{CO}_2$  experiment could not, of course, have been performed. Indeed, the result of the coupled perturbation empha-

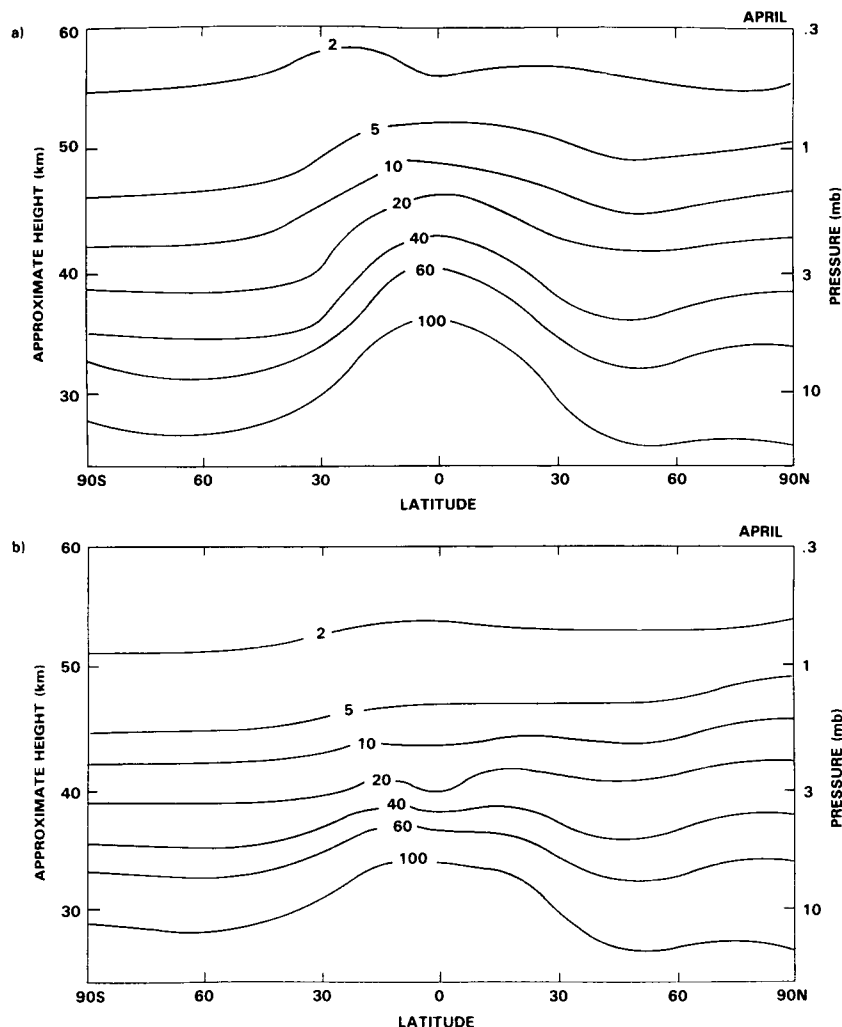
sized the importance of radiation feedback since the two perturbations were found not to be linearly additive. This was because of the different temperatures in the three runs acting differently on the temperature-dependent catalytic cycles. Figure 12-13 shows the ozone concentration change at the equator for these three calculations.

Figure 12-14 shows distributions of  $N_2O$  calculated with the above model (Gray and Pyle, 1985). Figure 12-14a shows a standard model calculation (similar to that described in Jones and Pyle 1984) in which the  $N_2O$  maximum is at the equator and little of the structure revealed by the SAMS experiment on Nimbus 7 (see Chapter 10) is seen. Figure 12-14b shows a model calculation in which the model is subjected to a prescribed equatorial momentum forcing, chosen so as to reproduce the equatorial semiannual oscillation of the zonal wind. The momentum forcing drives a circulation which modulates the net circulation and gives rise to features akin to the "double-peaks" described by Jones and Pyle (1984). Such a simple experiment, which suggests the importance of equatorial dynamics on some aspects of the tracer distributions, is only possible in a model in which the circulation can be calculated. Moreover, the validity of the experiment is not particularly compromised either by the crudeness of the momentum forcing or indeed by any other



**Figure 12-13.** Percentage change in ozone concentration calculated for the year 2045 due to (a) increased  $CO_2$  (b) increased fluorocarbons (c) the coupled perturbation, from Haigh and Pyle 1982.

## ASSESSMENT MODELS



**Figure 12-14.** Modelled  $N_2O$  for April from the 2-D model study of Gray and Pyle (1985); (a) is the basic model run (b) includes the semi-annual oscillation.

deficiencies in the model. Simple, physically-limited models can play an important role in increasing our understanding of stratospheric processes.

Turning to the transformed circulation models, the simplest of these use a fixed diabatic circulation. Prabhakara (1963) developed the first such model (although he, apparently, did not treat the circulation as being a 'residual' in any sense). He experimented with various  $K_y$  and  $K_z$  coefficients - the eddy transport was purely Fickian diffusion - and succeeded in obtaining a reasonable latitudinal distribution of total ozone.

A more detailed model using the residual mean circulation deduced from a spectral 3-D model (see Holton, 1981) was used to simulate the distribution of  $N_2O$ . Other models have used fixed diabatic heating rates to compute the diabatic/residual circulation. Miller *et al.* (1981), Guthrie *et al.* (1984) and Stordal *et al.* (1985), for instance, use Murgatroyd and Singleton's calculated heating rates above 25 km multiplied by 0.4. Although the use of the scaling factor could partially be justified by the argument that the summer stratosphere is probably much closer to equilibrium than suggested by Murgatroyd and Singleton, such

an arbitrary adjustment is somewhat unsatisfactory. These models, however, use different methods to obtain the heating rate below 25 kms. Miller *et al.* (1981) used simple extrapolation of the Murgatroyd and Singleton values. Their model was probably not very sensitive to the choice of circulation in the lower stratosphere because of the large eddy diffusion coefficient adopted. Guthrie *et al.* (1984) and Stordal *et al.* (1985) adopted the heating rate from Dopplick (1979). Another approach to specifying heating rates is that of Ko *et al.* (1985) who obtained a global fit of the data of Murgatroyd and Singleton and Dopplick by using a sum of hyperbolic functions and thus avoided any problem of mismatch at the boundary.

Although the use of residual/diabatic circulations has been adopted in model studies since about 1981, the choice of values for the eddy coefficients to be used in conjunction with the diabatic/residual circulation remains open. Miller *et al.* (1981) and Cariolle and Brard (1984) chose to use the coefficients from Luther (1973). In contrast, Holton (1981) and Tung (1982) argued that the eddy mixing may play a secondary role relative to advective transport and large values of Ks in residual circulation models appear to be in conflict with the theoretical estimates of Kida (1983) and Tung (1984) if the eddy term is to represent mixing from transient motions. However, the work of Pyle and Rogers (1980 a,b) indicated that the chemical eddy term could have Ks whose values may be comparable to those of Luther's.

The work of Guthrie *et al.* (1984) and Ko *et al.* (1985) helps clarify the role of eddy mixing in transport of trace gases. Guthrie *et al.* used values of  $K_{yy} \sim 2 \times 10^5 \text{ m}^2 \text{ s}^{-1}$  and  $K_{zz} \sim 0.2 \text{ m}^2 \text{ s}^{-1}$  to simulate the distribution of upward 'diffusing' trace gases such as  $\text{N}_2\text{O}$ , F-11, and F-12. By comparing their model results with models using large values of  $K_{zz}$ , they concluded that altitude profiles of upward 'diffusing' trace gases can be simulated better with smaller values of  $K_{zz}$  when used with the residual circulation. However, as noted by Ko *et al.* (1985), the distributions of upward 'diffusing' species, while sensitive to  $K_{zz}$ , are not very sensitive to the values of  $K_{yy}$ . Ko *et al.* argued that it is more advantageous to deduce  $K_{yy}$  from the observed distributions of downward 'diffusing' species which show large latitudinal gradients. One such candidate species for which extensive global data are available is  $\text{HNO}_3$ . By systematically varying the values of  $K_{yy}$  and comparing the model simulated column abundance of  $\text{HNO}_3$  with observation from LIMS, they concluded that values of  $K_{yy} \sim 3 \times 10^5 \text{ m}^2 \text{ s}^{-1}$  would be appropriate for use with the diabatic circulation. Figure 12-15 shows the observed latitudinal variation of nitric acid column compared with model calculations using various values of  $K_{yy}$ . The low latitude values are best fit with values close to  $3 \times 10^5 \text{ m}^2 \text{ s}^{-1}$ . Notice, though, the weaker (or smaller) diffusion leads to considerable underestimation of the column abundance.

Values of  $K_{yy}$  and  $K_{zz}$  of  $\sim 10^5$  and  $10^{-1} \text{ m}^2 \text{ s}^{-1}$ , respectively, are closest to the numbers suggested by Kida (1983), Tung (1984), and Plumb and Mahlman (1985) (away from the zero wind line 'surfzone', actually  $\sim 30^\circ - 40^\circ$  in latitudinal extent). There is some consensus among modellers that values of this order are suitable for the residual circulation approach. However, Miller *et al.* (1981) and Cariolle and Brard (1984) produce satisfactory tracer distributions with larger Ks. The uncertainty in the derived Ks due to limitations in GCMs and inadequate resolution in atmospheric data should not be forgotten.

Rogers and Pyle (1984) allowed some degree of radiation/dynamics feedback in their diabatic model by calculating the heating rates, although they used precomputed, time-varying temperatures from a classical Eulerian model. Secondly, they included the chemical eddy transport which arises when a tracer is not inert. The eddy correlations  $\overline{v'^2}$ ,  $\overline{v'w'}$  and  $\overline{w'^2}$ , which along with the photochemical lifetimes define the Ks, were calculated using a planetary wave model forced by climatological 100 mb heights. (Notice that Rogers and Pyle assumed linear, small amplitude waves and thus arrived at expressions involving Eulerian statistics).

## ASSESSMENT MODELS

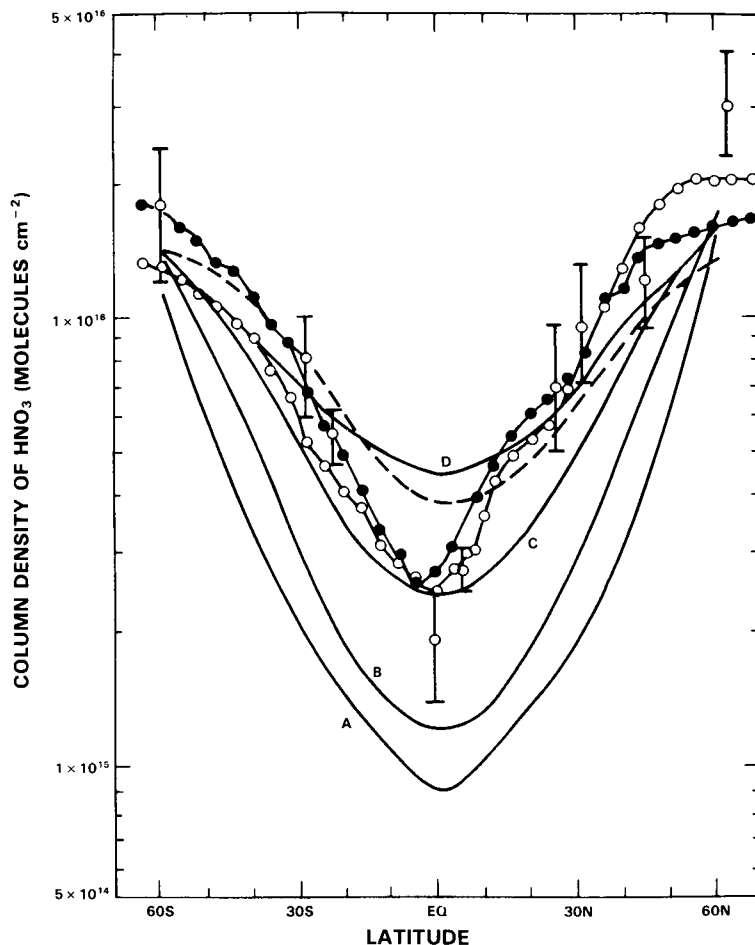


**Figure 12-15.** Calculated latitudinal distribution of the stratospheric column density of  $\text{HNO}_3$ . The calculated results are for (curve A)  $K_{yy} = 0$ , (curve B)  $K_{yy} = 1 \times 10^9 \text{ cm}^2 \text{ s}^{-1}$ , (curve C)  $K_{yy} = 3 \times 10^9 \text{ cm}^2 \text{ s}^{-1}$  and (curve D)  $K_{yy} = 1 \times 10^{10} \text{ cm}^2 \text{ s}^{-1}$ . The data are April/May 1980 (bars) from Girard *et al.* [1982], May (dash-solid circle curve) and December (dash-open circle curve) from Gille *et al.* [1984b]. The calculated column density from the classical Eulerian model of Ko *et al.* [1984] (dashed curve) is included for comparison. From Ko *et al.* (1985).

Two conclusions may be drawn from their work. Firstly, in agreement with Guthrie *et al.* (1984) they conclude that the absence of a large cancellation between mean and eddy motions in the diabatic model helps physical interpretation. For example, Figure 12-16 shows the ozone budget at 64 mb from two model runs, a) the classical Eulerian model and b) the diabatic model. In Figure 12-16a the evident feature is the close cancellation between eddies and mean motion terms. The photochemistry appears negligible. Figure 12-16b shows, on the contrary, that the net transport is in fact comparable with the photochemistry. For time scales appropriate to two-dimensional models ozone in the lower stratosphere cannot be regarded as inert.

Secondly, the chemical eddies can play a role in determining the distribution of tracers. In their experiments Pyle and Rogers (1984) showed that using the correct chemical eddy K coefficient (dependent on the appropriate lifetime) can make significant differences to the calculated column abundances. For

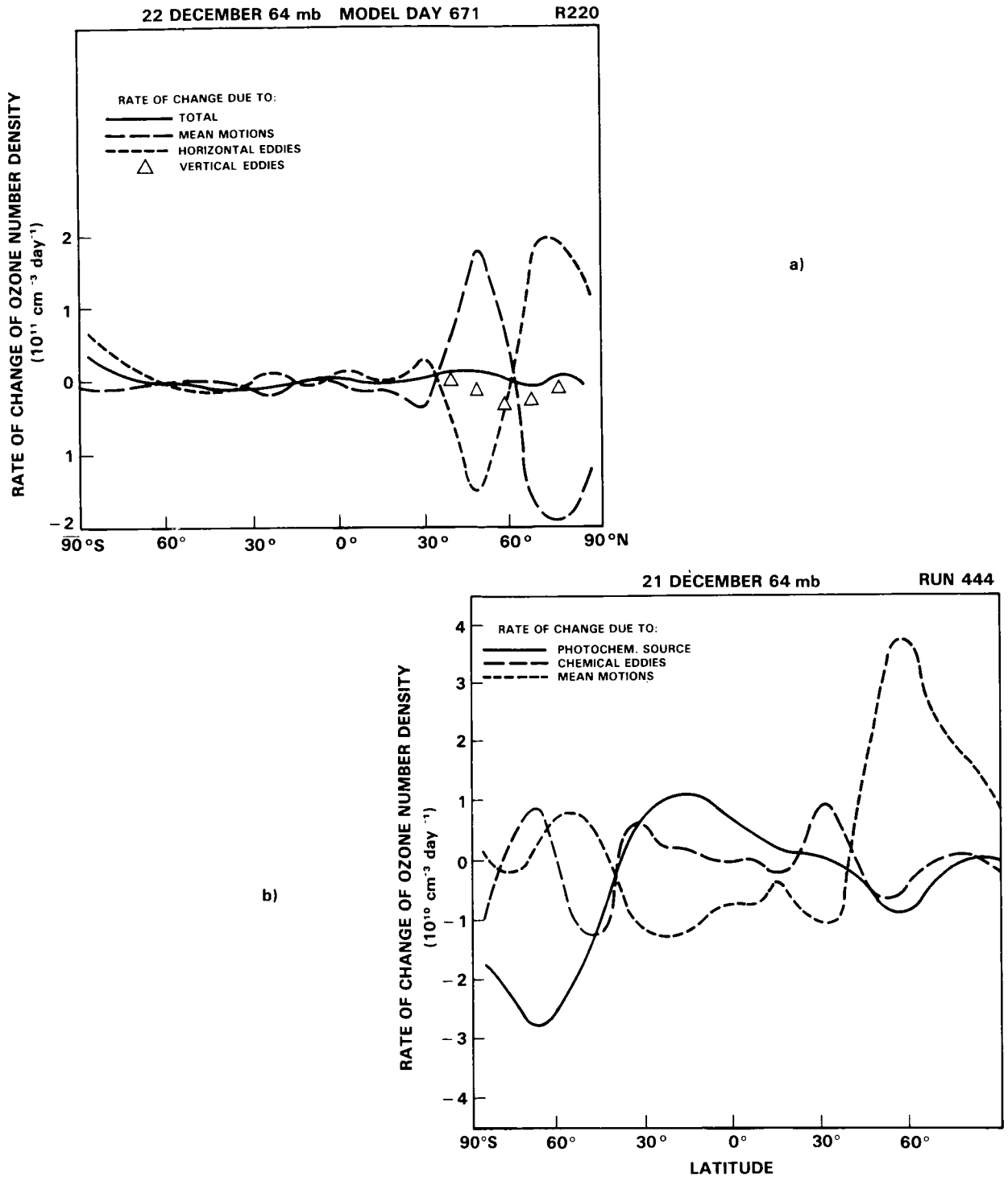


**Figure 12-16.** a) Zonal mean meridional section of the ozone tendency at 64 mb for December from a typical Eulerian circulation simulation (after Harwood and Pyle 1975). b) Zonal mean meridional section of the ozone tendency at 64 mb for December from a modified diabatic circulation simulation. Pyle and Rogers (1984).

## ASSESSMENT MODELS

example, using a  $K$  appropriate to  $\text{NO}_x$  leads to changes in the  $\text{O}_3$  and  $\text{HNO}_3$  high latitude columns of approaching 10% and 50% respectively.

Another residual circulation model which includes some dynamical feedback is that developed by Garcia and Solomon (1983). They solved the coupled thermodynamic and momentum equations above 100 mb and include some eddy forcing by diffusive heat and momentum fluxes, treated as a Rayleigh friction. Radiation is modelled using Newtonian cooling. The calculated circulation, temperature structure and distribution of chemical species generally agree satisfactorily with observations. In their first experiments, they used a  $K_{yy}$  of  $10^5 \text{m}^2 \text{s}^{-1}$ , but their  $K_{zz}$  increased from a small value ( $10^{-1} \text{m}^2 \text{s}^{-1}$ ) in the lower stratosphere to rather large values ( $\sim 10^1 \text{m}^2 \text{s}^{-1}$ ) in the middle and upper stratosphere. As a consequence, their vertical distribution of  $\text{N}_2\text{O}$  did not fall off with altitude as sharply as the data or as in Guthrie's *et al.* model. Their more recent calculations with smaller  $K_{zz}$  produce much closer agreement with observations. The model also includes chemical eddy transport parameterized in terms of the photochemical relaxation time constant which, as expected, is found to be important in the transition region where the photochemical and zonal transport time scales are comparable. The model has been used in a detailed investigation of the nitrogen budget of the stratosphere. The polar distributions of the nitrogen compounds are sensitive to the use of the residual circulation. The model supports the idea that  $\text{NO}_2$  is carried down from the lower thermosphere to the stratosphere in the polar night. An important model conclusion (Solomon and Garcia 1984 a,b) is that  $\text{N}_2\text{O}_5$  is the major  $\text{NO}_y$  reservoir in high latitudes (see Ko *et al.* 1984) and the model calculations appear to be consistent with the observations of the Noxon cliff (1979).

An important addition to the above model is the representation of breaking gravity waves. The seasonal behaviour of the model meridional temperature and circulation in the mesosphere is then in good agreement with observations and the computed eddy diffusion coefficients are consistent with the behaviour of mesospheric turbulence inferred from MST radar echoes. (Garcia and Solomon 1985) Figure 12-17

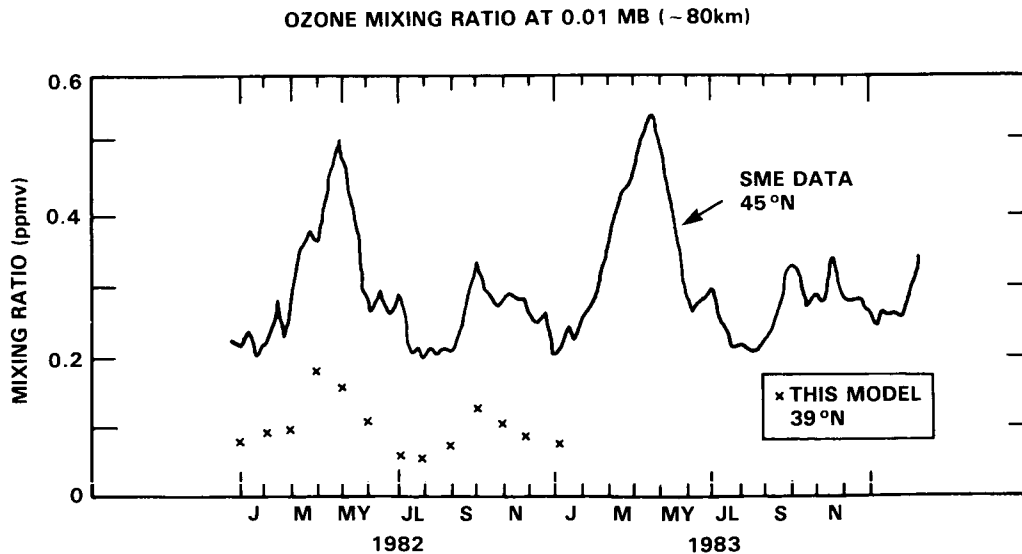


**Figure 12-17.** Observed [Thomas *et al.*, 1984a] and calculated  $\text{O}_3$  mixing ratios near 85 km as a function of season at mid-latitude. From Garcia and Solomon (1985).

shows SME ozone data at  $\sim 80$  km compared with model calculations. The qualitative agreement is excellent with maxima in March and September, corresponding to times of weak winds in the middle atmosphere and hence enhanced absorption of propagating gravity waves. This absorption leads to reduced gravity wave breaking, and hence mixing, in the upper mesosphere. Water vapour, and hence hydrogen radicals, are then reduced in the spring and autumn, leading to enhanced  $O_3$ .

Finally, the work of Plumb and Mahlman (1985) should be stressed. They are developing a model whose transport is derived from general circulation model statistics. This has the advantage that the transport circulation can be derived self-consistently with the K tensor (see Section 6.6.2). It is expected that this approach will continue to yield much useful information about stratospheric transport processes and their inclusion in two-dimensional models. A disadvantage of the model is that the validity of the transport depends on the GCM, with its own strengths and weaknesses.

This review of current two-dimensional modelling efforts suggests two conclusions, one general and one specific. Firstly, it is clear that the variety of models, using sometimes quite different approaches, has contributed to the understanding of stratospheric processes. The richness of approach is an advantage and no one approach can necessarily be regarded as always superior. This is particularly exemplified by simple model experiments where the nature of the feedback processes is the important consideration.

Secondly, major problems are still associated with the treatment of eddy processes. This applies to whichever two-dimensional approach is followed. The residual circulation approach has the advantage that the steady, conservative waves need not be considered. However, it is precisely the situations when the non-acceleration conditions break down that the eddies are important and need to be treated. A consensus appears to be developing, based on observations, general circulation model results and experience with 2-D models, that smaller K values should be used in residual circulation models with perhaps  $K_{yy}$  being a few  $\times 10^5 \text{m}^2 \text{s}^{-1}$  (but see the comments above). It must be stressed that this smaller  $K_{yy}$  does not mean that the modelled eddy transports are any less important. This is shown by reference to Figure 12-15. The model is still sensitive to the choice of  $K_{yy}$  for species with large mean latitudinal gradients.

Some current residual circulation models employ constant K coefficients. Plumb and Mahlman's results argue against this, and this too is perhaps supported by Figure 12-15 where a  $K_{yy}$  increasing in the winter subtropics might produce a better fit to the data.

The progress in recent years is encouraging. For example, the consensus regarding the size of Ks is based not just on experience with models but also on theoretical arguments or models in which the large scale waves are treated explicitly. Despite some difficulties, it can be said that two-dimensional modelling is on a firmer footing than hitherto. While much work remains to be done, the physical basis of the models and, perhaps as important, the model limitations (most important being the treatment of non-conservative eddy processes) are generally well understood.

## 12.6 A COMPARISON OF TWO-DIMENSIONAL MODELS

The models discussed in this section are shown in Table 12-3.

### (i) *Source gases*

The simulation of long-lived trace gases gives a good indication of the diversity of two-dimensional models. It also indicates a chief advantage of two- over one-dimensional models: the ability to simulate latitudinal

## ASSESSMENT MODELS

Table 12-3. 2-D Models Used In This Report

	TYPE	INVESTIGATORS
MPI	Eulerian	Schmailzl, Crutzen
RAL	Eulerian	Gray, Pyle
AER	Eulerian	Ko, Sze
L'Aquila	Diabatic	Visconti
EERM	Diabatic	Cariolle
GSFC	Diabatic	Guthrie
Du Pont	Diabatic	Owens
NOCAR	Residual Circulation	Garcia, Solomon
AER	Diabatic, Isentropic	Ko, Sze, Tung
Oslo	Diabatic	Stordal, Isaksen
RAL	Diabatic	Rogers, Pyle

and seasonal variations. In this section we will concentrate on model results for the long-lived tracers  $N_2O$ ,  $CH_4$ , CFC-11 and CFC-12. The calculations that will be discussed were nominally performed with the same set of chemical reaction rate constants, solar fluxes, and photolytic absorption cross sections (see Appendix A and Chapter 7), so model differences due to chemistry have been minimized. There are still some differences, including the radiative treatment, diurnal model formulation, and treatments of the Schumann-Runge bands, as discussed in greater detail below.

For the simulation of source gases, two-dimensional models fall roughly into two general classes - those in which advection and diffusion play approximately equal roles, and those in which advective transport dominates. The former include classical Eulerian models (eg. MPI, RAL) and those with a diabatic circulation but with eddy diffusion coefficients of the same order as those of Eulerian models (eg. Du Pont, EERM) while the latter (eg. L'Aquila, LLNL, NASA GSFC, the NOAA/NCAR model (NOCAR), Oslo) use diabatic or residual circulations and small eddy diffusion coefficients ( $K_{zz} \sim 10^{-1} m^2 s^{-1}$ ,  $K_{yy} \sim 10^5 m^2 s^{-1}$ ,  $K_{yz} \sim 0$ ). These coefficients are about a factor of ten smaller than in the former models. The advective models have a Brewer-Dobson type atmospheric circulation, with rising air motions in the tropics and descending motions towards the poles.

Long-lived trace gases with sources in the troposphere (eg.  $N_2O$ ,  $CH_4$ , CFC-11, CFC-12) are injected into the stratosphere primarily in the tropics ( $20^\circ S$  to  $20^\circ N$ ). As the tropical air parcel is transported upward by the mean circulation, destruction of source species occurs by photolysis or reactions with  $O(^1D)$  and  $OH$ . Destruction continues as the parcels are advected poleward in the stratosphere, and the parcels then descend at high latitudes with lower concentrations of the source gases. The source gas mixing ratios are thus greater at the equator than at the poles, and the isolines descend to lower altitudes near the poles.

In models with larger eddy coefficients, horizontal mixing reduces the equator-to-pole gradients, giving flatter isolines. For all the source gases, as will be discussed below, this same general picture emerges.

Figure 12-18 shows the calculated  $N_2O$  mixing ratio as a function of altitude and latitude for July in three models, two (GSFC, NOCAR) advective and one with large eddy diffusion (Du Pont). The advective

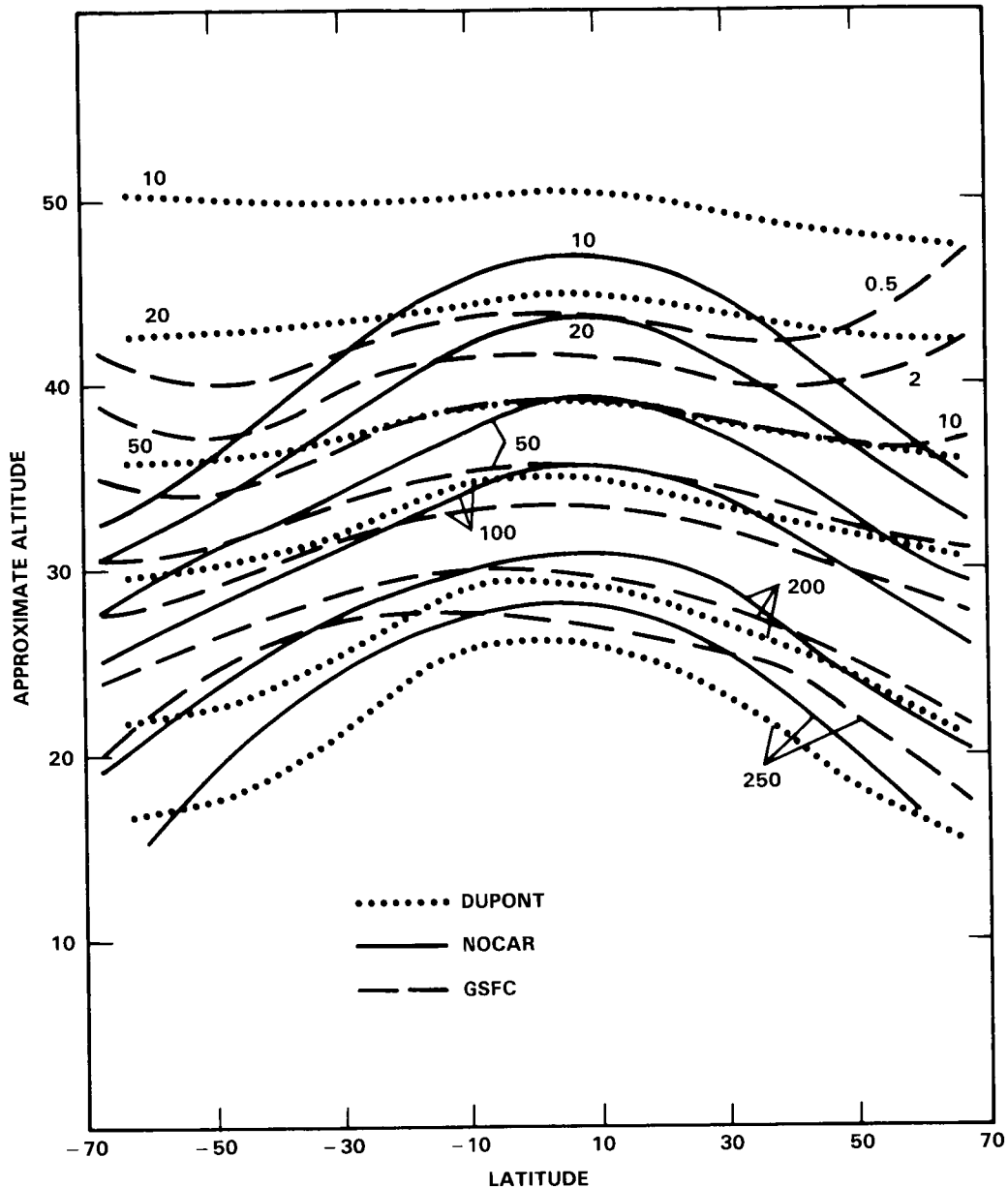


**Figure 12-18.** Latitude-height cross-section of the N<sub>2</sub>O distribution (ppbv) from three different 2-D models.

models gives more rapidly downward-sloping contour lines at low and mid latitudes. The NOCAR model in particular strongly mirrors the underlying equator-to-pole circulation. Toward the poles, the upturn in the GSFC model is due to the structure of the Murgatroyd and Singleton (1961) wind field.

Figures 12-19a and 12-19b show the vertical profiles of N<sub>2</sub>O calculated by several of the models at the equator and midlatitudes, respectively. Because of the differing latitudinal gradients illustrated in Figure 12-18, there is a large spread in the predicted profiles, especially in the mid to upper stratosphere. The

# ASSESSMENT MODELS

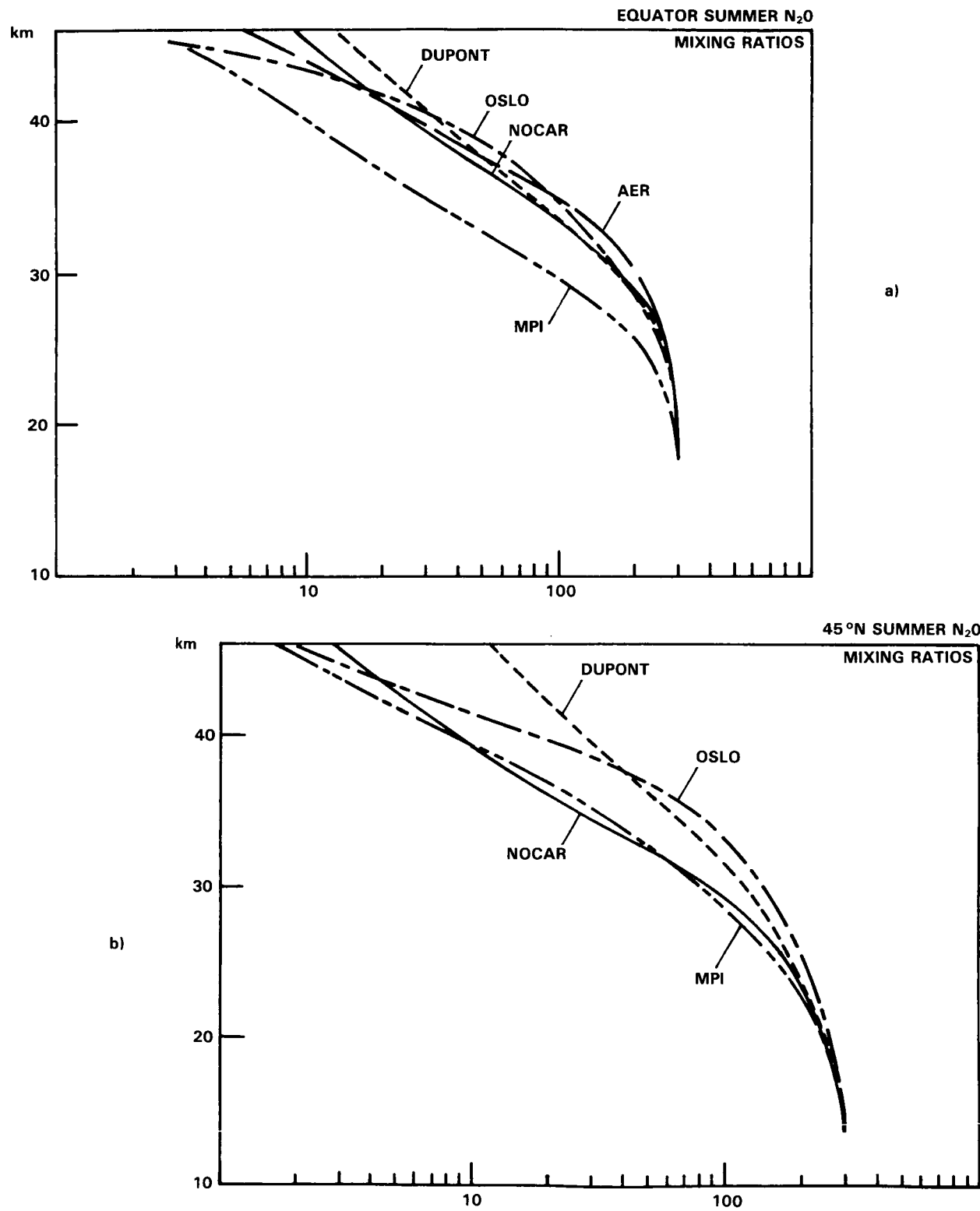


**Figure 12-19.** Vertical profiles of N<sub>2</sub>O (ppbv) calculated by various models. a) Summer, 0°; b) Summer, 45°N.

model range approaches a factor of two for both low and mid latitudes at 30-35 km altitude and a factor of four at 40 km.

A latitude section of the modelled  $N_2O$  mixing ratio at the 35 km level is shown in Figure 12-20. The latitudinal distribution is quite flat in the MPI (Eulerian) model, although considerably more structure is evident between 30S and 30N in RAL's classical Eulerian model. Interestingly, the RAL model has similar structure in this low-latitude region to the residual circulation NOCAR model. In high latitudes the models are quite different, with the NOCAR model showing a continued decrease. The RAL model, with a strong high latitude indirect cell, predicts increasing  $N_2O$  with latitude.

An interesting feature of the satellite observations of  $N_2O$  is the presence of a 'double peak' structure in March, April and May when, on a given pressure surface, there is a local minimum in mixing ratio at the equator with maxima in the sub-tropics. This is in contrast to the usual situation with a single low latitude maximum. Jones and Pyle (1984) discussed this feature in detail. Using a classical Eulerian two-dimensional model they were unable to reproduce the double peak. Using the same model, Gray and Pyle (1985) have now satisfactorily modelled the feature (Figure 12-14). They hypothesise that it is related to the low latitude semiannual oscillation. The circulation induced by a low latitude westerly forcing (chosen to reproduce the observed semiannual oscillation of the zonal wind) has descending motion at the equator, sufficient to produce the local minimum there. The model also reproduces somewhat similar features in  $CH_4$  and  $O_3$  and leads to a significantly improved low latitude seasonal variation.

Some representative mixing ratio cross sections for  $CH_4$  are shown in Figure 12-21. As is the case for  $N_2O$ , the residual circulation model (NOCAR) shows a much larger latitudinal gradient than the classical Eulerian model (MPI). The large difference in latitudinal gradient between a model with large eddy diffusion values (Du Pont) and one with small coefficients, both using essentially the same wind field, is shown

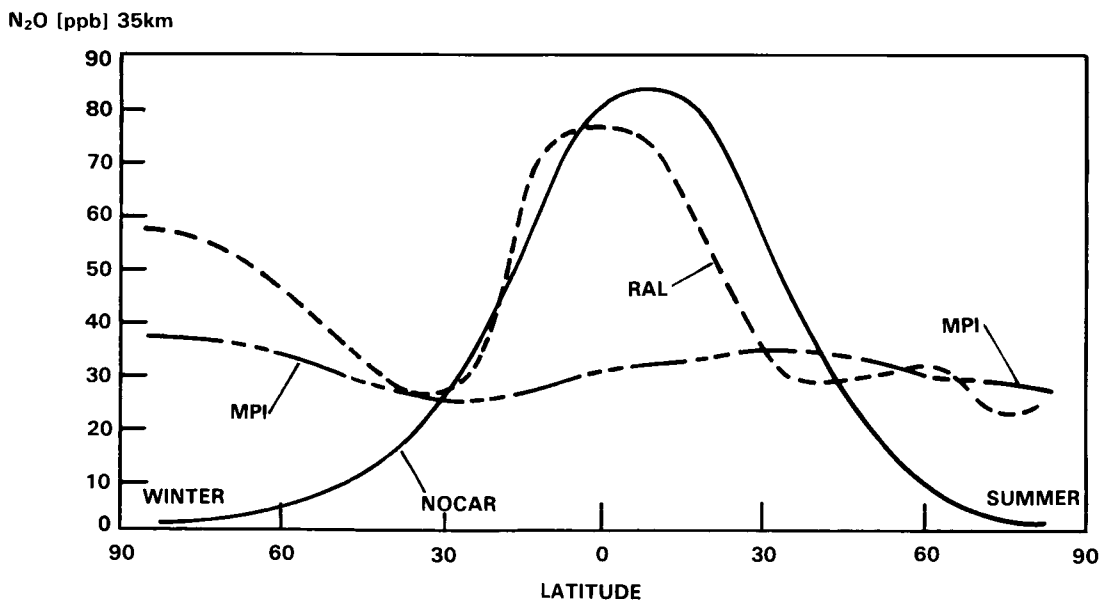


**Figure 12-20.** Latitude section of  $N_2O$  volume mixing ratio at 35 km for three different 2-D models.

## ASSESSMENT MODELS

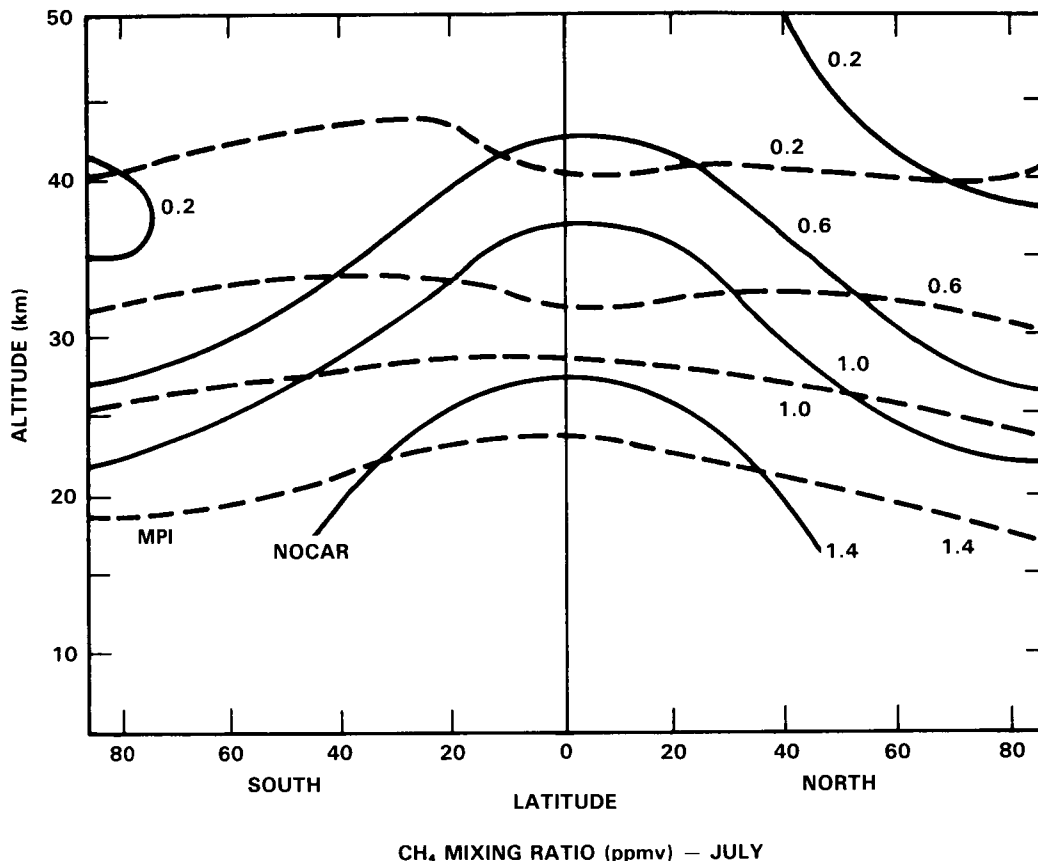


**Figure 12-21.** Cross-sections of CH<sub>4</sub> from the MPI and NOCAR 2-D models.

in Figure 12-22. While the latitudinal change from equator to 60 degrees at 40 km altitude in the summer hemisphere is less than a factor of 2 in the Du Pont model, it is an order of magnitude in the GSFC model. This large difference in model predictions for CH<sub>4</sub> in the upper stratosphere is one point on which satellite data may provide a significant test.

Vertical profiles for methane computed in several models are shown in Figure 12-23 for the equator and midlatitude (summer). The models with classical diffusion coefficients (Du Pont, RAL) fall off far less rapidly above 40 km than the residual circulation model (AER). The range of model predictions approaches a factor of 2 at midlatitudes near 30 km, while at the equator all the models agree within about 50% for all altitudes below 40 km. At higher latitudes, the upper-stratospheric differences between the various model predictions are considerably larger.

The modelled vertical profiles for CFC-11 at the equator and 45°N are shown in Figure 12-24. There is good agreement between the models (after scaling to the same tropospheric mixing ratio) at midlatitudes, with agreement at all altitudes better than a factor of two. Model agreement is not so good at the equator or at high latitudes. The reason for the good gross agreement between models for CFC-11 may be its relatively rapid destruction rate in the lower stratosphere, so that its vertical profile is dominated by the photochemical sink. Nevertheless, important differences in transport are evident in discrepancies between the models.

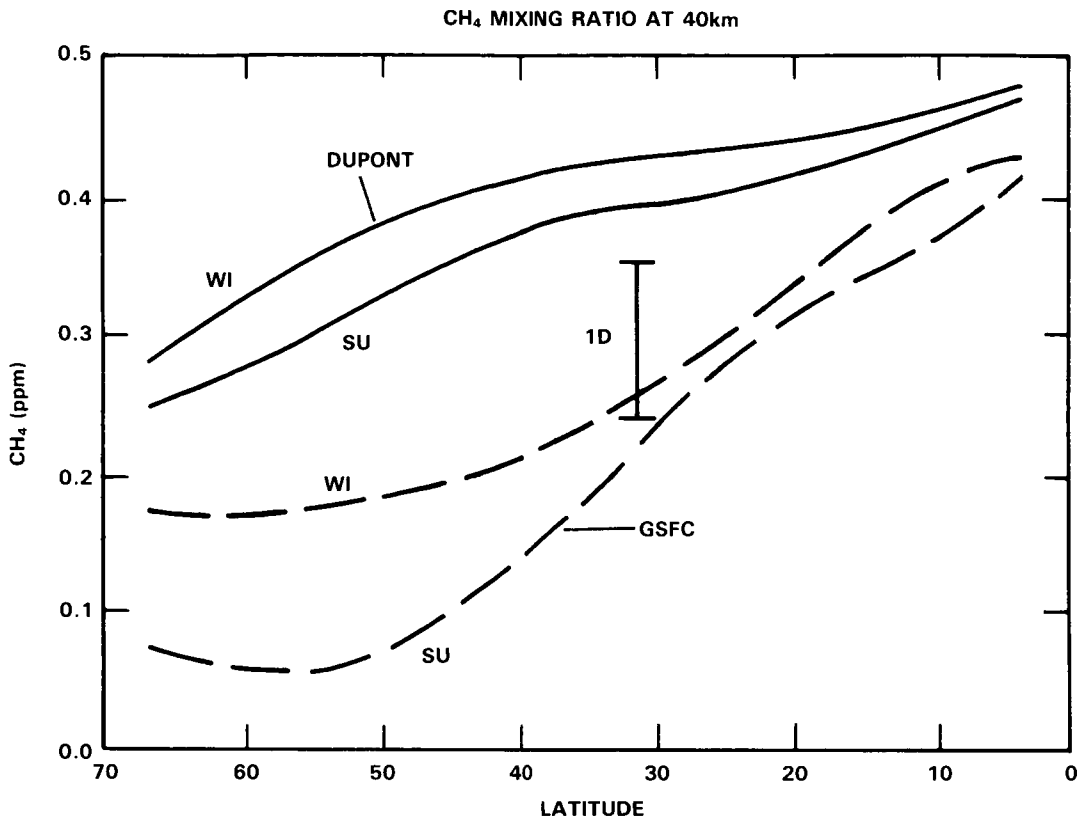


Figure 12-22. CH<sub>4</sub> mixing ratios versus latitude at 40 km for two different models for winter and summer. The range of 1-D model values is also shown.

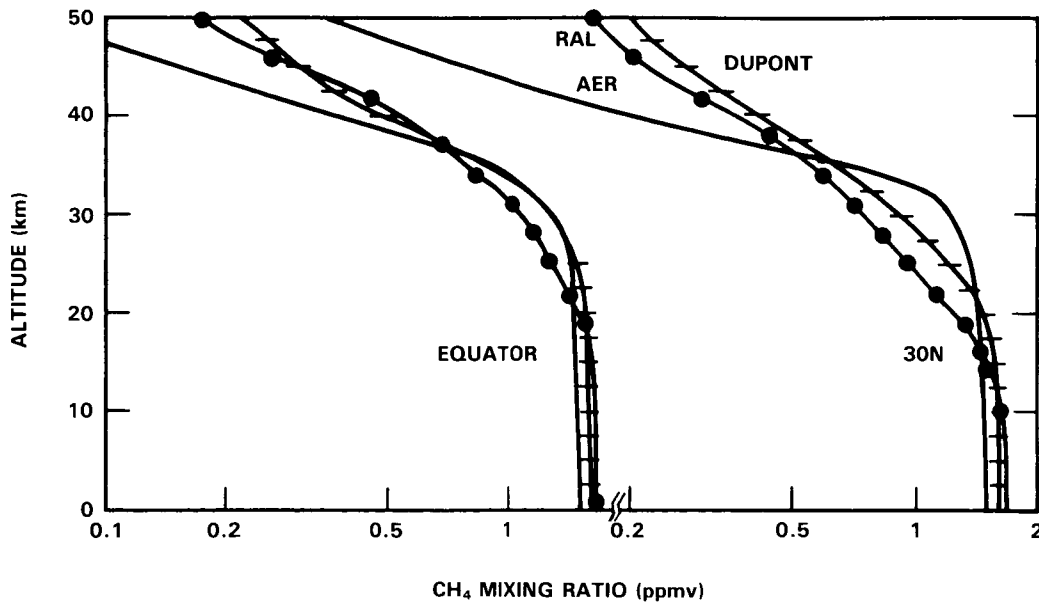


Figure 12-23. Vertical profiles of CH<sub>4</sub> calculated by various models at the equator and 30°N.

ASSESSMENT MODELS

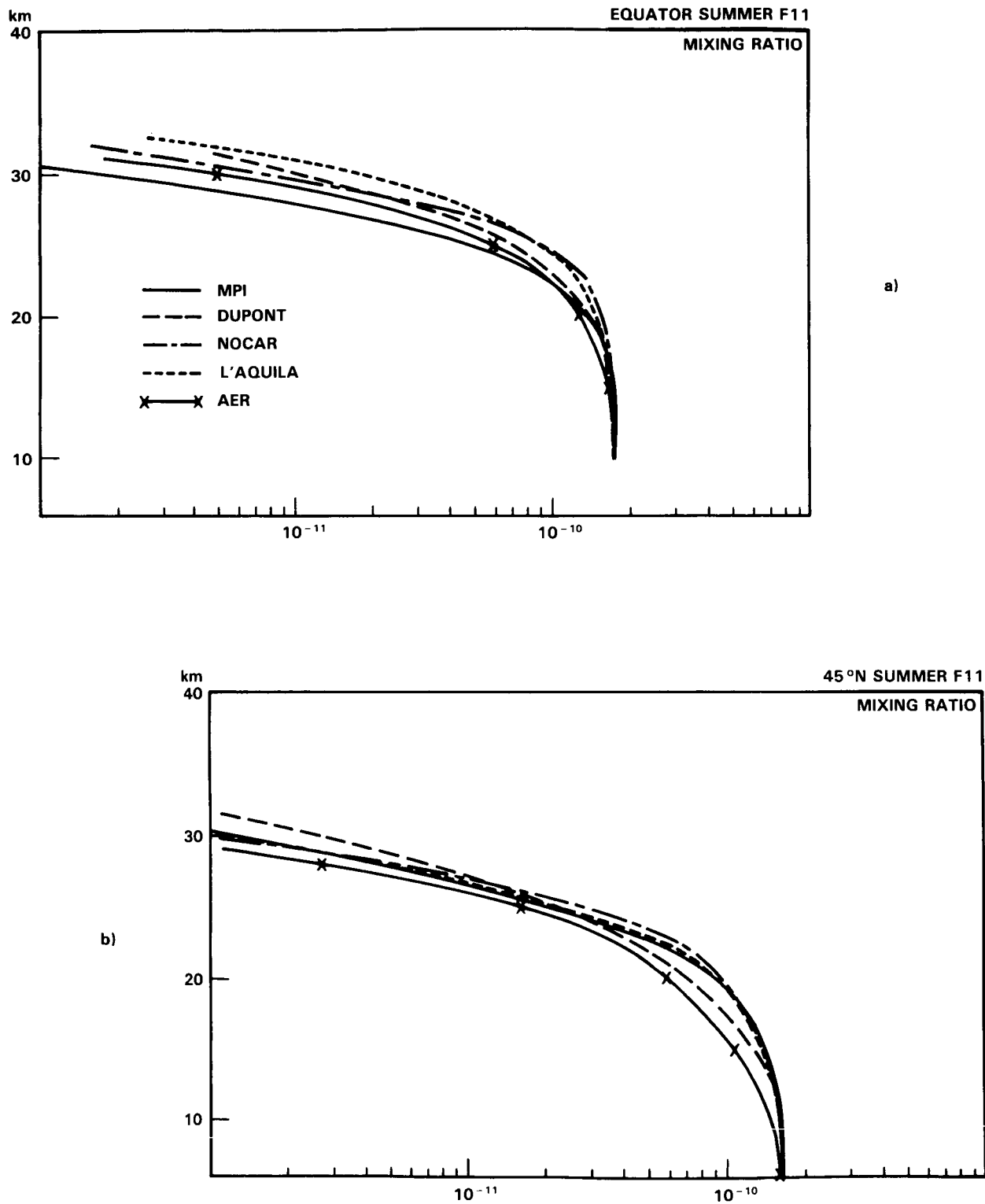


Figure 12-24. Vertical profiles of CFC<sub>13</sub> volume mixing ratio calculated by various models. a) Summer, 0°; b) Summer, 45°N.

For the longer-lived CFC-12, the model agreement is poorer at both equatorial and midlatitudes, as shown in Figure 12-25. As is the case for N<sub>2</sub>O, a greater latitudinal gradient is shown by the residual circulation models. The model range is a factor of two at 25-30 km and continues to be large at higher altitudes. The difference in latitudinal gradient between Eulerian (MPI) and residual (NOCAR) transport schemes are shown in Figure 12-26. At 25km altitude, the modelled equatorial values of 200ppt decrease to 40 ppt at 50 degrees latitude for the NOCAR model but only to 140 ppt for MPI.

In summary, there is a distinct difference in the results between models with large eddy diffusion compared with those with small eddy diffusion. The latter consistently show larger latitudinal and seasonal variations in the middle and upper stratosphere, as expected. Differences are still found between models of the same basic type. For example, for long-lived tracers with sources in the troposphere, the diabatic circulation in some models produces an upward bend in the isolines, while the residual circulation in other models gives isolines that continue to slope downward toward the pole. Furthermore, general conclusions regarding the relative performance of classical Eulerian compared with the transformed models are difficult to make. For example, there is some suggestion that the satellite CH<sub>4</sub> and N<sub>2</sub>O data show latitudinal gradients more characteristic of the advection-dominated models, although there are still important differences from model to model. Moreover, the classical Eulerian RAL model reproduces the CH<sub>4</sub> and N<sub>2</sub>O data well. In fact, in low latitudes, the satellite data shows flatter fields than are found in the model (Jones & Pyle 1984). Of course, the argument is not really about the size of the eddy diffusion but about the balance between mean and eddy transport.

One of the major problems in developing a diabatic circulation model is the lack of a definitive set of self-consistent atmospheric heating and temperature fields. The Murgatroyd and Singleton wind field, used in many models (Du Pont, EERM, LLNL, NASA, Oslo), is based on very old data and does not give a summer stratosphere near radiative equilibrium, as recent studies have implied. For diagnostic studies in the near term, more realistic ozone fields and more sophisticated radiation schemes for infrared cooling should provide an improved estimation of stratospheric winds.

Because of the large differences in source gas latitudinal gradients predicted by the models with either large or small horizontal and vertical mixing, satellite data with good coverage of the globe (from, e.g. SAMS and LIMS) should prove useful in validating transport schemes. The satellite data have already become a useful tool for testing 2-D models and their transport schemes.

In this discussion, we have not mentioned one-dimensional models. Three one-dimensional models (Du Pont, Harvard, LLNL) were compared with the mid-latitude vertical profiles shown in Figures 12-19, 23, 24 and 25 (for N<sub>2</sub>O, CH<sub>4</sub>, CFC-11 and CFC-12). In general, the 1-D models fall within the range of values spanned by the 2-D models and have a similar degree of consistency within themselves. The long standing problem of simultaneously fitting the observed midlatitude vertical profiles of these four tracers using the same eddy diffusion profile is shared to some extent by two-dimensional models. In two dimensions, it is, for example, possible for a model to fit the midlatitude profiles of these species satisfactorily (eg. Guthrie *et al.*, 1984), but then to have difficulty in reproducing the profiles at lower and higher latitudes.

#### (ii) HO<sub>x</sub>

The models show striking similarity in the morphology of the HO<sub>x</sub> distributions. Figure 12-27 shows a height-latitude cross-section for daytime average OH. The salient features are the broad peak between 40 and 45 km, the steep gradient toward the winter pole, and the saddle-shaped minimum near the tropopause.

ASSESSMENT MODELS

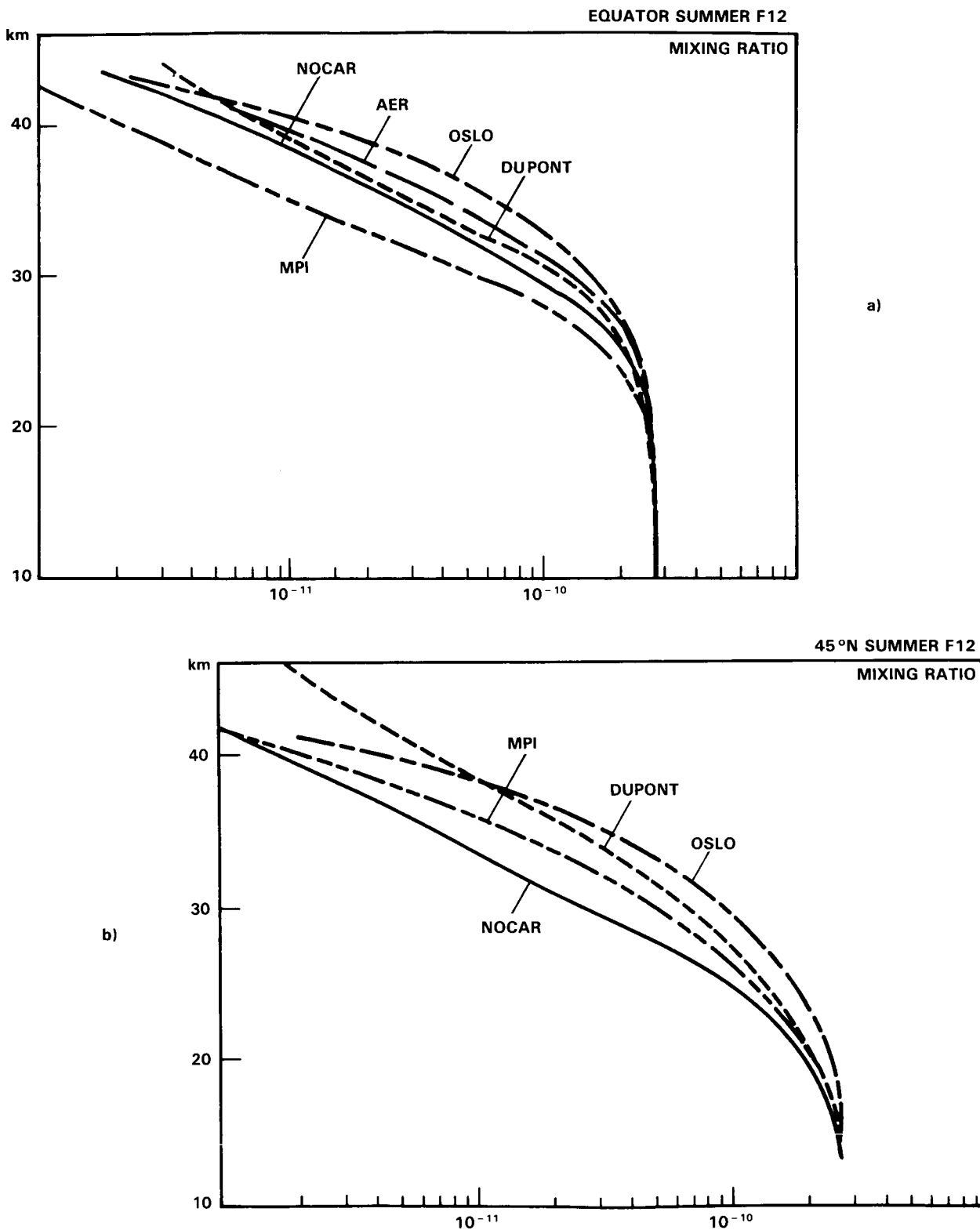
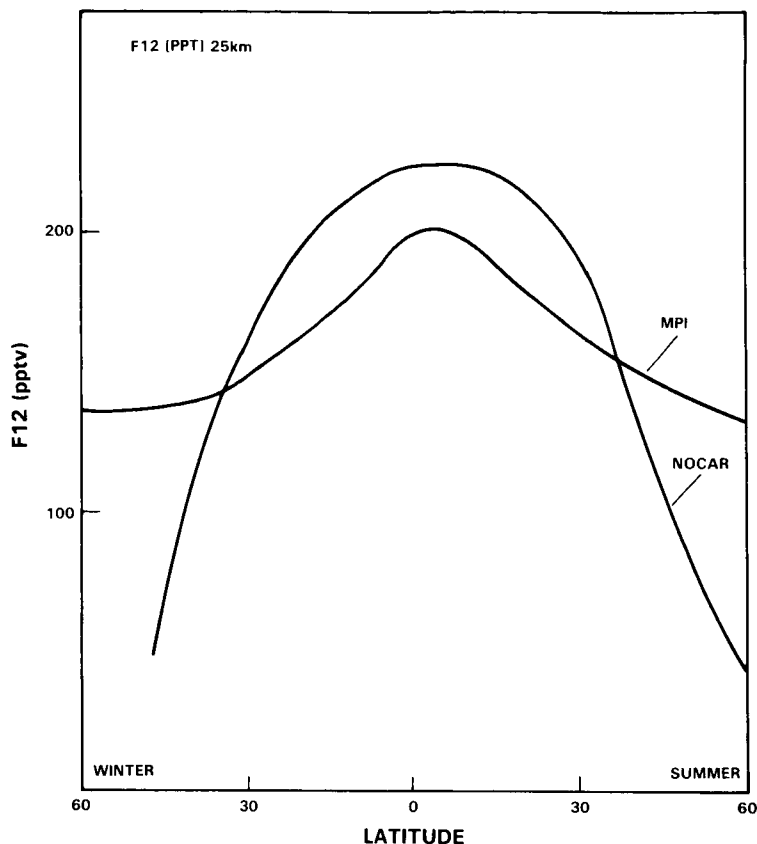


Figure 12-25. Vertical profiles of  $CF_2Cl_2$  volume mixing ratio calculated by various models. a) Summer,  $0^\circ$ ; b) Summer,  $45^\circ N$ .



**Figure 12-26.** Latitude section of  $\text{CF}_2 \text{Cl}_2$  volume mixing ratio at 25 km for the MPI and NOCAR models.

All of the models considered here show peak values of  $2$  to  $2.5 \times 10^7$  molecules/ $\text{cm}^3$ . The exact height of the saddle minimum and the slope of the poleward decrease at the saddle vary slightly between models, (presumably due to small differences in ozone, water vapour, and temperature distributions).

Similar structures appear in the  $\text{HO}_2$  and  $\text{H}_2\text{O}_2$  cross sections, although the peaks are substantially broader and flatter than in the case of OH (Figures 12-28 and 12-29). As might be expected, the centroids of the distributions follow the sun northward and southward through the course of a year with little or no phase lag.

In comparing the model distributions with available data, some discrepancies appear. The range of model profiles for daytime average OH is shown in Figure 12-30, along with measurements. The agreement seems quite good, with the intermodel range and the range of the measurements being quite comparable (see Chapter 9 for a more complete discussion).

The situation seems quite different for  $\text{HO}_2$  (Figure 12-31). The models again agree well with each other but there is barely overlap between the range of model profiles and the range of measurements, although the available measurements are extremely limited. The difference between range centers is at least a factor of three and approaches an order of magnitude. Both ranges (model and measurement) include seasonal differences.

# ASSESSMENT MODELS

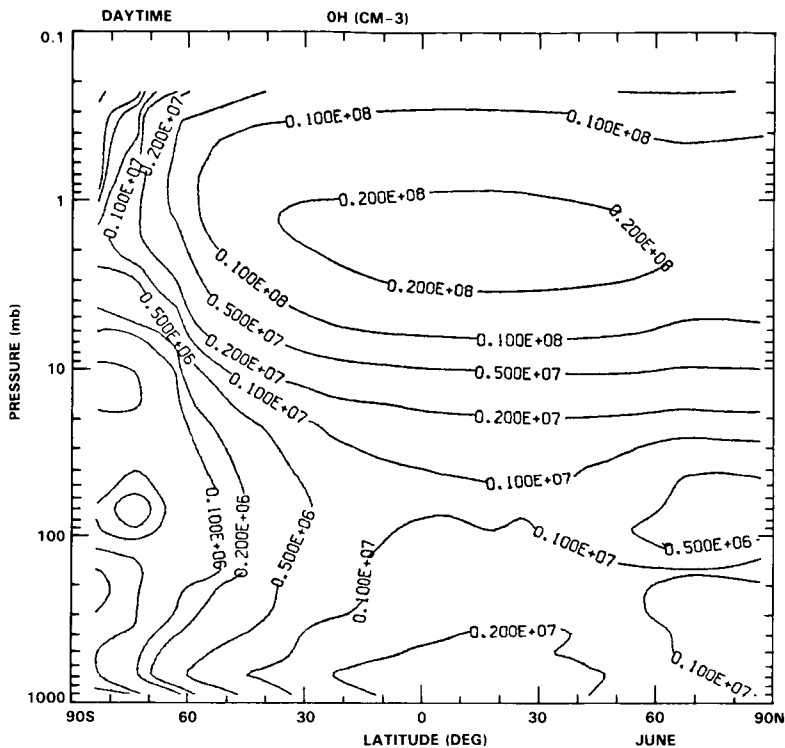


Figure 12-27. Latitude-height cross section of daytime average OH (molecules  $\text{cm}^{-3}$ ) from the GSFC 2-D model.

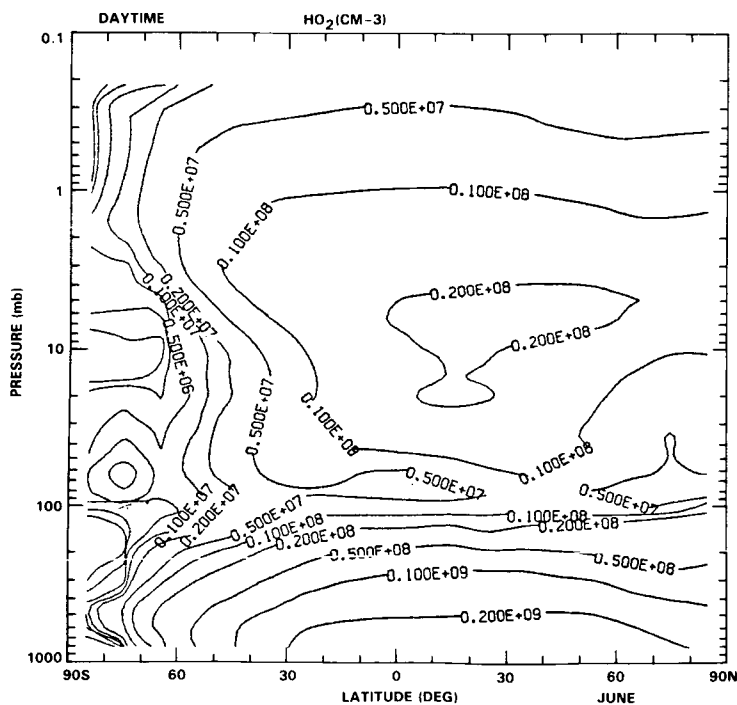


Figure 12-28. As Figure 12-27 for  $\text{HO}_2$ .

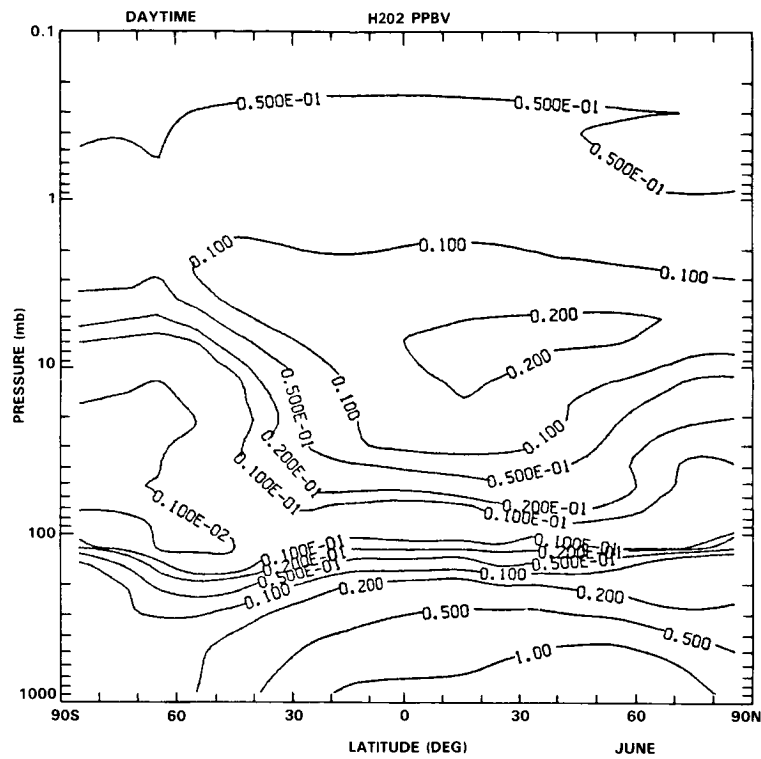


Figure 12-29. As Figure 12-28 for H<sub>2</sub>O<sub>2</sub> volume mixing ratio (ppbv).

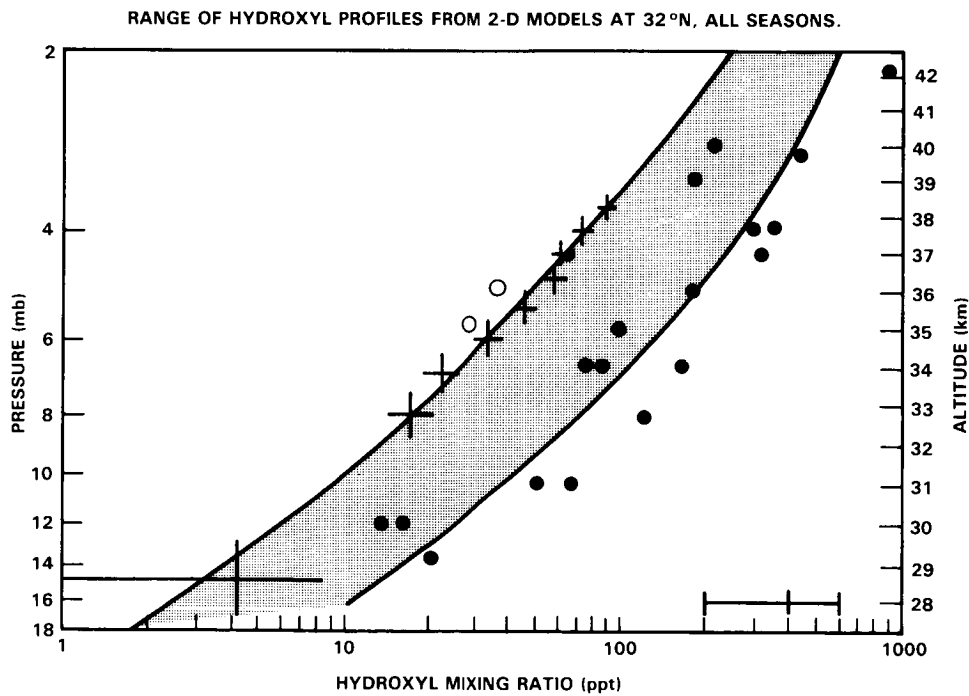


Figure 12-30. Shaded region shows the model range of 2-D model calculated OH at 32°N compared with available observations (see Chapter 9).

ASSESSMENT MODELS

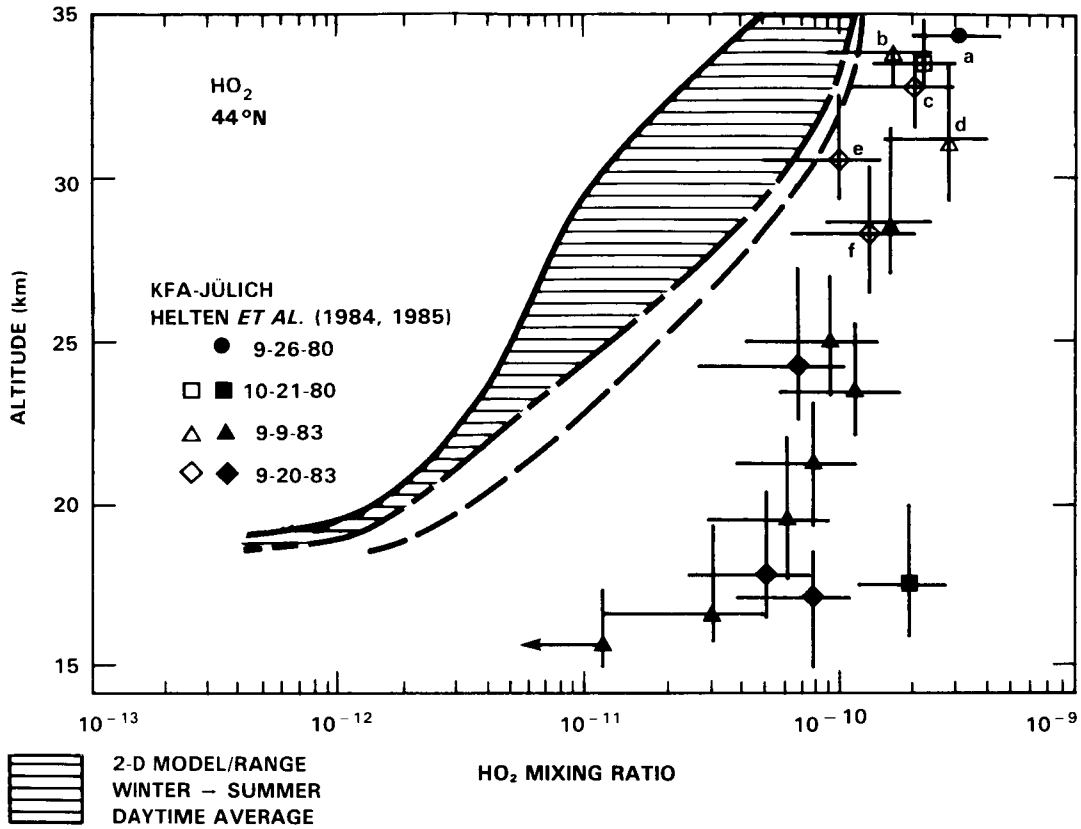


Figure 12-31. As Figure 12-30 for HO<sub>2</sub>.

In the case of hydrogen peroxide (H<sub>2</sub>O<sub>2</sub>) the range, defined by reported detections and the upper limits from both Chance and Traub (1984) and de Zafra *et al.* (1984) is very broad and the detailed profile is essentially undefined. The range of model profiles for 30°N, winter is shown in Figure 12-32. Although the model range is fairly broad, it clearly falls above the upper limit of Chance and Traub between 24 and 32 km.

The increased model spread for H<sub>2</sub>O<sub>2</sub> can be understood by the quadratic dependence of H<sub>2</sub>O<sub>2</sub> on HO<sub>2</sub>, and then on total HO<sub>x</sub>. Any model differences in the production of HO<sub>x</sub> (due, for example, to the different ozone distributions) or in the HO<sub>2</sub>/HO<sub>x</sub> ratio (due, for example, to differences in temperature distributions) will be magnified in the H<sub>2</sub>O<sub>2</sub> comparison. It is this particular sensitivity which prompted the suggestion by Connell *et al.* (1985) that measurements of H<sub>2</sub>O<sub>2</sub> along with other members of the HO<sub>x</sub> family would make a very useful test of atmospheric chemistry.

If the difference between models and measurements persists with additional HO<sub>2</sub> and H<sub>2</sub>O<sub>2</sub> measurements it will indicate a possible problem with our understanding of the partitioning of the HO<sub>x</sub> family,

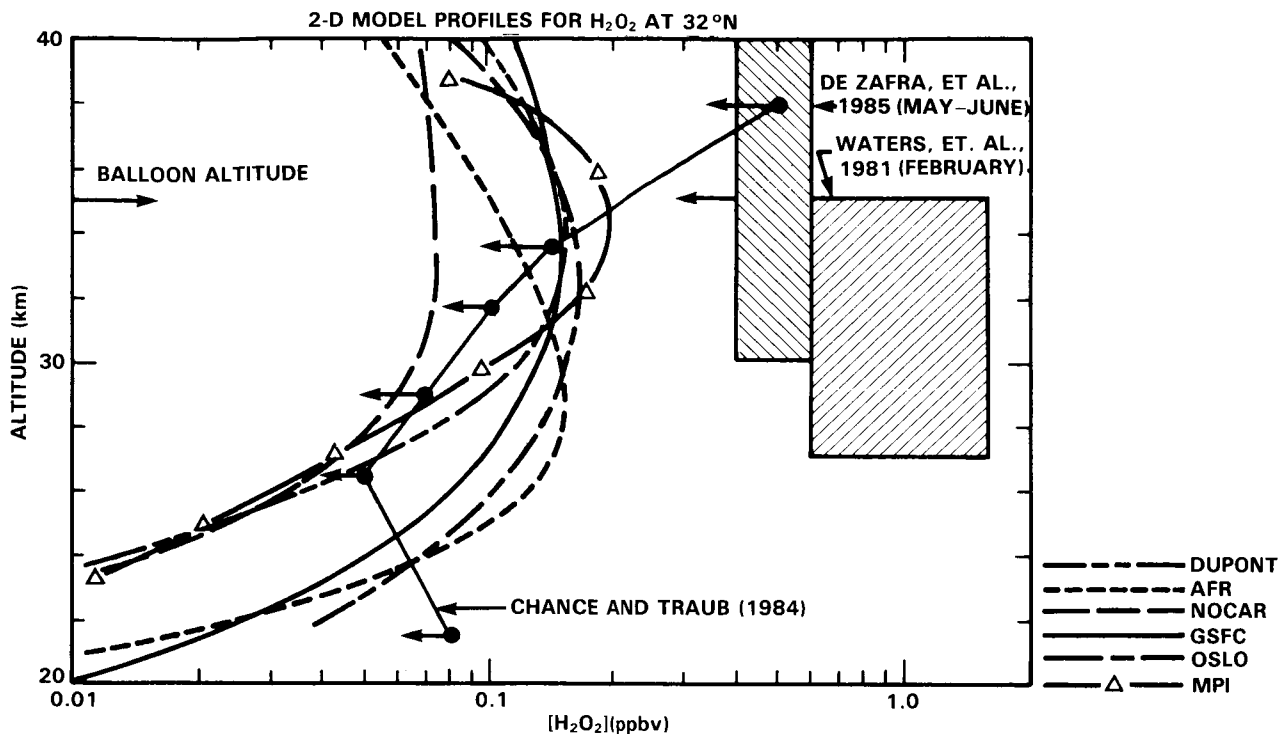


Figure 12-32. Range of 2-D model calculated  $\text{H}_2\text{O}_2$  at  $30^\circ\text{N}$ , winter compared with measured upper limits.

although that partitioning would appear to be controlled by well-understood photochemical processes. This is discussed further in Chapter 9. Any such problem must be common to all the models given the agreement between them.

### (iii) Odd nitrogen

In this subsection, distributions of odd nitrogen species calculated by a number of two-dimensional models will be compared. Differences in their behaviour will be discussed, with particular emphasis on the origin of variations in model calculated abundances of total odd nitrogen ( $\text{N} + \text{NO} + \text{NO}_2 + \text{NO}_3 + 2 \times \text{N}_2\text{O}_5 + \text{HNO}_3 + \text{HNO}_4 + \text{ClONO}_2$ ). This parameter is of critical importance to the ozone balance in the contemporary atmosphere, as well as to the evaluation of possible future perturbations in ozone.

Figure 12-33 presents contour plots of the  $\text{NO}_y$  distributions calculated in the models by Ko *et al.* (1985) and Gray and Pyle (1985), which are respectively formulated in the residual and classical Eulerian frameworks. Like  $\text{CH}_4$  and  $\text{N}_2\text{O}$ ,  $\text{NO}_y$  is very long-lived in the lower stratosphere, and its horizontal gradients depend sensitively on the competition between horizontal mixing and advection by the mean meridional circulation. Therefore the meridional cross section of  $\text{NO}_y$  calculated in the advection-dominated model of Ko *et al.* (1985) exhibits a steeper slope with latitude than does the classical Eulerian model.

Figure 12-34 presents vertical profiles of the calculated  $\text{NO}_y$  abundances from several two-dimensional models. The model by Pyle *et al.* makes use of the  $\text{NO}$  photolysis parameterisation of Cieslik and Nicolet (1973), while the others employ the parameterisation by Allen and Frederick (updated to account for re-

ASSESSMENT MODELS

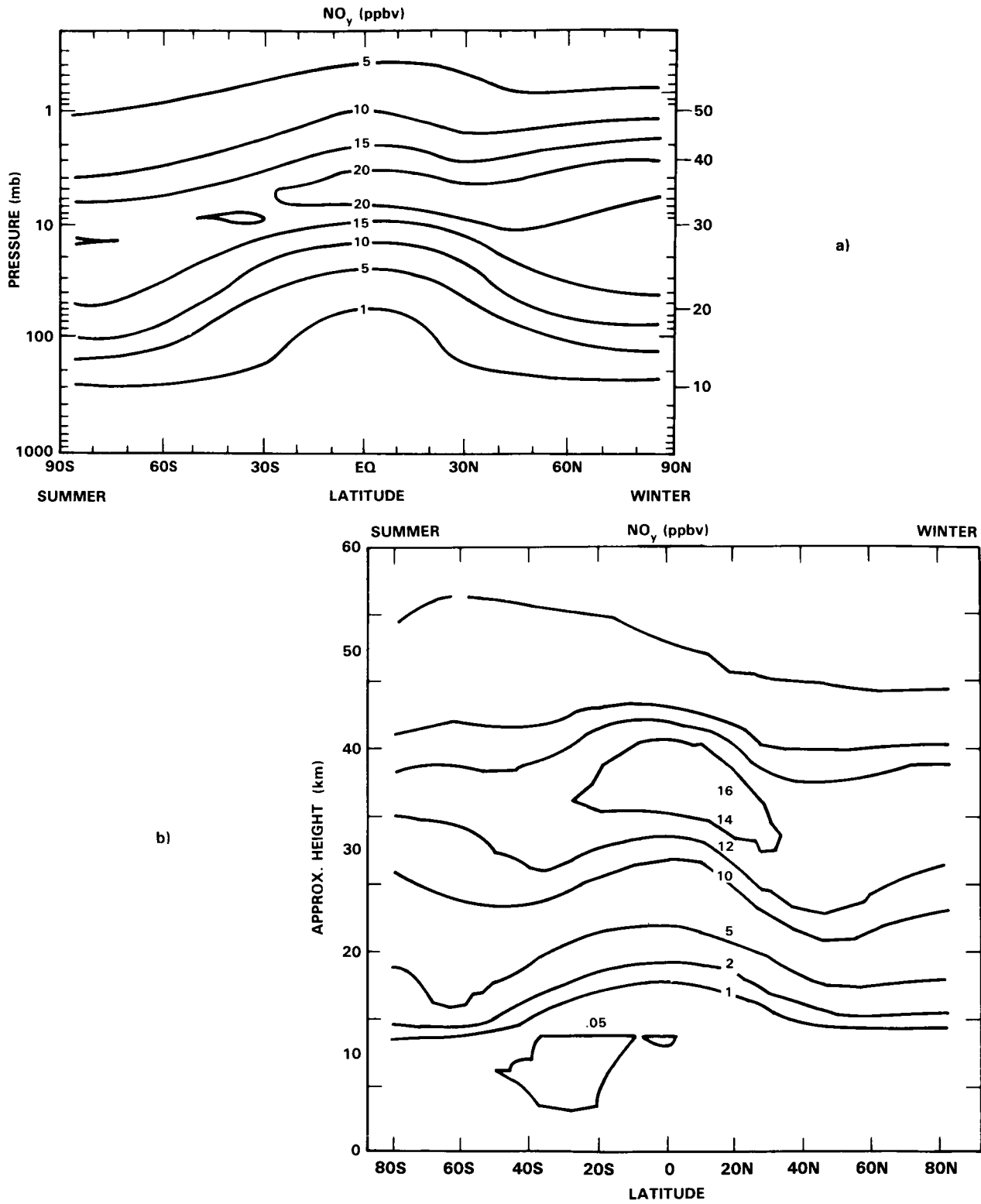
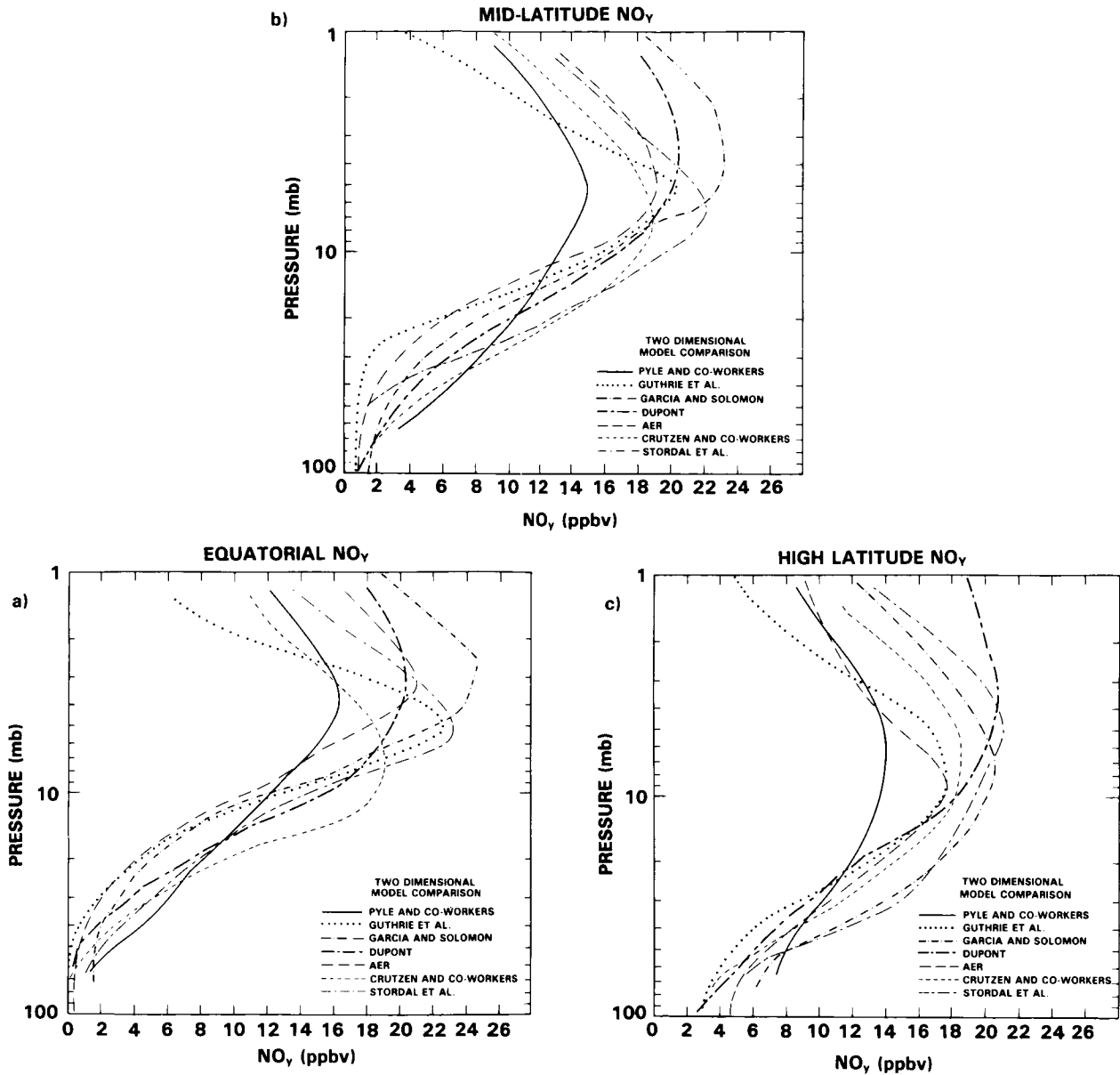


Figure 12-33. Latitude-height cross sections of  $\text{NO}_y$  (ppbv) from a) The AER diabatic model (Ko et al., 1985); b) The RAL Eulerian model.



**Figure 12-34.** 2-D model profiles of  $\text{NO}_y$  at various latitudes. a)  $0^\circ$ ; b) Mid-latitude,  $26\text{--}35^\circ\text{N}$ . c) High latitude

cent changes in our knowledge of the  $\text{O}_2$  Herzberg continuum and Schumann-Runge band cross sections), or the similar parameterisation presented by Frederick *et al.* (1983a), which is used in the model of Garcia and Solomon (1983). The latter parameterisation includes the effect of self-absorption by the NO molecule, and the corresponding NO photolysis rates are therefore smaller (order of 40% for a  $60^\circ$  solar zenith angle without this effect near 40 km.). On the other hand, the NO photolysis rates obtained by Cieslik and Nicolet are larger than those presented by Frederick and co-workers in this region. As discussed in more detail in the subsection comparing one-dimensional models, the calculated abundance of  $\text{NO}_y$  near and above the peak at about 40 km is very sensitive to the NO photolysis rate, which controls the density

## ASSESSMENT MODELS

of atomic nitrogen and the loss of  $\text{NO}_y$  through the reaction  $\text{N} + \text{NO}$ . The model variations in  $\text{NO}_y$  abundance near the peak are consistent with these differences in the adopted photolysis rates.

Another factor that plays a critical role in the differences between modelled  $\text{NO}_y$  abundances, particularly in the lower stratosphere, is the approach taken for the transport of  $\text{NO}_y$  and for the  $\text{HNO}_3$  rainout around the tropical tropopause region. This is perhaps easiest to examine conceptually by assuming transport in the residual Eulerian framework. The air parcels entering the stratosphere probably do so principally in the tropics, as discussed above. In residual Eulerian models, then, the  $\text{NO}_y$  mixing ratio of air ascending into the lower stratosphere is highly dependent on the treatment of transport (i.e. the vertical velocity near the tropopause and the vertical eddy diffusivity between the tropopause and the  $\text{NO}_y$  peak near 40 km), and, on the treatment of  $\text{HNO}_3$  rainout in the tropical upper troposphere. The meridional transport in the lower stratosphere has equator to poleward flow in both hemispheres in such models (and the rate of vertical eddy mixing is very slow by comparison), so that the  $\text{NO}_y$  content of the extra-tropical lower stratosphere will also be strongly influenced by variations in the  $\text{NO}_y$  that is input in the tropics. These effects should be expected to be less pronounced in classical Eulerian models due to more mixing, both in the vertical and horizontal directions. These differences are clearly manifested by the comparison of the calculated  $\text{NO}_y$  abundances of the models of Guthrie *et al.* (residual Eulerian with rapid  $\text{HNO}_3$  rainout in the tropics) and Pyle *et al.* (classic Eulerian with slower  $\text{HNO}_3$  rainout). The Garcia-Solomon model has no troposphere, and prescribes an inflow of  $\text{NO}_y$  at the tropical tropopause as a boundary condition, based on the measurements reported by Loewenstein *et al.* (1978a).

In the low stratosphere, the  $\text{NO}_y$  budget is a balance between slow photochemistry and slow vertical transport. Given the great difficulty in modelling the net radiation sources and sinks in the equatorial lower stratosphere (Houghton 1978) which determines the vertical velocity in these models, the large differences in  $\text{NO}_y$  shown in Figure 12-34 are not surprising.

More recently, the LIMS data on  $\text{NO}_2$  and  $\text{HNO}_3$  have become available, providing a database against which our knowledge of  $\text{NO}_y$  may be tested. These data will be discussed in Chapter 10 and compared to the models. It should be noted that a more complete database of  $\text{NO}_y$ , particularly around the tropical tropopause and lower stratosphere, could be of great value in improving our knowledge of this very important aspect of stratospheric modelling. That these fluxes are important in determining  $\text{NO}_y$  can be seen by results from the RAL model. Using the Allen & Frederick parameterisation instead of the Ciezlik and Nicolet values for NO photolysis, leads to an increase in  $\text{NO}_y$  at the peak of only  $\sim 3$ ppbv and makes little difference to the slope of the profile.

The partitioning of odd nitrogen among NO,  $\text{NO}_2$ ,  $\text{NO}_3$ ,  $\text{N}_2\text{O}_5$ ,  $\text{HNO}_4$  and  $\text{HNO}_3$  is determined largely by fast photochemistry (outside of the polar night region). The ratio of  $\text{HNO}_3$  to  $\text{NO}_2$  depends upon the model OH abundances and  $\text{HNO}_3$  photolysis rates. Figure 12-35 presents a comparison of model calculated  $\text{HNO}_3/\text{NO}_2$  ratios at about  $30^\circ$  in summer, showing that these models are in rather good agreement on this photochemical parameter. The differences are probably largely due to differences in calculated  $\text{O}_3$  and associated optical depth effects. Figure 12-36 shows the  $\text{HNO}_3$  profiles calculated by these models. Comparison of Figures 12-36 and 12-35 reveals that the differences in model  $\text{HNO}_3$  profiles are driven principally by the calculated differences in  $\text{NO}_y$ , and thus similar ranges should be expected to apply to the calculated abundances of NO,  $\text{NO}_2$ , etc. Because of the large amount of data available for many of the  $\text{NO}_y$  species, presentation of the data and remarks regarding the comparison to models will be deferred to the chapter devoted to  $\text{NO}_x$ .

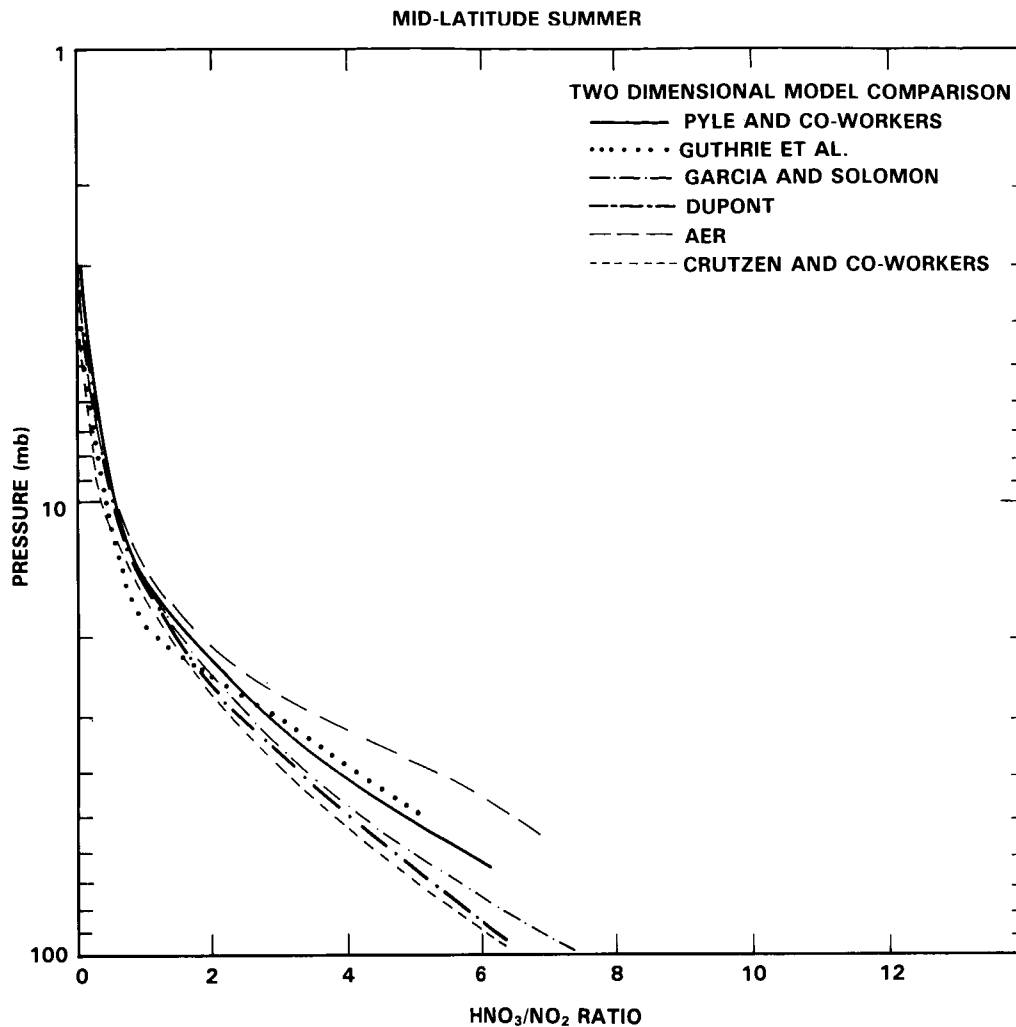


Figure 12-35. 2-D model profiles of HNO<sub>3</sub>/NO<sub>2</sub> at ~30°, Summer.

Finally, we will briefly mention the morphology of a few constituents that have not yet been measured, at least not as a function of latitude. Figure 12-37 presents contour plots of the computed N<sub>2</sub>O<sub>5</sub> distributions from the residual Eulerian model of Stordal *et al.* In addition to the variations in these constituents driven by the calculated gradients in NO<sub>y</sub> (eg. Figure 12-34 above) and the sharply descending contours at high latitude characteristic of the residual circulation models, there are also strong variations with latitude which are due to calculated gradients in photochemical production and loss terms. This is particularly pronounced in the calculated N<sub>2</sub>O<sub>5</sub> distribution in high latitude winter, where almost all the available NO<sub>x</sub> (N + NO + NO<sub>2</sub> + NO<sub>3</sub> + 2 x N<sub>2</sub>O<sub>5</sub>) is chemically converted into N<sub>2</sub>O<sub>5</sub> in present models.

The sequestering of NO<sub>x</sub> in the N<sub>2</sub>O<sub>5</sub> reservoir species has potentially important consequences on O<sub>3</sub> in high latitudes, as discussed by Ko *et al.* (1984) and suggests the need for global measurements of this species.

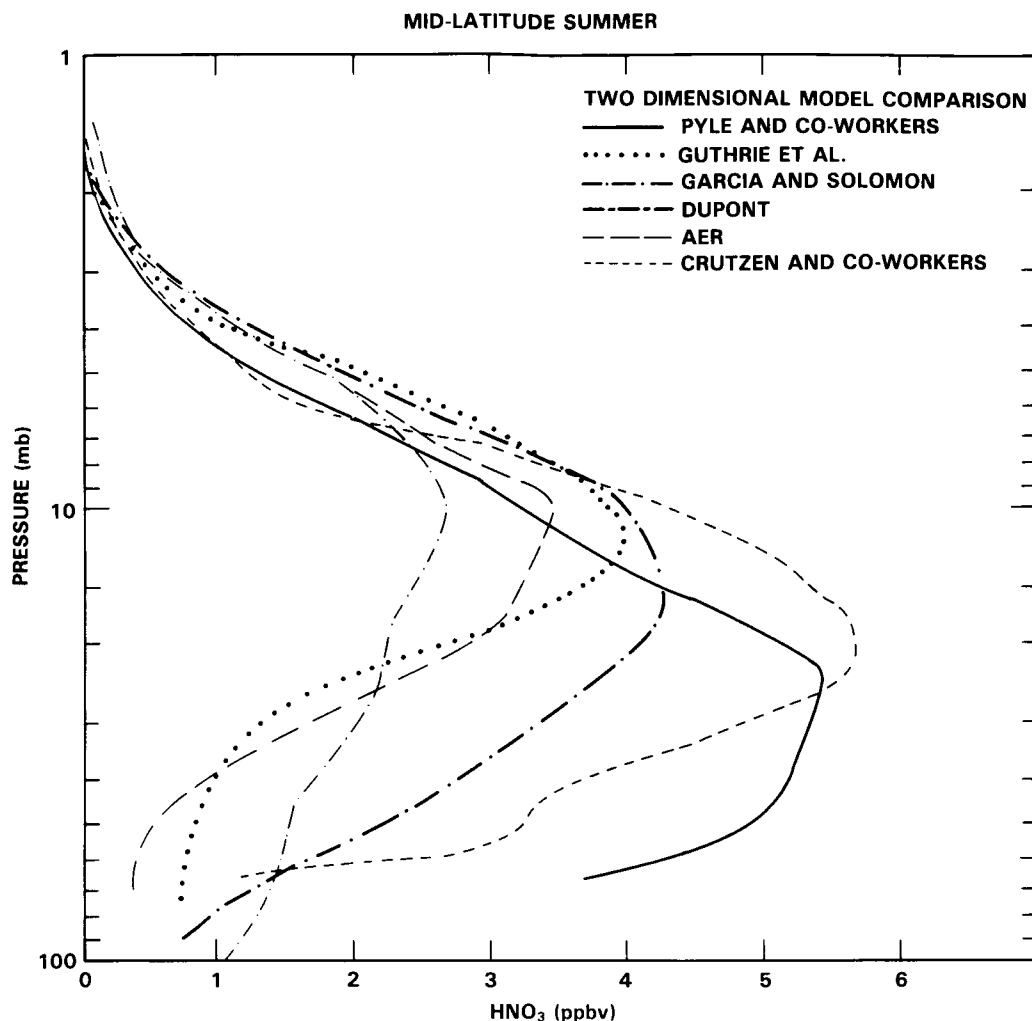


Figure 12-36. 2-D model profiles of HNO<sub>3</sub>, ~30°N.

(iv) ClO<sub>x</sub>

This subsection will provide an overview of model results for odd chlorine species, beginning with a discussion of the latitude-altitude distributions of the species from 2-D model calculations. The overall morphology of the species' behaviour as functions of altitude and latitude is sufficiently similar that only the results from one model (the AER model) will be given. In anticipation of the comparison of model results with observations to be presented in the ClO<sub>x</sub> chapter (Chapter 11), a comparison of the calculated profiles for ClO, HCl, and ClNO<sub>3</sub> from different models will be presented. Detailed description of the diurnal behaviour of the chlorine species will be discussed in Chapter 11.

In the models, production of total chlorine (Cl<sub>y</sub>) is from the photodecomposition of the halocarbons (CH<sub>3</sub>Cl, CCl<sub>4</sub>, CH<sub>3</sub>CCl<sub>3</sub>, F-11 and F-12) and removal is via transport into the troposphere followed by rainout and other deposition. Figure 12-38 shows the latitude-altitude cross-section of model calculated Cl<sub>y</sub>. Cl<sub>y</sub> is well mixed in the upper stratosphere because of the lack of photochemical removal processes.

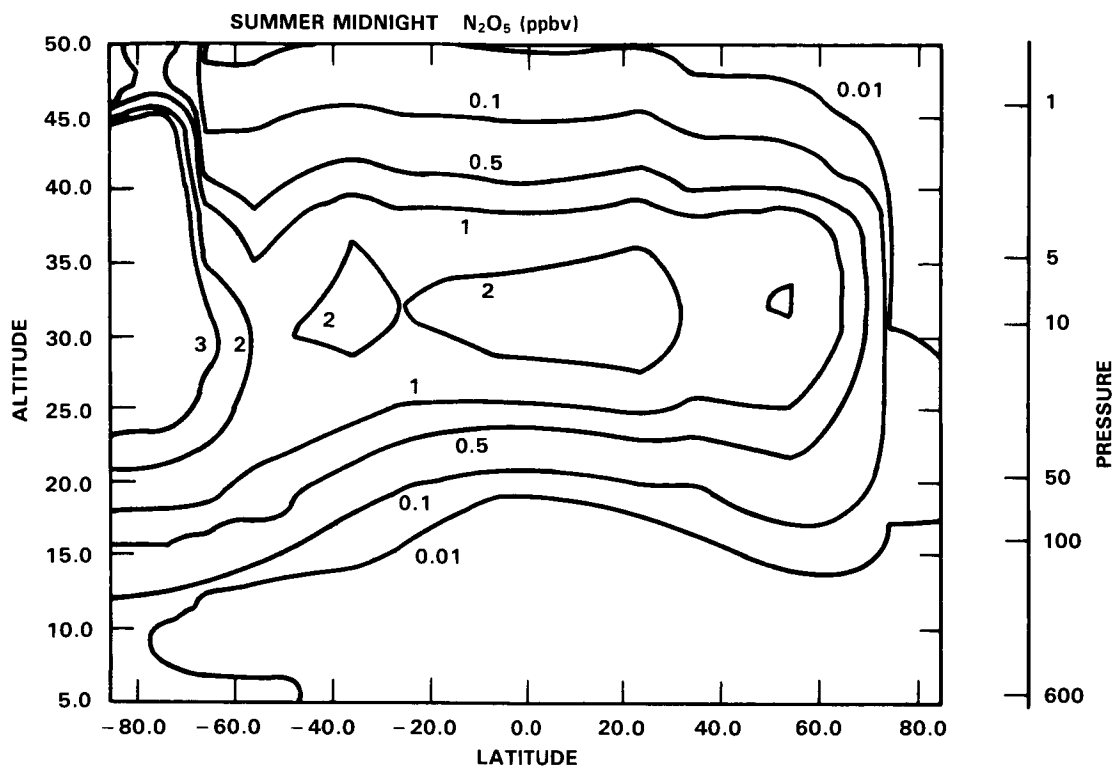


Figure 12-37. Latitude-height cross-section of  $\text{N}_2\text{O}_5$  from the model of Stordal *et al.* (1985).

The calculated distributions in the lower stratosphere differ in various models and are dependent on the transport scheme used and the heterogeneous removal process assumed in the troposphere.

In the stratosphere, the chlorine species can be conveniently separated into HCl and  $\text{Cl}_x$  which comprises Cl, ClO, and  $\text{ClONO}_2$  and HOCl. The species in the  $\text{Cl}_x$  group have interconversion lifetimes of a few hours or shorter, while transformation between HCl and  $\text{ClO}_x$  has a typical time constant of approximately one day or longer (Ko and Sze, 1984). Species in the  $\text{ClO}_x$  group exhibit large diurnal variation, but the concentrations of HCl and the  $\text{ClO}_x$  group show little variation throughout the day.

Figure 12-39 shows the calculated altitude-latitude cross-section of HCl. In the upper stratosphere, the bulk of the  $\text{Cl}_y$  is in the form of HCl as evident from the similarity between the distributions of HCl and  $\text{Cl}_y$ . The distribution in the lower stratosphere is influenced by the formation of  $\text{ClONO}_2$  where its concentration reaches comparable magnitude to that of HCl.

Figure 12-40 shows the calculated altitude-latitude cross-section of the noontime concentration of  $\text{ClO}_x$ . Note the factor of 2 increase in concentration of  $\text{ClO}_x$  from the equator to  $60^\circ$  around 40 km in the northern hemisphere. This feature in the model results is consistent with the model results on  $\text{CH}_4$  which show a factor of 2 decrease from the equator to the high latitudes around 40 km. Since  $\text{CH}_4$  mediates the conversion of  $\text{ClO}_x$  to HCl via the reaction  $\text{Cl} + \text{CH}_4 \rightarrow \text{HCl} + \text{CH}_3$ , lower concentrations of  $\text{CH}_4$  in the high latitudes should favour formation of  $\text{ClO}_x$  at high latitudes (cf. Solomon and Garcia, 1984b). Superimposed on the latitudinal behaviour is the seasonal variation reflecting the change in OH concentration where

## ASSESSMENT MODELS

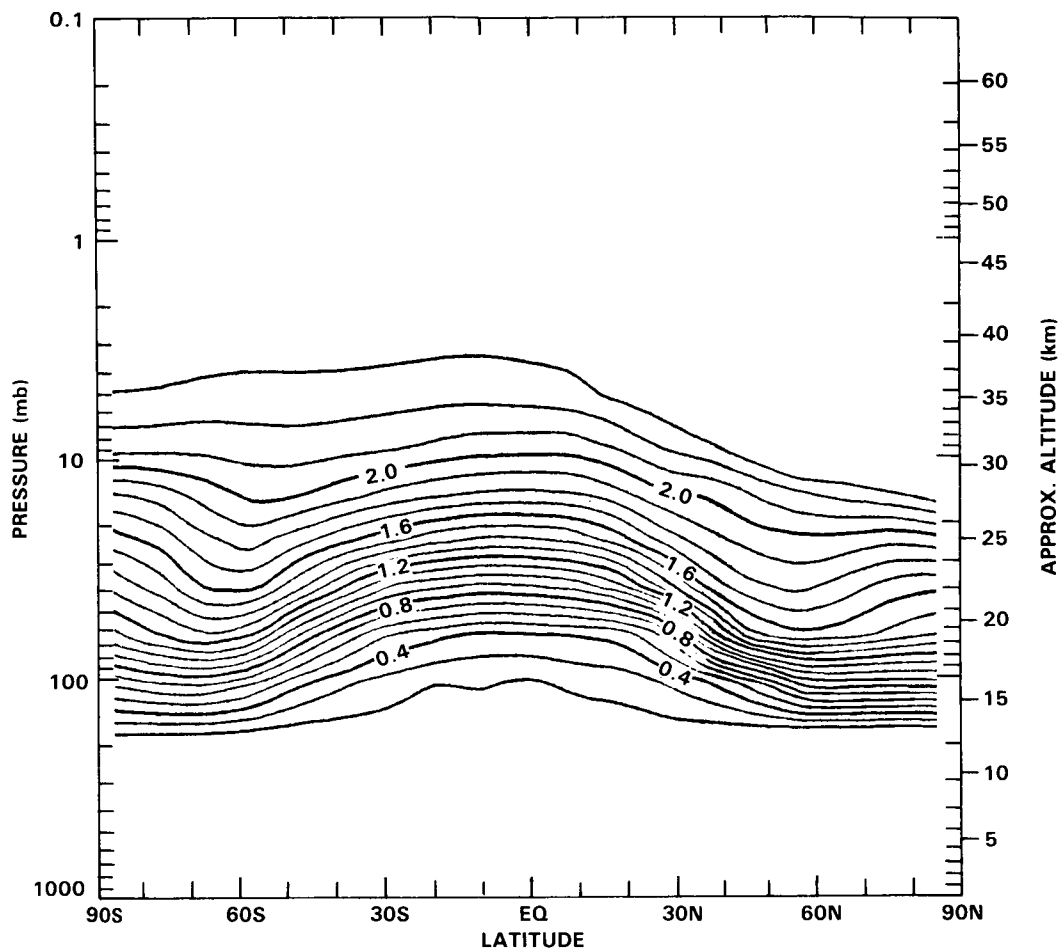


**Figure 12-38.** Calculated volume mixing ratio of  $\text{Cl}_y$  as a function of latitude and altitude for April. The contour levels are labelled in units of ppbv. The result is from the AER model. The photochemical scheme is identical to that in Ko *et al.* (1984) except for updating of reaction rates. The dynamical scheme is a refinement of the scheme described in Ko *et al.* (1985). The source of  $\text{Cl}_y$  is from photodecomposition of  $\text{CH}_3\text{Cl}$ ,  $\text{CH}_3\text{CCl}_3$ ,  $\text{CCl}_4$ , CFC-11, and CFC-12 and removal is by washout and rainout in the troposphere with lifetime of about ten days.

higher OH concentration in the sunlit hemisphere will also help to convert HCl to  $\text{ClO}_x$  via the reaction  $\text{OH} + \text{HCl} \rightarrow \text{H}_2\text{O} + \text{Cl}$ .

The calculated cross-sections for the noontime concentrations of Cl, ClO,  $\text{ClNO}_3$ , and HOCl are shown in Figure 12-41. The figures show that  $\text{ClNO}_3$  has the highest concentration in the lower stratosphere whereas ClO and HOCl become more important in the upper stratosphere. The species ClO and  $\text{ClNO}_3$  exhibit latitudinal features similar to that of  $\text{ClO}_x$ .

The above features are common to all model results although the latitudinal gradient in upper stratospheric  $\text{ClO}_x$  in the classical Eulerian models are less pronounced because of the smaller latitudinal contrast in  $\text{CH}_4$  (see above).

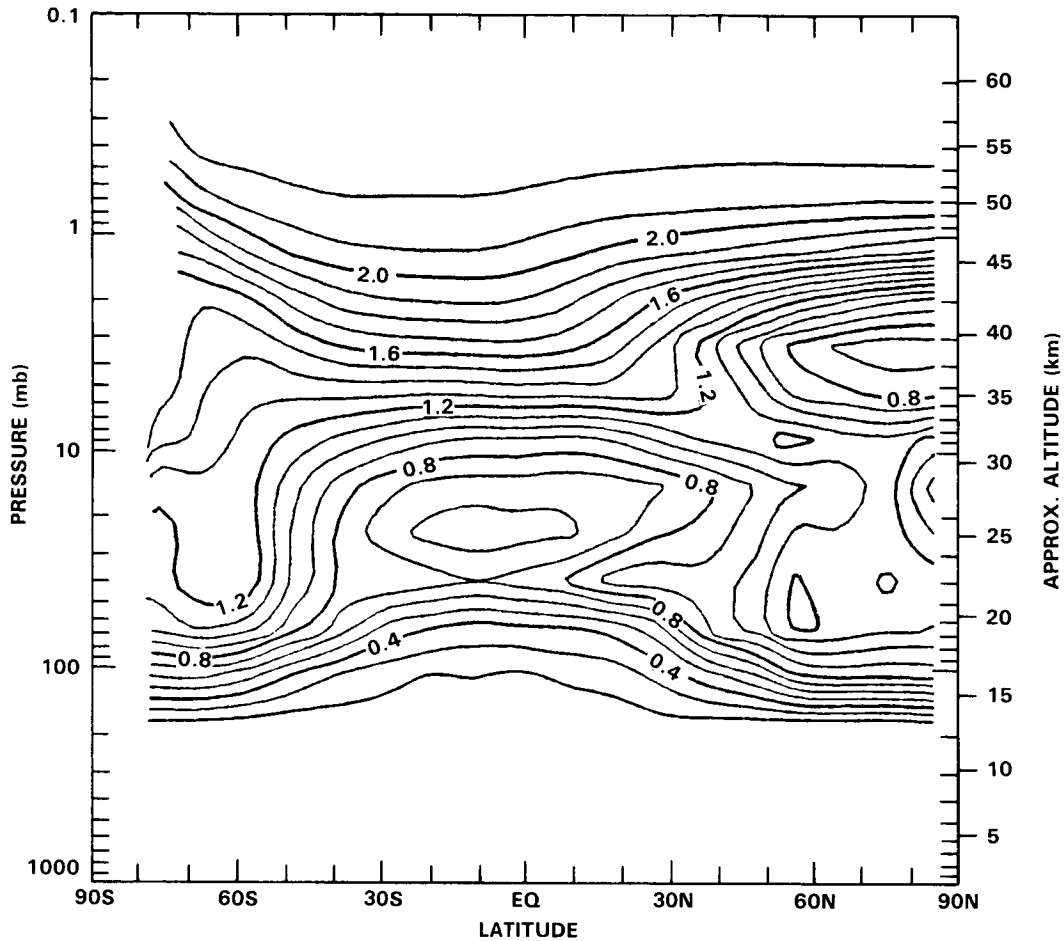


Figure 12-39. Same as Figure 12-38, for HCl (ppbv).

Figure 12-42 gives the altitude profiles of  $\text{Cl}_y$  from different models. The relatively small spread (2.1-2.5 ppbv) in the calculated values in the upper stratosphere results from the slightly different scenarios for the halocarbon emissions and transport parameters assumed in the models. The spread of values among the models in the lower stratosphere is, however, larger. In general, compared to models using the classical Eulerian circulation, those models using a diabatic or residual circulation and small eddy diffusion coefficients have lower concentrations at the tropical regions and higher concentrations at the high latitudes in the lower stratosphere. This is best illustrated by the calculated column abundances of HCl, which will be discussed in more detail in Chapter 11. In a classical Eulerian model (e.g. MPI), the ratio of the abundance at  $60^\circ\text{N}$  to that at the equator is about a factor of 2. In models using diabatic/residual circulations (NOCAR, AER), the ratio is about 3:1 which is in better agreement with the observations.

Figure 12-43 shows calculated profiles of  $\text{ClO}$ , HCl, and  $\text{ClNO}_3$  from different models corresponding to mid-latitudes ( $\sim 30^\circ\text{N}$ ) and summer condition. Given the diversities in the treatment of dynamic transport and diurnal variation in the various models, it remains difficult to isolate a single cause for the discrepancies. However, much of the difference could be explained in terms of the differences in the calculated  $\text{Cl}_y$  (Figure 12-42) and then differences in the partitioning of  $\text{Cl}_y$  species related to the coupling to the  $\text{NO}_x$  chemistry. To isolate the effect of partitioning, the ratios  $\text{ClNO}_3/\text{ClO}$  and  $\text{ClO}/\text{HCl}$  are plotted

## ASSESSMENT MODELS

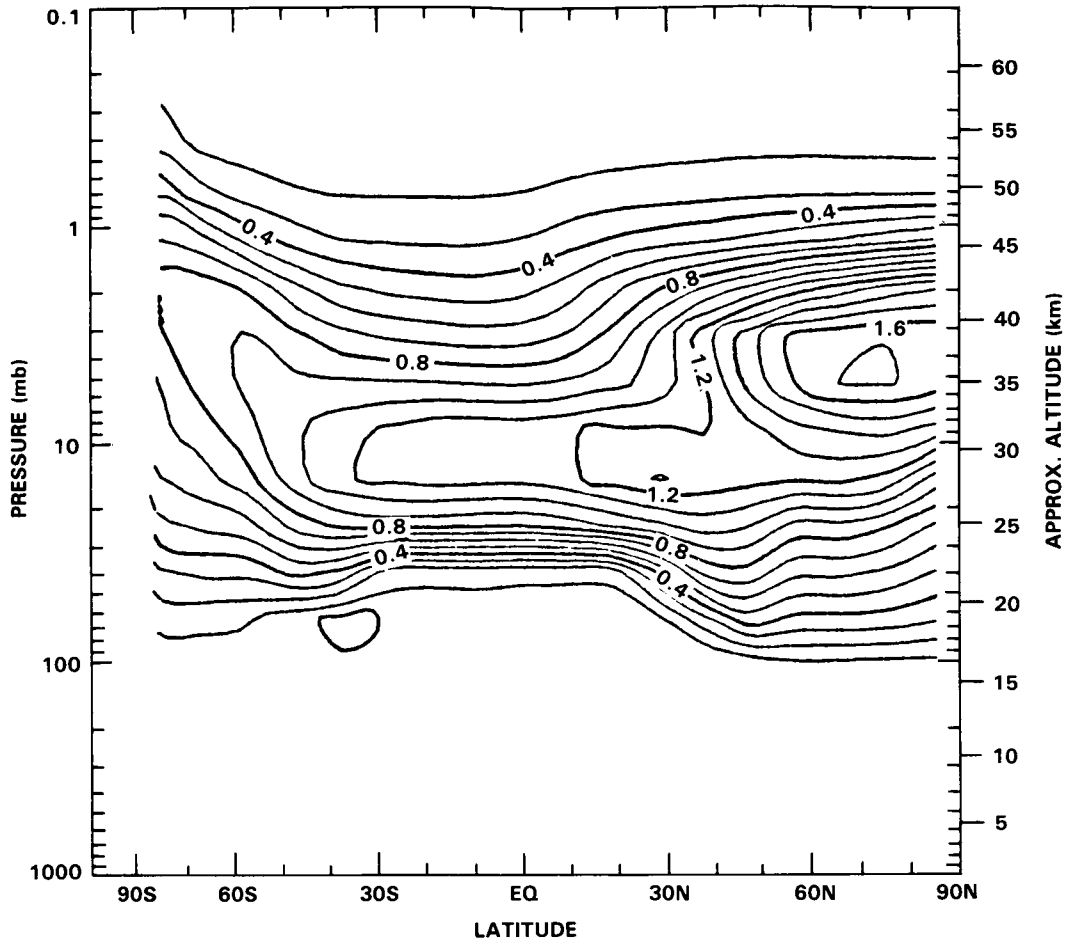


Figure 12-40. Same as Figure 12-38, for  $\text{ClO}_x$ , which is the sum of Cl, HOCl,  $\text{ClNO}_3$  and ClO.

in Figure 12-44. The factor of 2 discrepancy in the ratios among the models below 30 km can be attributed in part to the differences in the calculated  $\text{NO}_y$ , where higher  $\text{NO}_y$  tends to favour the production of  $\text{ClNO}_3$  at the expense of ClO, resulting in a larger  $\text{ClNO}_3/\text{ClO}$  ratio and smaller ClO/HCl ratio.

### (v) $O_x$

The observed seasonal and latitudinal distribution of the total ozone column is shown in Figure 12-45a. Important features that models should simulate are: low equatorial abundances; an increase towards high latitudes; the seasonal variations at mid and particularly high latitudes; the spring maximum in both hemispheres, at the polar region in the Northern Hemisphere but at  $50^\circ - 60^\circ$  latitude in the Southern Hemisphere; a fall minimum in both hemispheres around  $60^\circ$  latitude.

In general, models with high diffusion (mostly classical Eulerian models) underestimate the latitudinal contrasts (Figure 12-45b-e). The equatorial abundances are generally overestimated due to too strong an eddy transport. The seasonal variation at high latitudes is usually less than observed.

ASSESSMENT MODELS

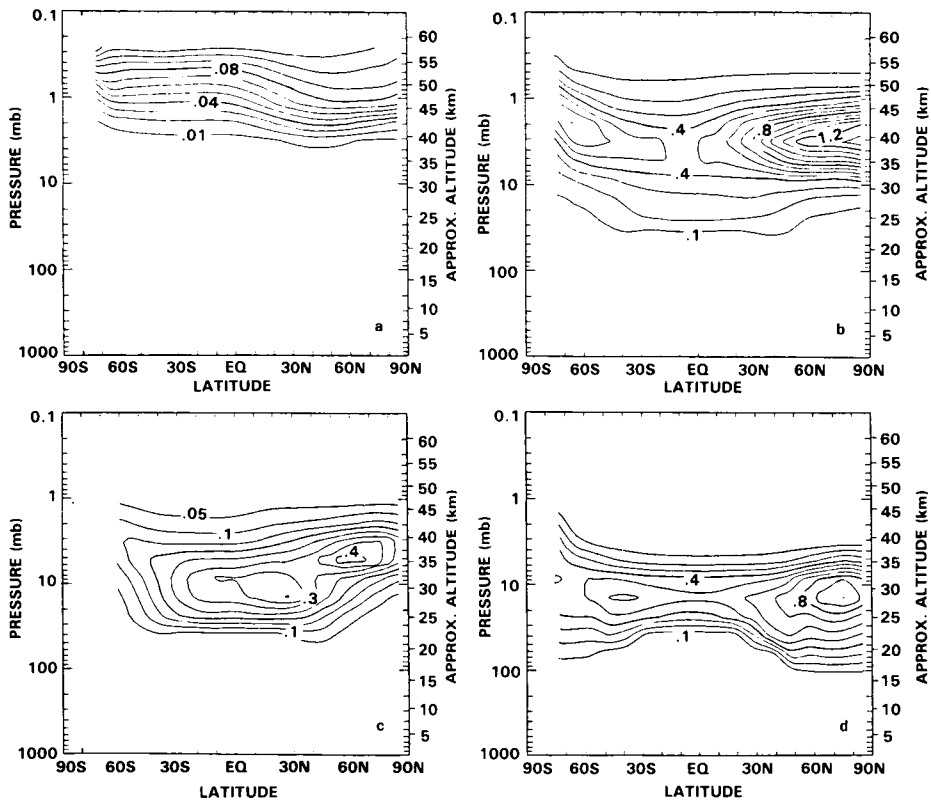


Figure 12-41. Same as Figure 12-38, for Cl in (a), ClO in (b), HOCl in (c), and ClNO<sub>2</sub> in (d).

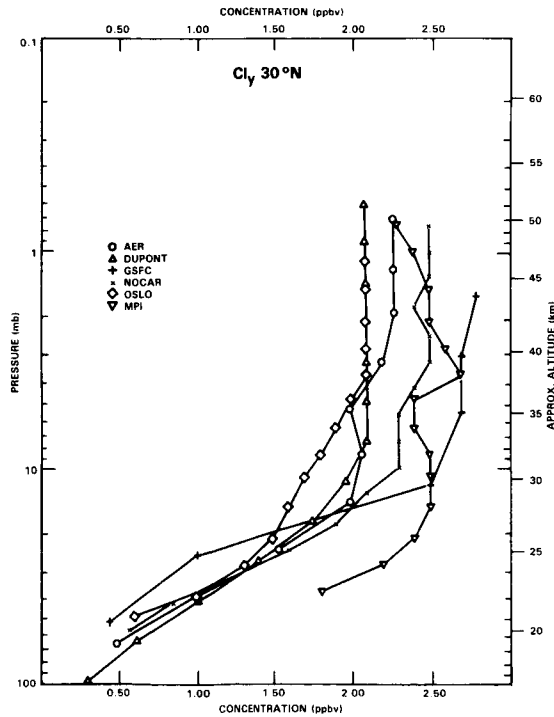


Figure 12-42. Calculated profiles of Cl<sub>γ</sub> from different models for ~30°N for summer conditions.

ASSESSMENT MODELS

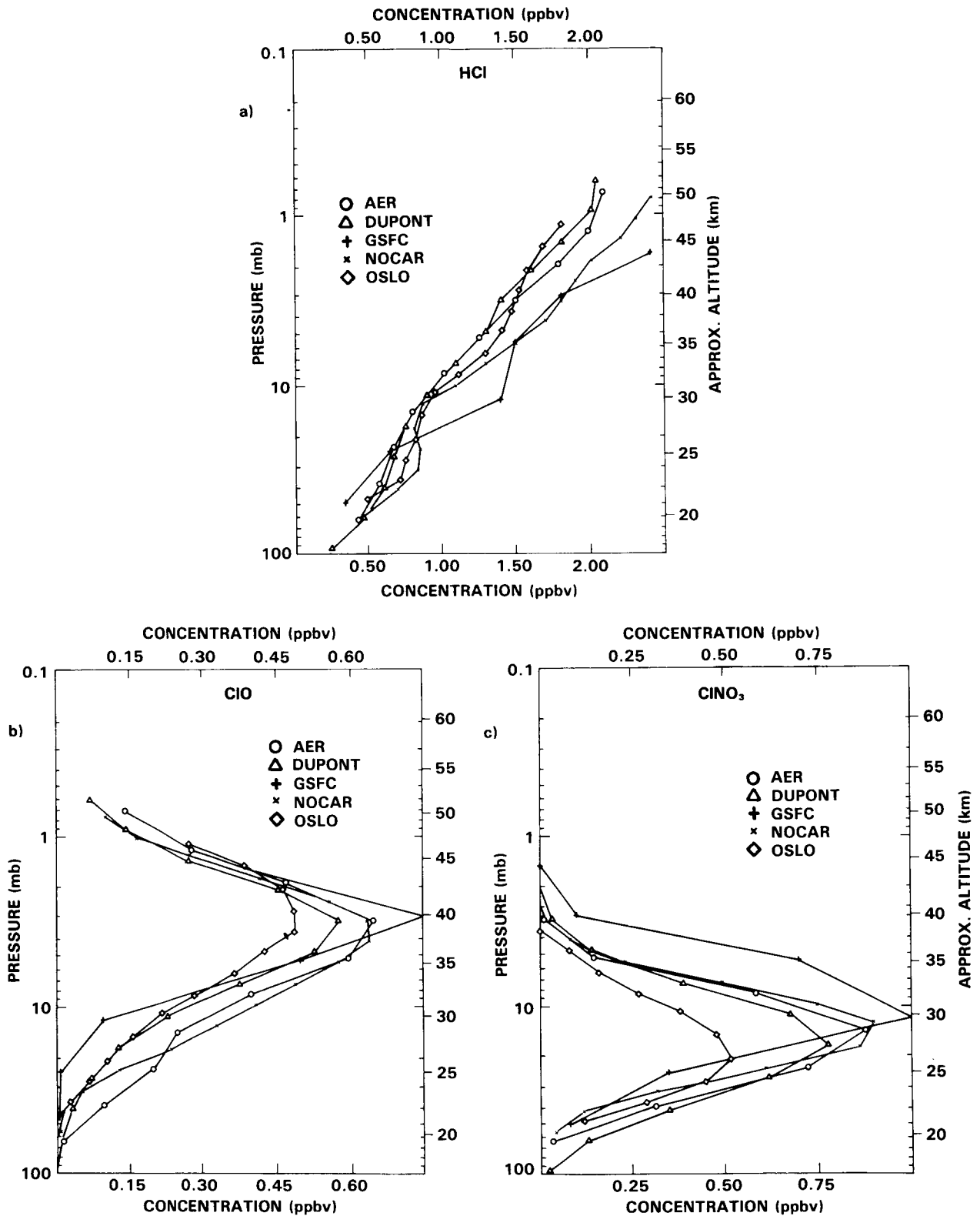


Figure 12-43. Calculated profiles of (a) HCl, (b) ClO, and (c) ClONO<sub>2</sub> for different models for mid latitudes (~30°N) for summer conditions.

ASSESSMENT MODELS

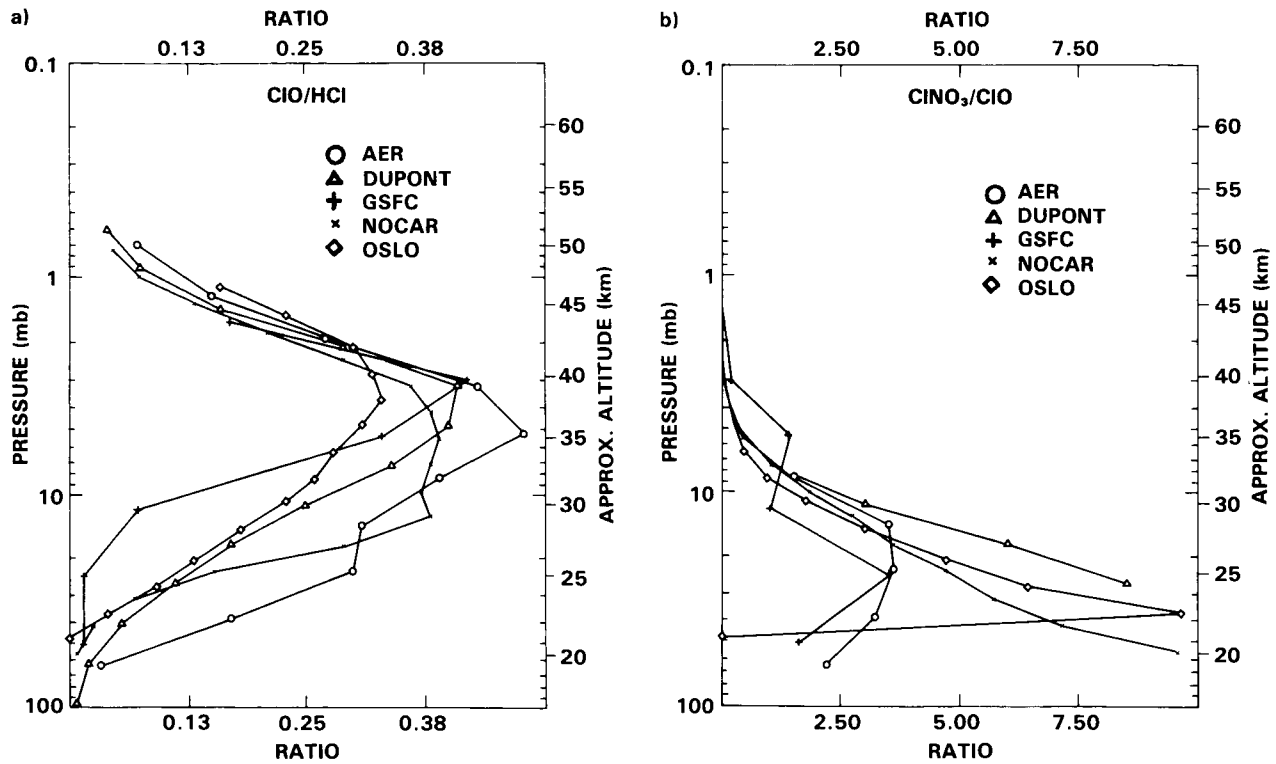


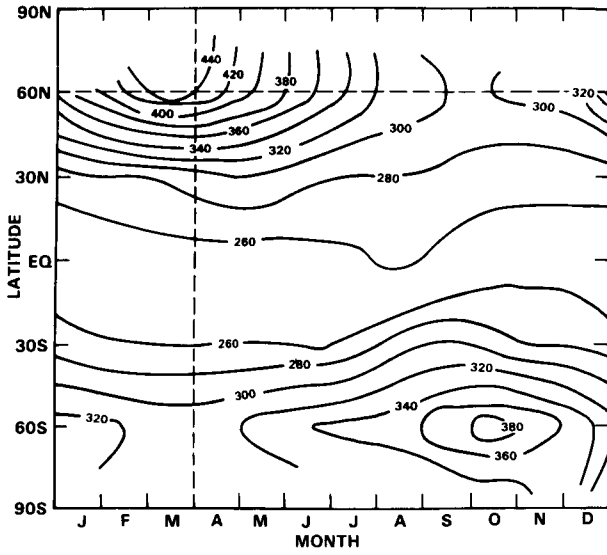
Figure 12-44. Calculated ratio of (a) ClO/HCl and (b) ClONO<sub>2</sub>/ClO from different models as deduced from results indicated in Figure 12-43.

The agreement with the observations varies from model to model and essentially reflects how well the cancellation between the mean Eulerian circulation and the eddy fluxes is achieved. The Eulerian model of Crutzen and Schmailzl (1983) simulates the ozone columns in reasonable agreement with the observations, not surprising since the diffusion coefficients in this model are chosen to give the best fit to observed ozone abundances (Hidalgo and Crutzen, 1977).

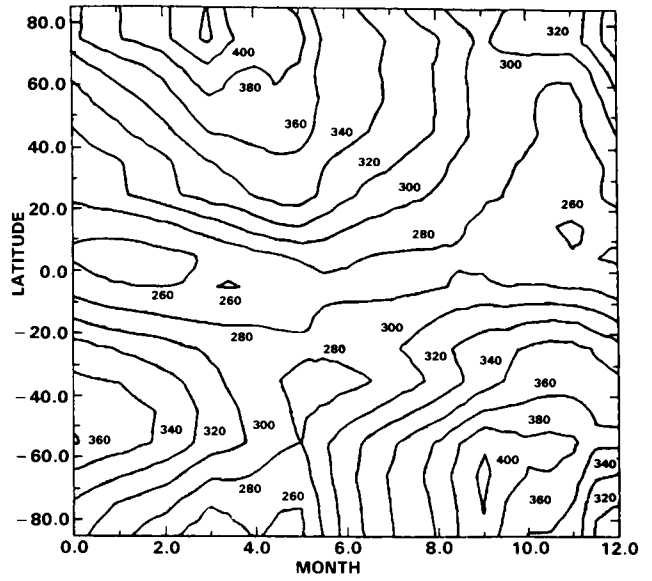
The diabatic circulation models all get equatorial abundances in good agreement with the observations (see Figure 12-45). Since only low horizontal diffusion is used, larger latitudinal gradients in the observed range can be obtained. Indeed, the abundances at high latitudes are sometimes too high (Ko *et al.*, 1985 Figure 12-45h). Figure 12-45f-h show that there is a substantial individual variation between the diabatic and residual circulation models, reflecting mostly differences in adopted values of diabatic heating rates and diffusion coefficients. For instance, the model of Ko *et al.* (1985) uses hemispherically symmetric heating rates giving only small differences in the ozone columns of the two hemispheres. In the model of Stordal *et al.* (1985) (Figure 12-45g) the adopted asymmetric heating rates give rise to an interhemispheric asymmetry in ozone which is even larger than observed, with the spring abundances in their model considerably lower than observed in the Southern Hemisphere.

Figure 12-46a presents mid-latitude O<sub>3</sub> height profiles for summer and winter conditions from a 2D model (Solomon and Garcia, 1984b), chosen to illustrate the seasonal variations at mid-latitude. This model represents values in the middle of the model range and has a seasonal variation which is typical of all the models. The seasonal variation in the upper stratosphere is small. It increases at lower altitudes and

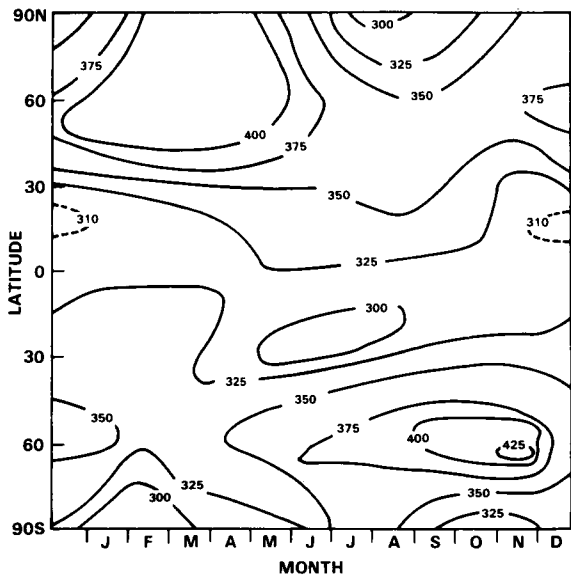
**ASSESSMENT MODELS**



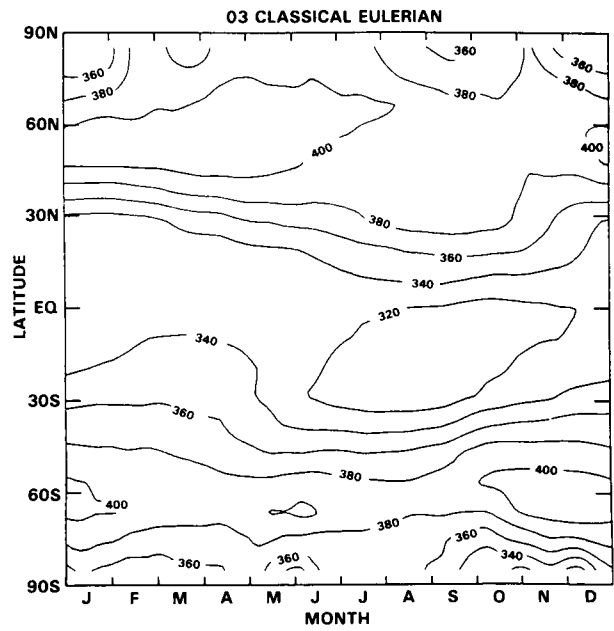
a) Observations



b) MPI



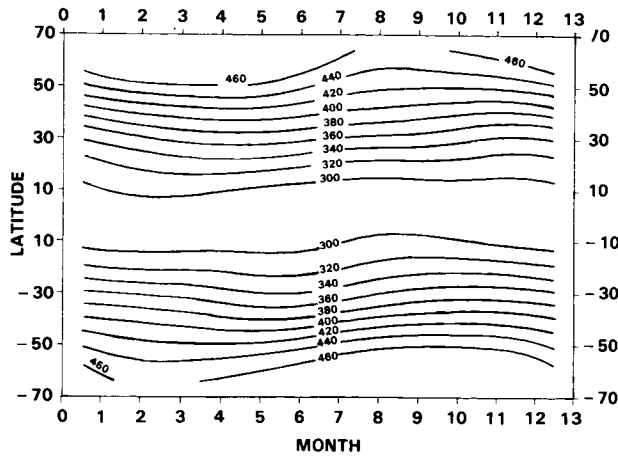
c) RAL (Eulerian)



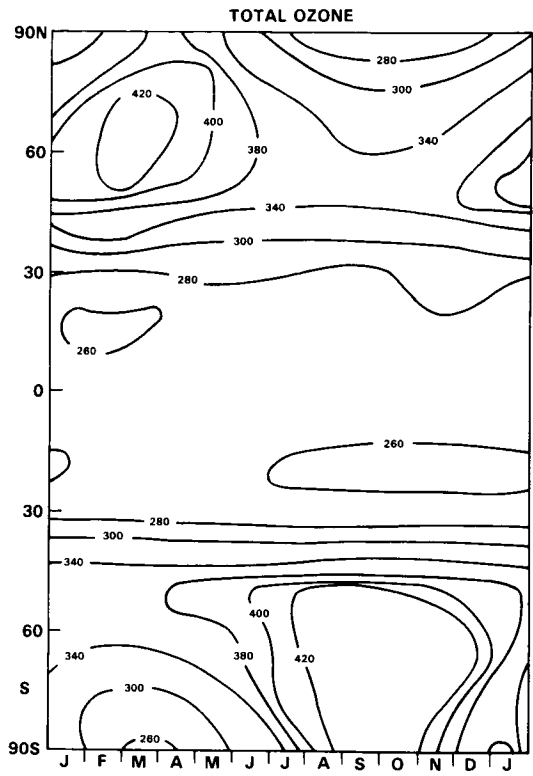
d) AER (Eulerian)

**Figure 12-45.** Total ozone columns as function of latitude and time of the year (m. atm cm).

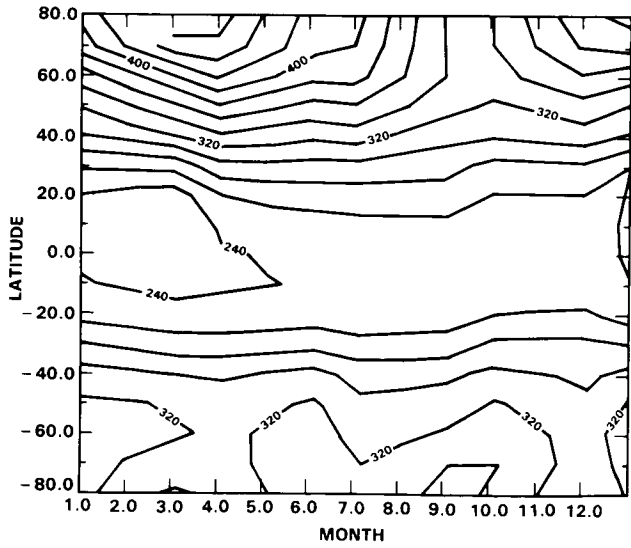
ASSESSMENT MODELS



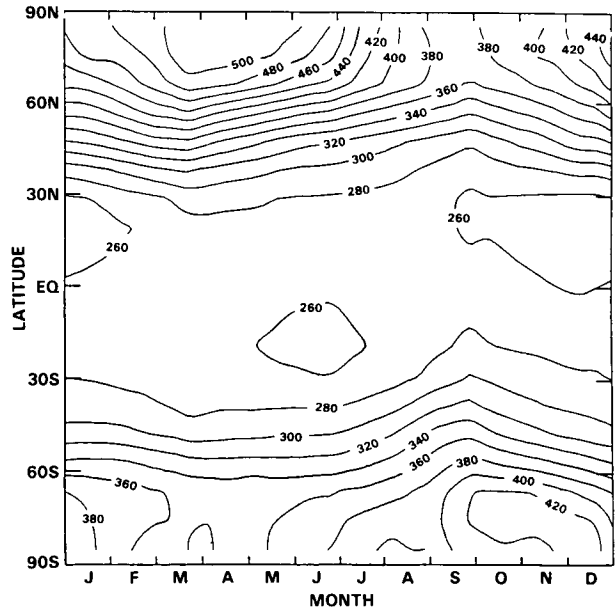
e) DuPont



f) RAL (Diabatic)



g) UOslo



h) AER (Diabatic)

Figure 12-45. Continued

ASSESSMENT MODELS

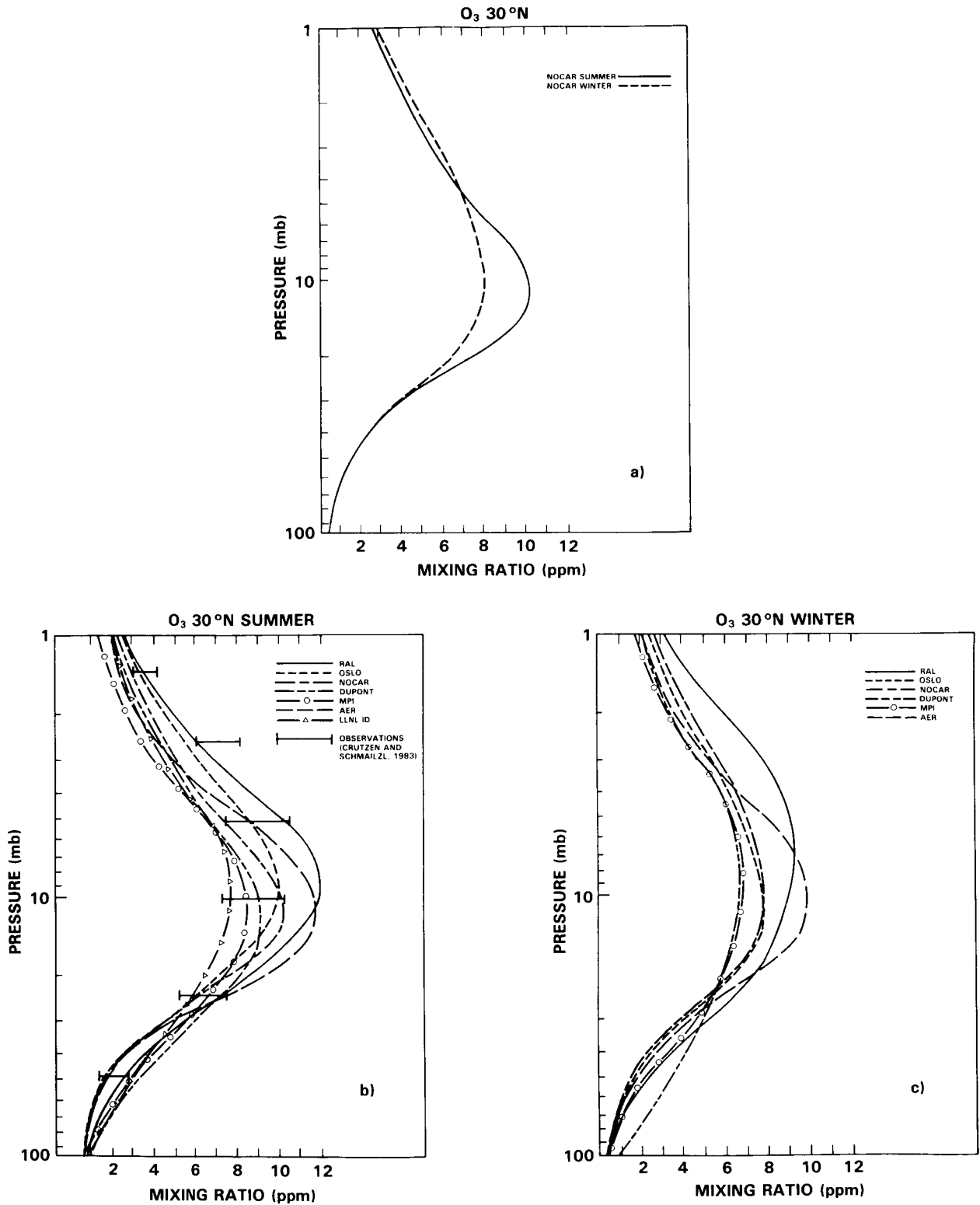


Figure 12-46. Altitude profiles of O<sub>3</sub> volume mixing ratio, 30°N. a) Summer and Winter, NOCAR model; b) Summer profiles, various models; c) Winter profiles, various models;

amounts to about 2 ppm in the peak region. There is no substantial seasonal variation in the altitude of the peak.

The summer profiles for 30° latitude for several models are shown in Figure 12-46b. In the 40 km region the models consistently underestimate O<sub>3</sub> compared to the observations except for the RAL model which has low concentrations of ClO<sub>x</sub> and NO<sub>x</sub> (see Figure 12-34). In this region, ozone is photochemically controlled, and the direct effect of transport is of minor importance. However, transport processes influence the ozone abundances indirectly through transport of NO<sub>y</sub> and Cl<sub>y</sub>. The discrepancy between models and observations could be due to lack in the present understanding of the ozone loss chemistry, possibly in all of the HO<sub>x</sub>, NO<sub>x</sub> and ClO<sub>x</sub> cycles, since they all contribute similarly to the ozone loss in the altitude region in question. The other possibility is that the production of ozone through the oxygen photolysis is not presently represented adequately in the models. The inability of models to simulate ozone in the photochemically controlled upper stratosphere represents a major limitation of current photochemical theory. This must be kept in mind when estimated effects of photochemical perturbations are evaluated. For illustrative purposes the profile from a 1-D model (LLNL) is included in Figure 12-46b. The 1-D profile falls within the range of 2-D model profiles. The problem of modelling ozone in the 40 km region appears to be independent of the dimensionality of the models.

From Figure 12-46c where winter profiles are shown, it is seen that the models underestimate ozone around 40 km regardless of the time of year. Note that the spread between the models is about the same in the winter as in the summer season.

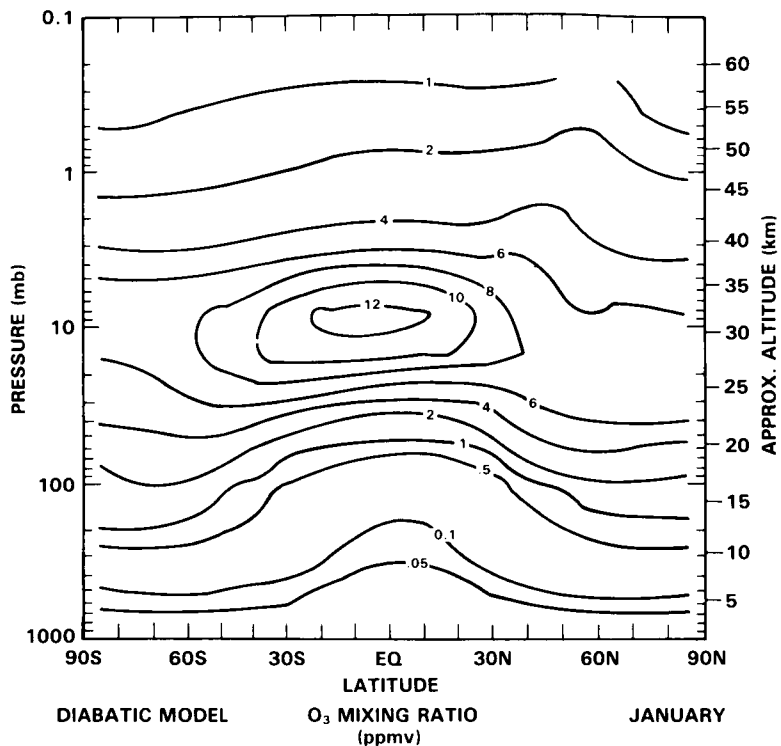
Figure 12-47a-b shows latitude-altitude cross sections of ozone mixing ratios under solstice conditions. Results from the two AER models (one diabatic and one Eulerian) have been chosen since the two models have identical photochemistry and only differ in the transport representation. However, all the 2-D models from which data is used in this chapter show common features in the photochemically controlled domain. The region of maximum mixing ratios is located in the tropics at about 30 km in all models. The peak values range from about 9 to 12 ppm, which is also the range of the values observed from satellites. The modelled latitudinal extent of the peak is also similar in the models.

The most significant differences between the models occur in the lower stratosphere in the dynamically controlled region. In general, the mixing ratio surfaces slope more steeply downward and poleward at mid and high latitudes in the diabatic type of models (Figure 12-47a) than in the classical Eulerian models (Figure 12-47b). This behaviour can be attributed mainly to the difference in horizontal mixing in the two kinds of models and has important consequences for the latitudinal distribution of the total ozone columns. The highest ozone concentrations occur in the lower stratosphere. The slope of the mixing ratio surfaces in this region will therefore determine the latitudinal variation of the maximum ozone concentrations and thereby the total columns as well. The large latitudinal gradient in the distribution of total ozone columns in the AER diabatic model (Figure 12-45h) is therefore a reflection of the steep downward and poleward slopes of the mixing ratio surfaces in the lower stratosphere in this model (Figure 12-47a).

## 12.7 CHEMISTRY IN THREE-DIMENSIONAL MODELS

During the past decade a number of three-dimensional atmospheric models incorporating a formulation of chemically active trace species has been developed. The complexity of both the physics and chemistry in these models varied widely. Earlier studies of ozone transport with three-dimensional models had been conducted by Hunt (1969) and by London and Park (1973, 1974), but the study of Cunnold *et al.* (1975,

**ASSESSMENT MODELS**



a)

b)

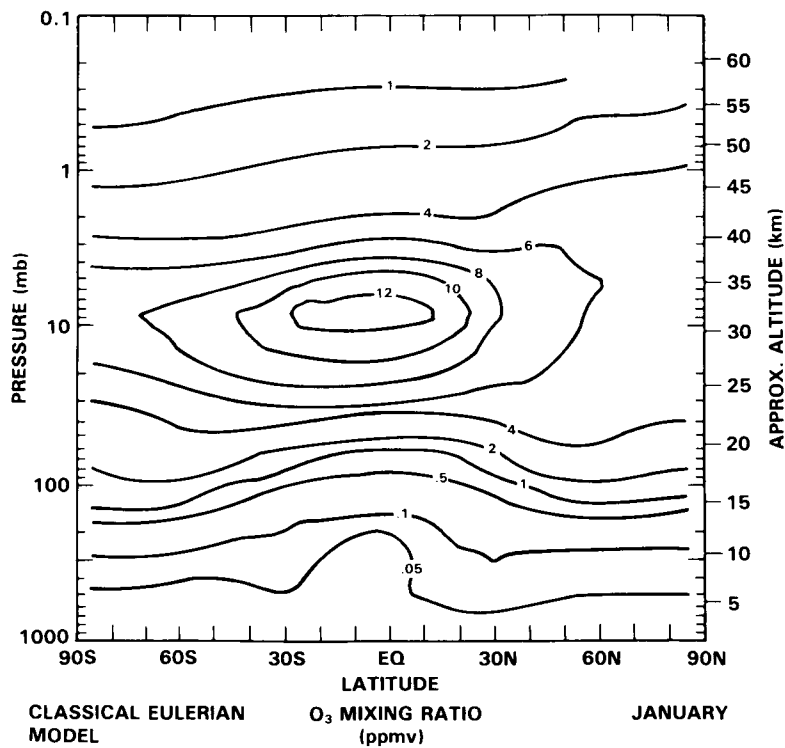


**Figure 12-47.** Ozone mixing ratio cross-sections, solstice conditions (ppmv). a) AER Diabatic model; b) AER Eulerian model.

1980) was notable in that for the first time multi-year simulations were conducted to study the relative importance of chemistry and dynamics in maintaining the distribution of ozone. A low resolution (six zonal wave-numbers) quasi-geostrophic model was used to simulate the gross features of the wind and temperature fields of the atmosphere. The model included simplified ozone chemistry and a specified (altitude dependent only)  $\text{NO}_x$  distribution. Despite the extremely simplified treatment of both the chemistry and the dynamics, the model was successful in simulating a number of features of the observed ozone fields, in particular the seasonal evolution of total column ozone. Schlesinger and Mintz (1979) employed the same simplified treatment of the chemistry in a primitive equation GCM which included comprehensive physics. Unfortunately, the model was integrated for such a short time (six weeks from winter solstice), that the ozone had insufficient time to evolve to a satisfactory wintertime distribution. In addition, the model winter hemisphere had an extra meridional cell in both the troposphere and stratosphere not present in the observations.

Mahlman *et al.* (1980) conducted two ozone tracer experiments using the general circulation model described by Manabe and Mahlman (1976). They employed the 'off-line' approach adopted by Mahlman and Moxim (1978) in which wind and temperature fields from the GCM simulations are stored and later used as input to a separate tracer model. In this approach the constituents (ozone in this instance) are free to react chemically as they are transported, but the chemistry cannot affect the dynamics. In the first experiment, the ozone mixing ratio at the top model level (10 mb) was specified constant everywhere. At other model levels the ozone was treated as an inert tracer with parameterized removal in the troposphere. In the second experiment, a simplified ozone chemistry was incorporated at the 10 mb level with  $\text{NO}_y$  ( $\text{NO} + \text{NO}_2 + \text{HNO}_3$ ) specified. At all other levels the treatment of ozone was identical with that for the first experiment. These experiments were integrated for four model years. The intent of these studies was to examine the roles of chemical and dynamical processes in maintaining the ozone distribution, and determine the role of those processes in producing the observed poleward and downward slope of isolines of quasi-conserved species in the lower stratosphere. These studies indicated an important role for transient waves in irreversibly mixing constituents into the winter polar vortex. Mahlman *et al.* (1980) concluded that inclusion of ozone photochemistry in the lower stratosphere was necessary to obtain a good ozone simulation.

Grose *et al.* (1984, 1985) have recently conducted simulations of the transport of stratospheric constituents using a spectral, primitive equation model (Blackshear *et al.* 1986) with a detailed formulation of the chemistry, including those species and reactions currently thought to be important for determining the ozone distribution in the stratosphere. The transport simulation is done 'off-line'. Chemistry is incorporated by grouping certain species together into families. This family concept partitions the species into groups so that, although there may be rapid chemical conversions between individual members of the family, the characteristic lifetime of the family is long in comparison to that of individual species. A 5-month simulation was conducted transporting  $\text{O}_x$ ,  $\text{NO}_y$ ,  $\text{Cl}_y$ , and  $\text{HNO}_3$ . The results of the simulations were quite encouraging, when compared with LIMS and other satellite observation. These simulations share deficiencies common to most model studies of the stratospheric ozone distribution. In particular, the ozone mixing ratio is lower than observed in the upper stratosphere, and the nitric acid maximum in winter high latitudes is underpredicted. These deficiencies appear to be associated with our understanding of the chemical mechanisms involved, rate coefficients, spectroscopic data, or some combination thereof. Cariolle and Deque (1984) have also utilized a spectral, primitive equation model to study ozone transport. Although the ozone chemistry in the model has been coupled with the dynamics, the chemistry has been linearized using relaxation times inferred from a 2-D photochemical model. The results from a first integration of 45 days show a successful simulation of the zonally averaged total  $\text{O}_3$  column in the Southern Hemisphere that deviates from the observation by less than 10%. In this hemisphere the ozone variability is found

## ASSESSMENT MODELS

to be the result of the action of transient medium-scale waves with zonal wavenumbers 4, 5 and 6, in fairly good agreement with observation. Due to the short integration time compared to the photochemical relaxation time, the O<sub>3</sub> content simulated in the winter northern hemisphere was underpredicted. These results have now been improved by increasing the integration period to 6 months and by replacing the simple Newtonian cooling approximation by a more comprehensive radiative code.

Rose and Brasseur (1985) have utilized a hemispheric, primitive equation model with coupled ozone chemistry and lower boundary at 10 km to study ozone transport during a stratospheric warming. A simplified ozone chemistry was included with a zonally average chemical source term and specified NO<sub>x</sub> (altitude dependent). The integration period was 21 days and the preliminary results presented make it difficult to judge the degree of success of this study.

As yet there are no reported results of simulations conducted using a GCM with a complete formulation of the chemistry but progress has been demonstrated with a variety of approaches as described in the foregoing discussion. Due to the severe computational burden imposed by this problem, the most fruitful approach in the near term will probably result from use of a comprehensive GCM with coupled chemistry, but using the 'family' concept. However, it should be noted that even with the development of such a model, a number of problems exist in our current understanding of both dynamics and chemistry which will inhibit our ability to achieve an accurate ozone simulation. These problems are addressed in other sections of this document.

### 12.8 ON THE USE OF MODELS FOR ASSESSMENT STUDIES

1- and 2-D models are now commonly used in studies of the middle atmosphere. Given the approximations in these models and their inability to explain adequately some of the limited number of measurements available, how do these limitations affect our confidence in assessment studies? How do we relate the 1- and 2-D model assessment calculations; has the use of 2-D models improved our assessment capability? In this section we consider these questions. Two problems are considered. First, how might certain model deficiencies in treatments of photochemistry affect assessment studies? Secondly, in what way do the 2-D models improve assessment studies? One of the advantages of 2-D models is the increased potential for radiative-dynamical-photochemical coupling. This is considered in some detail at the end of the section.

Turning first to limitations in photochemistry, we ask how discrepancies in models for the current atmosphere affect our ability to make such assessments. Consider the inability of most models to match the observations of stratospheric ozone. Calculated ozone abundances are generally 20 to 50% below observed values at ~ 40 km and above but are as much as 20% greater than the observed concentration near the ozone peak between 20 and 30 km. The magnitude of this discrepancy varies from model to model (and also depends on which observations are selected for comparison). The pattern is common to both 1-D and 2-D models, and points possibly to a fundamental problem with photochemical theory. Various hypotheses have been put forward, ranging from revisions in the molecular oxygen cross-sections, readjustments of kinetic rates within possible uncertainties or proposals of heretofore unknown chemical reactions. No simple solution is currently acceptable and resolution of these differences may have to result from a gradual evolution of the models combined with continued observations with greater absolute accuracy.

If we accept that the models are deficient somehow in their photochemistry then we should determine how these errors would affect our predictions for the perturbed stratosphere. For example, it is hard to imagine that small changes ( $\pm 50\%$ ) in the kinetic rate constants or a revision in O<sub>2</sub> photolysis rate would

grossly alter the calculated ozone depletions at high levels of chlorine. However, a new, hidden chemical cycle might have significant impact on our ability to make assessments. Any of these revisions are likely to alter the calculations of small perturbations to ozone, and research is needed to test how the proposed solutions to the high-altitude ozone problem would affect models of a hypothetical high-chlorine, high-methane atmosphere of the future.

The key element in determining the onset of major ozone reductions predicted by 1-D models at high levels of chlorine is the abundance of odd-nitrogen ( $\text{NO}_y$ ) in the middle stratosphere. The 1-D model intercomparison described above found differences as large as 50% in peak  $\text{NO}_y$  around 36 km, but generally less than 20% in modelled values for  $\text{NO}_y$  between 20 and 30 km. This range in  $\text{NO}_y$  translates into a 20% uncertainty in the amount of chlorine (i.e. from 16 to 19 ppbv) needed to achieve major ozone reductions in current 1-D models.

Observations of stratospheric odd-nitrogen species show large latitudinal and seasonal gradients which are reasonably reproduced in the upper stratosphere by 2-D models (see Chapter 10). The 1-D model results are generally representative of the mid-latitude profiles from the 2-D models. However, there are large differences between the 2-D models in  $\text{NO}_y$ , especially in the equatorial lower stratosphere where the agreement with data is generally poor. For example, the diabatic models predict low  $\text{NO}_y$ , especially below 25 km in the tropics. These results (see Section 12-7) point to the importance of a satisfactory treatment for tropospheric  $\text{NO}_y$  (its rainout, possible lightning source, etc.) and of the vertical transport in the equatorial lower stratosphere if the  $\text{NO}_y$  budget is to be modelled adequately.

How would these large differences in  $\text{NO}_y$  in 2-D models affect the calculated ozone depletions at high chlorine? At first, one might believe that the chlorine levels, at which large ozone depletions are predicted, should scale with the  $\text{NO}_y$  as is found in 1-D models. However, this scaling may not be applied directly to 2-D models because the source of the  $\text{NO}_y$  differences is related to transport phenomena. For example, in the residual circulation models, the subtropical lower stratosphere has low  $\text{NO}_y$  values. Similarly this region would have low levels of active chlorine ( $\text{Cl}_x$ ) relative to organic chlorine (e.g. CFCs). In this case, the importance of high-chlorine scenarios may only be judged on the basis of latitudinally and seasonally averaged destruction of ozone. The 1-D models attempt to simulate this averaging through their sluggish vertical transport of ozone,  $\text{NO}_y$  and  $\text{Cl}_x$ . The 2-D models include realistic seasonal variations. We may regard the diversity in  $\text{NO}_y$  concentrations of the lower stratosphere in current 2-D models as a range in the ages of air injected into the stratosphere, and hence as a range in the time over which the photochemistry has had a chance to perturb stratospheric ozone. Thus the range in stratospheric  $\text{NO}_y$  may imply a proportional range in the amount of  $\text{Cl}_x$  from tropospheric sources, with corresponding differences in the impact of photochemical perturbations to ozone. In any case it is clear that the 2-D model response is more complex than the 1-D case.

When one represents a three-dimensional system such as the atmosphere in a model of lower dimensionality (1-D or 2-D) one must in some sense average out some of the physical behaviour which occurs in the real system. When such models are used to predict the results of perturbations to the system, there is always the possibility that the averaging process has constrained the model so as to miss important interactions in the real atmosphere. One way of testing models in this context is to ask whether models of the same system at high dimensionality reveal phenomena which would affect the perturbation assessment. In particular one can look at two-dimensional models of the atmosphere to understand the effects that a more complete treatment of transport and seasonal variation would have on the global or mid-latitude 'average' profiles which are calculated by one-dimensional models. Based on such comparison it appears

## ASSESSMENT MODELS

that there are systematic differences between profiles generated by the two types of models, but that the differences can be understood in terms of the different transport representations.

A conclusion of a comparison of 1- and 2-D models, for both present day and perturbed atmospheres, is that there is at present no indication that the addition of meridional transport in 2-D models invalidates in a gross sense the results of 1-D perturbation assessments. Thus both types of model predict ozone depletions in a stratosphere with increased chlorine content. Because of the non-linear nature of the problem, this does not preclude the possibility of such a discrepancy for a different perturbation problem. Furthermore, it is clear that there are some questions (for example, possible latitude-dependent ozone changes) which 1-D models are incapable of answering. Moreover, there are systematic differences between 1- and 2-D model assessment studies (see Chapter 13) which remain to be explained.

Agreement in a gross sense between 1- and 2-D models is perhaps not surprising. For example, the transport parameterisation in 1-D models must describe broadly the flux of source gases from troposphere to stratosphere and agreement for these gases in low latitudes is inevitable. Since the latitude band from 30°S to 30°N encompasses half the volume of the atmosphere, gross agreement between a 1-D model and the globally averaged results of a 2-D model can be expected. However, detailed agreement at a particular latitude must be regarded as fortuitous. Furthermore, the hybrid nature of the 1-D model - part low latitude model, part global model and part local model - makes difficult the interpretation of assessment studies.

The difference between the diffusive transport in a 1-D model and predominantly advective transport in a 2-D model (especially in the residual mean or diabatic formulation) shows up quite strongly in the case of total  $\text{NO}_y$ . Figure 12-48a shows the budget of  $\text{NO}_y$  taken from the AER model for the mid-latitude

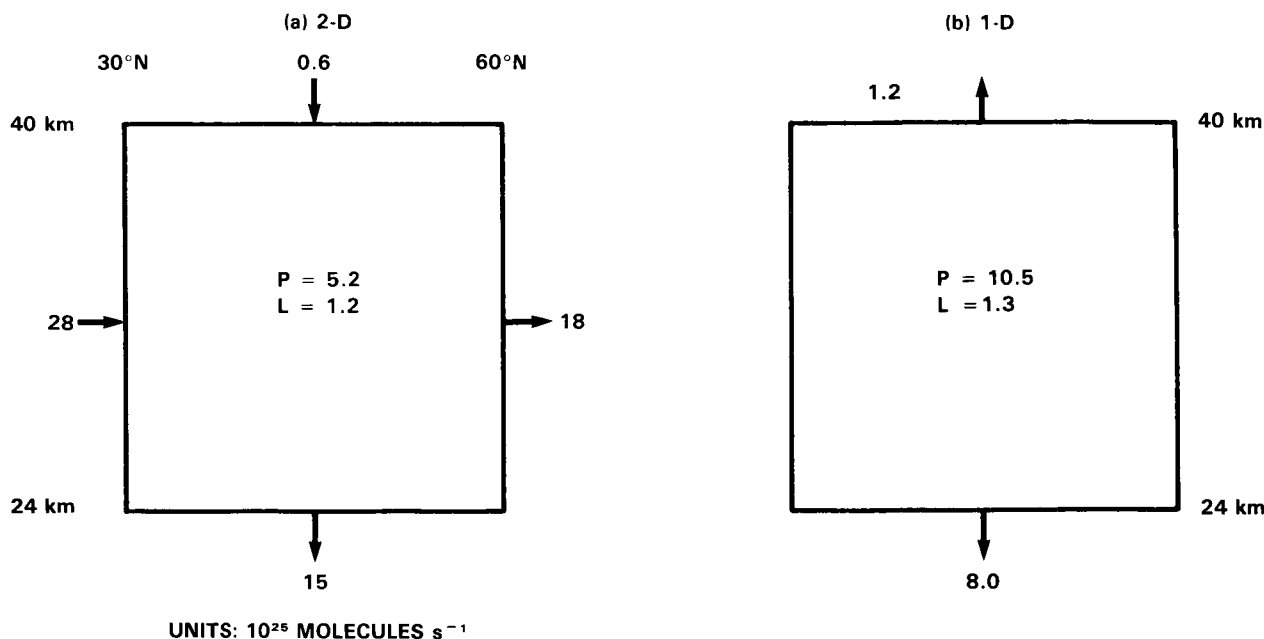


**Figure 12-48.** The budget of  $\text{NO}_y$  as calculated by 2-D (a) and 1-D (b) models. The integrated photochemical production rate ( $P$ ) and removal rate ( $L$ ) in the region are given in units of  $10^{25}$  molecules/sec.) The calculated fluxes across the boundary (in units of  $10^{25}$  molecules/sec) are also given for the region indicated. For comparison purpose, the values for the 1-D model are scaled to correspond to the same volume and surface areas given in Figure (a).

region ( $30^\circ$  to  $60^\circ$ ) between 24 to 40 km. The local concentration of  $\text{NO}_y$  is determined by the balance of the horizontal and vertical transport fluxes with the photochemical term playing a relatively minor role. In contrast, the calculated concentration in a 1-D model is maintained by the net photochemical production with diffusive transport out of the region. However, these differing effects are not surprising given that  $\text{NO}_y$  is effectively a long lived tracer and that, in its conceptual formulation, the 1-D model should approximate global averaged (not  $30^\circ$  to  $60^\circ$ ) fluxes.

In summary, while the 1-D models remain useful tools for assessment it is becoming clear that 2-D models provide a much more detailed picture of the atmospheric response to perturbations. For example, 2-D model studies indicate that ozone changes will be largest in high latitudes and that there will be some local ozone production due to the self healing effect in low latitudes. The high latitude changes suggest that some monitoring efforts should be centered on this region.

Turning to the question of the degree of feedback in 2-D models, we note that the continuity equation for ozone contains transport and photochemical terms. In one- and two-dimensional models, the transport terms can be formulated in a number of different ways and they can either be specified or calculated. If calculated, they are dependent on the radiative heating and on the eddy fluxes of heat and momentum. The photochemical term depends on the ultraviolet flux and on the distribution of the other interacting species. To make predictions of changes to the ozone layer, the interactions among all these terms must be considered.

If the coupling between chemistry, radiation and dynamics is ignored (if, for example,  $K_z$  is specified in a 1-D model, or if the meridional velocities are specified in two-dimensional models) then it is possible to make a rough estimate of the error in an assessment, since this just depends on the errors in individual species concentrations.

However, the stratosphere is highly coupled with, for example, the wind fields dependent on the radiative heating which depends on the ozone field which itself is transport dependent. At first sight this appears to suggest a major limitation of 1-D and 2-D models as assessment tools. Indeed, experiments with a 2-D model (Harwood and Pyle, 1980) show that changes in the mean meridional circulation, changes in the eddy coefficients and changes in the specified eddy momentum fluxes all have a major impact ( $> 10\%$ ) on the calculated ozone column amounts. Assessment of a perturbed stratosphere seems to require that changes in radiative and dynamical processes be modelled to high accuracy.

It is possible that the above limitations of simplified models may not be quite so serious as they seem. Perturbation experiments with a 2-D model (Haigh and Pyle, 1982) and with a GCM (Fels *et al.*, 1980) suggest that the primary adjustment of the stratosphere to changes in solar heating rates is radiative rather than dynamical. Solar heating changes due to ozone perturbations can lead to adjustments of the dynamical fields, of the longwave cooling, or both. In the two papers cited the main change is to the longwave cooling, giving rise to an altered temperature structure but with only small changes to the meridional circulation. An important exception in the calculations by Fels *et al.*, was in the region around the tropical tropopause where the dynamical adjustment was significant.

Some insight into the radiative/dynamical adjustment problem can be gained from consideration of the equations governing the global mean meridional circulation. If the quasi-geostrophic approximation is

## ASSESSMENT MODELS

made, the steady-state zonal mean fields must obey the following momentum and thermodynamic equations in the residual Eulerian formulation:

$$-f\bar{v}^* = -K_R\bar{u} + F \quad (12.13)$$

$$\bar{w}^* \frac{HN^2}{R} = Q - C - \alpha\bar{T} \quad (12.14)$$

where for simplicity, nonlinear terms have been omitted and where infrared cooling has been written in terms of a global cooling rate,  $C$ , plus Newtonian relaxation with coefficient  $\alpha$ . In the momentum equation a Rayleigh friction term,  $K_R$ , has been included. The terms  $Q$  and  $F$  represent externally imposed radiative and momentum forcing, respectively.

In the stratosphere,  $Q$  is due principally to absorption of UV radiation by ozone and  $F$  to the convergence of the Eliassen-Palm flux of planetary waves.

In addition to 12.13 and 12.14, the zonal mean fields also obey the continuity equation

$$\bar{v}_y^* + \bar{w}_z^* = 0 \quad (12.15)$$

(where compressibility and spherical geometry have been neglected), and the geostrophic balance equation

$$-f\bar{u}_z = \frac{R}{H} \bar{T}_y \quad (12.16)$$

Straightforward manipulation of the set 12.13 - 12.16 leads to a second order partial differential equation for the mean meridional streamfunction,  $\chi^*$ :

$$\bar{\chi}_{zz}^* + \frac{N^2}{f^2} \frac{K_R}{\alpha} \bar{\chi}_{yy}^* = \frac{F_z}{f} + \frac{N^2}{f^2} \frac{K_R}{\alpha} \frac{Q_y}{\Gamma} \quad (12.17)$$

where  $\Gamma = HN^2/R$ . The mean meridional circulation can be obtained from  $\chi^*$  through the relationships

$$\begin{aligned} \bar{v}^* &= -\bar{\chi}_z^* \\ \bar{w}^* &= \bar{\chi}_y^* \end{aligned} \quad (12.18)$$

It is instructive to consider how Equation 12.17 depends on the magnitude of the ratio  $K_R/\alpha$ . In particular, if  $(K_R/\alpha) \ll 1$ , which appears to be the case throughout most of the stratosphere, Equation 12.17 reduces to

$$\bar{\chi}_{zz}^* \cong \frac{F_z}{f} \quad (12.19)$$

which implies that the mean meridional circulation is forced mainly by the EP flux convergence. If  $F$  is zero, then there is no mean meridional circulation and the stratosphere is in radiative equilibrium, i.e.

$$Q = C + \alpha\bar{T} \quad (12.20)$$

The work of Dickinson (1975) and Harwood and Pyle (1980) suggests that this is indeed the case in the summer stratosphere, where planetary wave activity is essentially absent.

It follows from these considerations that a change in the short wave heating rate  $Q$  due to ozone perturbations will be compensated for through adjustment of the temperature field (cf, Equation 12.20). The Fels *et al.* (1980) finding that significant dynamical adjustment occurred in the tropics is also consistent with the foregoing arguments since  $f \rightarrow 0$  at the equator and the factor  $N^2 K_R / f^2 \alpha$  in Equation 12.17 may not be small even if  $(K_R / \alpha) < 1$ .

Although the smallness of the ratio  $(K_R / \alpha)$  in the stratosphere implies that its mean meridional circulation is rather insensitive to changes in the solar heating rate, it must be borne in mind that circulation changes could still be produced indirectly if the wave forcing,  $F$ , is altered. For example, the temperature changes produced by perturbed solar heating will affect the zonal mean wind through geostrophic adjustment (Equation 12.16). One can then envisage a change in the propagation characteristics of planetary waves in the stratosphere which, in turn, could lead to a different EP flux divergence. Investigation of this possibility would of course require the simultaneous computation of the zonal mean state and at least one planetary wave harmonic.

If the main effect of coupling during a stratospheric perturbation is to change the temperature structure then a requirement is for the models to contain an interactive radiation scheme. Since the photochemistry is temperature dependent, the adjustment needs to be calculated accurately. (The requirement for the determination of temperature dependent rate constants is also emphasized.) In the upper stratosphere, 1- and 2-D models should be able to treat the radiation transfer to high accuracy. If simple treatments are still to be used, they should be based on the Planck function perturbation, rather than the temperature perturbation (as in Newtonian cooling approaches). The radiation transfer becomes more complex in the lower stratosphere (Houghton, 1978) and more difficult to model (Haigh, 1984). Nevertheless, when considering perturbations to the ozone layer this is a crucial area which must be modelled well before assessments can be treated with confidence.

## 12.9 CONCLUSIONS

Middle atmosphere models which include a detailed description of photochemistry have been discussed, with an emphasis on two-dimensional models whose use has increased considerably since the publication of WMO 1981. During this time, theoretical advances have led to major improvements in the formulation (and the understanding of the formulation) of 2-D models. The theoretical basis of 2-D models, and the associated limitations, are now generally well understood. The existing 2-D models provide a generally good description of the spatial and temporal variations of most stratospheric trace gases (or, at least, of those gases for which a reasonable observational data base exists). Practically, however, there are still some problems in overcoming the model limitations.

Improvements in 2-D models have stemmed from two areas of work. Firstly, important understanding of the relationship between eddies and the mean circulation has followed from the work of Andrews and McIntyre (1976) and many others. Secondly, the treatment of eddies in two-dimensional models has also received considerable attention.

Two-dimensional models can now be classified in at least two ways. Firstly, there are the classical Eulerian models. Secondly, there is a new generation of modified Eulerian models which use the residual

## ASSESSMENT MODELS

or diabatic circulation as the mean circulation and typically employ smaller eddy transport coefficients than the classical models. Eddy transport is important in both classes of models - finding the correct balance between the mean circulation and the eddies is necessary for a good model description. Secondly, some models use fixed temperature and circulation fields while others attempt to include a degree of feedback. Inclusion of feedback can help to elucidate the importance of particular radiative, dynamical or photochemical processes. Notice, though, that a completely interactive 2-D model would require an interactive description of eddy forcing, which we do not have.

While the theoretical basis of 2-D models is now well established, a comparison of the performances of various models reveals a number of practical problems. For example, comparison of classical Eulerian models with modified Eulerian models shows as large differences between models of a given type as between the two types of model.

The above differences make difficult general recommendations for the improvement of models. Nevertheless there are some clear problems. A comparison of the low-latitude profiles of odd nitrogen revealed large differences between the models. While the treatment of NO photolysis is important in defining the stratospheric sink of NO<sub>y</sub>, it is clear that the different model treatments are not the sole reason for the differences (and this was true for a similar comparison of 1-D models). In particular, there appear to be problems in the treatment of transport in the equatorial lower stratosphere/upper troposphere. In this region the radiative heating is the small, poorly defined difference of small heating and cooling terms. However, an accurate net heating rate is required for an adequate description of the flux of source gases into the mid-stratosphere. The equatorial lower stratosphere needs further study.

While recent studies have tended to point towards the need for smaller eddy transport coefficients in transformed models compared with classical Eulerian models, there remain important uncertainties. Some diabatic models, for instance, produce a good description of the stratosphere using larger Ks; the evidence for smaller Ks is partly based on the results of general circulation models, which have their own particular problems. More studies using satellite data, and any available data with finer spatial resolution, are required to address the question of the spatial and temporal structure of eddy transport coefficients for 2-D models.

Another problem requiring attention, particularly in view of the need to carry out assessment studies, is a more detailed analysis of the difference between 1- and 2-D model results. While the advantages of the 2-D models are obvious, the relationship between results of the 1- and 2-D model, and the systematic differences between them, are less clearly understood.

Finally, as models of the stratosphere have become increasingly complex, the testing of models has become no easier. Simple subjective comparison of a model and an observed profile does not constitute a particularly satisfactory test. While large data sets, for example, from satellites, improve the capability of making meaningful comparisons, it is clear that much depends on the ingenuity of the experimentalists and theoreticians to construct experiments, either in the field or on the computer, which can test isolated aspects of theory.